UNCERTAINTY QUANTIFICATION OF VOLUMETRIC AND MATERIAL BALANCE ANALYSIS OF GAS RESERVOIRS WITH WATER INFLUX USING A BAYESIAN FRAMEWORK

A Thesis

by

ASTI WULANDARI APRILIA

Submitted to the Office of Graduate Studies of
Texas A&M University
in partial fulfillment of the requirements for the degree of

MASTER OF SCIENCE

December 2005

Major Subject: Petroleum Engineering

UNCERTAINTY QUANTIFICATION OF VOLUMETRIC AND MATERIAL BALANCE ANALYSIS OF GAS RESERVOIRS WITH WATER INFLUX USING A BAYESIAN FRAMEWORK

A Thesis

by

ASTI WULANDARI APRILIA

Submitted to the Office of Graduate Studies of
Texas A&M University
in partial fulfillment of the requirements for the degree of

MASTER OF SCIENCE

Approved by:

Co-Chairs of Committee,	W. John Lee
	Duane A. McVay
Committee Member,	Eric J. Bickel
Head of Department,	Stephen A. Holditch

December 2005

Major Subject: Petroleum Engineering

ABSTRACT

Uncertainty Quantification of Volumetric and Material Balance Analysis of Gas Reservoirs With Water Influx Using a Bayesian Framework. (December 2005)

Asti Wulandari Aprilia, B.S., University of Indonesia

Co-Chairs of Advisory Committee: Dr. W. John Lee
Dr. Duane A. McVay

Accurately estimating hydrocarbon reserves is important, because it affects every phase of the oil and gas business. Unfortunately, reserves estimation is always uncertain, since perfect information is seldom available from the reservoir, and uncertainty can complicate the decision-making process. Many important decisions have to be made without knowing exactly what the ultimate outcome will be from a decision made today. Thus, quantifying the uncertainty is extremely important.

Two methods for estimating original hydrocarbons in place (OHIP) are volumetric and material balance methods. The volumetric method is convenient to calculate OHIP during the early development period, while the material balance method can be used later, after performance data, such as pressure and production data, are available.

In this work, I propose a methodology for using a Bayesian approach to quantify the uncertainty of original gas in place (G), aquifer productivity index (J), and the volume of the aquifer (W_i) as a result of combining volumetric and material balance analysis in a water-driven gas reservoir.

The results show that we potentially have significant non-uniqueness (i.e., large uncertainty) when we consider only volumetric analyses or material balance analyses.

By combining the results from both analyses, the non-uniqueness can be reduced, resulting in OGIP and aquifer parameter estimates with lower uncertainty. By understanding the uncertainty, we can expect better management decision making.

DEDICATION

Dedicated to my father and my mother, for their continuous support and prayers; my siblings, Mita and Adi; and my fiancé, Dolli, whose loving attention made writing this thesis easier.

ACKNOWLEDGMENTS

I would like to express my gratitude to Dr. John Lee and Dr. Duane McVay, co-chairs of my advisory committee, for their support and opinions; Prof. Eric J. Bickel, member of my committee, for giving me advice for my thesis; and Dr. Stephen A. Holditch for his advice during my first semester at Texas A&M University. I also thank my close friends Roy, for his superb support; Kalwant, Irene, Adi, Sulis, Memed, Evi, Buyung, Yenny, and Anto, whose friendship made the one and half years at College Station easier; and to the Indonesian community of College Station.

Last but not least, I would like to express my gratitude to my sponsor, PT Medco E&P Indonesia, without whose support I would not have been able to pursue my Master of Science degree.

TABLE OF CONTENTS

Page

ABSTRACT.. iii

DEDICATION.. v

ACKNOWLEDGMENTS.. vi

TABLE OF CONTENTS.. vii

LIST OF FIGURES.. ix

LIST OF TABLES.. xii

CHAPTER

I INTRODUCTION.. 1

II GAS-IN-PLACE ESTIMATION.. 4

Volumetric Method.. 4
Material Balance Method.. 5
Material Balance as a Straight Line (After Havlena and Odeh)........ 7
Water Influx.. 10
Fetkovich Model.. 11

III BAYES' THEOREM FOR COMBINING VOLUMETRIC AND MATERIAL BALANCE ANALYSIS.. 14

A *Priori* Distribution.. 17
Likelihood Distribution.. 18
A *Posteriori* Distribution.. 19
Comparison of the Prior and Posterior Parameter Covariance Matrices.. 19
Linear Regression Method.. 19
Numerical Method.. 20

IV APPLICATIONS.. 22

Lagan Gas Field.. 22

CHAPTER Page

A Synthetic Case by Dake.. 38
Higher Uncertainty in Prior.. 70
Lower Uncertainty in Prior.. 72
Less Uncertainty in the Pressure Data... 76

V CONCLUSIONS……………………………………………………….…..... 77

Future Work.. 77

NOMENCLATURE……………………………………..………………..…… 79

REFERENCES…………………………………………………………..……........... 81

APPENDIX A…………………………………………………………..…………… 83

VITA……………………………………………………………………..……... 107

LIST OF FIGURES

FIGURE Page

1 Diagnostic gas material balance plot (after Dake[11]) 9

2 Conventional p/Z plot (after Dake[11]) 9

3 Procedure to quantify fluids-in-place uncertainty using a Bayesian framework. 16

4 p/Z versus Gp for BB sand. 23

5 Prior distribution of G versus J for $W_i = 0.5\ W_{i\ max}$, BB sand. 25

6 Prior distribution of G versus W_i for $J = 0.5\ J_{max}$, BB sand. 26

7 Prior distribution of W_i versus J for $G = 0.5\ G_{max}$, BB sand. 27

8 Likelihood distribution of G versus J for $W_i = 0.5\ W_{i\ max}$, BB sand. 29

9 Likelihood distribution of G versus W_i for $J = 0.5\ J_{max}$, BB sand. 30

10 Likelihood distribution of W_i versus J for $G = 0.5\ G_{max}$, BB sand. 31

11 Posterior distribution of G versus J for $W_i = 0.5\ W_{i\ max}$, BB sand. 33

12 Posterior distribution of G versus W_i for $J = 0.5\ J_{max}$, BB sand. 34

13 The posterior distribution of W_i versus J for $G = 0.5\ G_{max}$, BB sand. 35

14 Composite plot for 50% of the maximum values of each parameter, BB Sand. 36

15 p/Z plot of synthetic gas field case (data from Dake[11]). 40

16 F/E_g versus G_p for synthetic gas field case (data from Dake[11]). 41

17 Prior distribution of G versus J for $W_i = 0.5\ W_{i\ max}$, synthetic field A. 43

18 Prior distribution of G versus W_i for $J = 0.5\ J_{max}$, synthetic field A. 44

FIGURE Page

19 Prior distribution of W_i versus J for $G = 0.5\ G_{max}$, synthetic field A. 45

20 Likelihood distribution of G versus J for $W_i = 0.5\ W_{i\ max}$, synthetic field A...... 47

21 Likelihood distribution of G versus W_i for $J = 0.5\ J_{max}$, synthetic field A......... 48

22 Likelihood distribution of W_i versus J for $G = 0.5\ G_{max}$, synthetic field A........ 49

23 Posterior distribution of G versus J for $W_i = 0.5\ W_{i\ max}$, synthetic field A......... 51

24 Posterior distribution of G versus W_i for $J = 0.5\ J_{max}$, synthetic field A. 52

25 Posterior distribution of W_i versus J for $G = 0.5\ G_{max}$, synthetic field A........... 53

26 Composite plot for 50% of the maximum values of each parameter, synthetic field A. 54

27 Composite plot for 25% of the maximum values of each parameter, synthetic field A. 55

28 Composite plot for 75% of the maximum values of each parameter, synthetic field A. 56

29 Pressure data with noise added.. 58

30 Likelihood distribution of G versus J for $W_i = 0.5\ W_{i\ max}$, synthetic Field B..... 60

31 Likelihood distribution of G versus W_i for $J = 0.5\ J_{max}$, synthetic field B. 61

32 Likelihood distribution of W_i versus J for $G = 0.5\ G_{max}$, synthetic field B. 62

33 Posterior distribution of G versus J for $W_i = 0.5\ W_{i\ max}$, synthetic field B......... 63

34 Posterior distribution of G versus W_i for $J = 0.5\ J_{max}$, synthetic field B. 64

35 Posterior distribution of W_i versus J for $G = 0.5G_{\mathrm{max}}$, synthetic field B. 65

36 Composite plot for 50% of the maximum values of each parameter, synthetic field B. 66

37 Composite plot for 25% of the maximum values of each parameter, synthetic field B. 67

FIGURE Page

38 Composite plot for 75% of the maximum values of each parameter, synthetic field B. 68

39 Composite plot for 50% of the maximum value of each parameter, synthetic field B, with higher uncertainty in prior. 71

40 Composite plot for 50% of the maximum values of each parameter, synthetic field B, with less uncertainty in prior. 74

41 Composite plot for 50% of the maximum value of each parameter, pressure SD = 20 psia. 75

LIST OF TABLES

TABLE Page

1 Performance Data from BB Sand 22

2 Mean and Standard Deviation of G, J, and W_i from Volumetric Analysis, BB Sand 24

3 Observed Data Used in Analysis, BB sand 28

4 Standard Deviations of G, J, and W_i from Prior and Posterior, BB Sand 37

5 PVT Data, Synthetic Gas Field Case 38

6 Field Performance Data, Synthetic Gas Field Case 39

7 Means and Standard Deviations of G, J, and W_i from Volumetric Analysis, Synthetic Field A 42

8 Observed Data Used in Analysis, Synthetic Field A 46

9 Prior and Posterior Standard Deviations of G, J, and W_i, Synthetic Field A 57

10 Observed Data Used in Analysis, Synthetic Field B 59

11 Prior and Posterior Standard Deviations of G, J, and W_i, Synthetic Field B 69

12 Mean and Standard Deviation of G, J, and W_i from Volumetric Analysis, Synthetic Field B, with Higher Uncertainty in Prior 70

13 Prior and Posterior Standard Deviations of G, J, and W_i, Synthetic Field B, with Higher Uncertainty in Prior 72

14 Mean and Standard Deviation of G, J, and W_i from Volumetric Analysis, Synthetic Field B, with Less Uncertainty in Prior 73

15 Prior and Posterior Standard Deviations of G, J, and W_i from Synthetic FieldB, with Less Uncertainty in Prior 73

CHAPTER I
INTRODUCTION

Estimating hydrocarbon reserves accurately is important. Bradley[1] states that reserves estimates may be used in formulating a company's policies for exploring and developing oil and gas properties; designing and constructing plants, gathering systems, and other surface facilities; determining the division of the ownership in unitized projects; determining the fair market value of a property to be bought or sold; determining the collateral value of producing properties for loans; establishing sales contracts, rates, and prices; and obtaining regulatory body approvals. But these estimates are always uncertain, since perfect information is seldom available in the oil and gas business. Thus, quantifying the uncertainty is extremely important. Better understanding of uncertainty can lead to better management decisions.[2]

Two common methods for estimating hydrocarbon reserves are volumetric and material balance methods. The volumetric method is convenient to calculate hydrocarbon reserves prior to availability of representative pressure and production data. This method uses static reservoir properties such as area of accumulation, pay thickness, porosity, and initial saturation distribution. The material balance method can be used later when sufficient amounts of performance data, such as pressure and production data, are available.

If the material balance calculation is properly applied, it can be used to estimate initial hydrocarbon volumes in place, predict future reservoir performance, and predict ultimate hydrocarbon recovery under various types of primary-drive mechanisms. The equation for the material balance method is structured to simply keep an inventory of all materials

---

This thesis follows the style and format of the *Journal of Petroleum Technology Monthly.*

entering, leaving, and accumulating in the reservoir. This method can be used as an independent check of volumetric estimates.

Bayes' theorem[3-5] provides a means to investigate the uncertainty of hydrocarbon reserves estimates. Bayes' theorem affords a mathematical basis for relating the degree to which an observation (or new information) confirms various hypothesized causes or states of nature. Floris *et al.*[6] applied Bayes' theorem to quantify uncertainty in production forecasts for reservoir models conditioned to both static and dynamic well data. Glimm *et al*.[7] showed that the Bayesian approach can reduce the uncertainty in the prediction error of unknown geological parameters in a simulation of an oil field. Daoud *et al.*[8] used the Bayesian approach to quantify the uncertainty of original oil in place and relative gas-cap size estimated using the Havlena and Odeh material balance equation. Galli *et al.*[9] also used the Bayesian approach to evaluate new information for choosing between different exploitation scenarios for a gas field.

In this work, using Bayes' theorem, I will modify *a priori* probability distributions from the result of volumetric analysis with likelihood probability distributions from the result of material balance analysis, and obtain new, *a posteriori* probability distributions. Then I will quantify the uncertainty of parameters from *a posteriori* probability distributions by approximation of the covariance matrix. Covariance is a statistical measure of correlation of the fluctuations of different quantities.[10]

This study will be based on a synthetic field case, reported by Dake,[11] and Lagan gas field, located in Indonesia and operated by PT Medco Exploration and Production Indonesia. Lagan field provides a considerable set of data from about 20 years of exploitation. The field has more than 15 reservoirs, but only six reservoirs are producing. In this work, only one reservoir, the BB sand, in Lagan field is examined. Both cases, the synthetic field and the BB sand, are known to have water-drive. The synthetic field has a strong water drive, while the BB sand has a very weak water drive.

For simplicity, and without significant sacrifice of accuracy, I will use a two-parameter aquifer model, and the original gas in place will be a parameter in my study. Thus, three parameters will control performance and contribute to uncertainty in production forecasts. They are original gas in place (G), aquifer productivity index (J), and the volume of water in the aquifer (W_i).

Since both cases have water drive, I will use Havlena and Odeh[12,13] material balance analysis, which includes water influx. Lee and Wattenbarger[14] state that if a gas reservoir is subjected to water influx from an aquifer, the pore volume of the gas reservoir is reduced by an amount equal to the volume of encroaching water. The water entering the reservoir provides an important source of energy that must considered in material balance calculations. In this work, I will use the Fetkovich method[15] to calculate water influx. The Fetkovich method uses an inflow equation to model the water influx from the aquifer into the reservoir.

This project will combine gas-in-place estimates from volumetric and material balance methods applied to the synthetic field case and the BB sand and will use Bayesian analysis to quantify the uncertainty of these parameters.

CHAPTER II
GAS IN PLACE ESTIMATION

Ikoku[16] states that reservoirs containing hydrocarbons fluids that exist totally in the vapor phase at pressures equal to or less than the initial pressure are defined to be gas reservoirs. Gas reservoirs may have water influx from an adjacent water-bearing portion of the formation or may be volumetric (i.e., have no water influx). Two approaches for estimating initial gas in place (G) are the volumetric method and the material balance method.

Volumetric Method

In volumetric analysis, the gas in the pore volume in the reservoir is calculated in terms of gas volume at standard conditions. Volumetric methods are particularly useful early in the life of a reservoir prior to significant development and production. However, volumetric methods can also be applied later in a reservoir's life and often are used to confirm estimates from material balance calculations. Before reservoir limits have been accurately defined, it is convenient to estimate gas in place per acre-foot of bulk reservoir rock. Multiplication of this unit figure by the best available estimate of bulk reservoir volume then gives gas in place for the lease, tract, or reservoir under consideration.

According to Lee and Wattenbarger,[14] accurately estimating gas in place using volumetric methods depends on the availability of adequate data to characterize the reservoir's areal extent and variations in net thickness, and also to determine the gas-bearing reservoir pore volume. Clearly, early in the productive life of a reservoir when few data are available to establish subsurface geologic control, volumetric estimates are least accurate. As more wells are drilled and more data become available, the accuracy of these estimates improves.

To determine net volume of reservoir rock containing the gas, we need information from cores, geophysical logs, drilling records, and drill stem and production tests. This information then can be used to build isopachous maps, from which the reservoir pore volume can be obtained.

The standard cubic feet of initial gas in place, G, is the product of three factors: the reservoir pore volume, the initial gas saturation, and a volume ratio (initial gas formation volume factor) that converts reservoir volumes to volumes at standard conditions. These factors are related as follows:

$$G=\frac{7{,}758\, A\, h\, \phi\left(1-S_{wi}\right)}{B_{gi}}, \quad \text{(1)}$$

where $B_{gi} = \frac{5.02\, z_i\, T}{p_i}$, ... (2)

The recovery factor from a gas reservoir is primarily a function of the abandonment pressure and permeability. For natural gas reservoirs under volumetric control (no water influx or water production), the recovery factor is usually 80 % to 90% of the original gas in place. Water-drive gas reservoirs usually have a lower recovery factor than volumetric gas reservoirs because of the high abandonment pressure due to water encroachment into the producing wells. For strong water drives where residual gas is trapped at high pressures, recovery factors may be 50 % to 60 %.

Material Balance Method

If enough production-pressure history is available for a gas reservoir, the initial gas in place and the gas reserves can be estimated without knowing area of the gas reservoir (A_r), pay thickness (h_r), porosity (ϕ), or water saturation (S_w) by using the material balance method.

A material balance process is an exact accounting of the materials that enter, accumulate in, and are depleted from a defined volume in the course of a given time interval of operation. The material balance equation for a gas reservoir may be applied to estimate initial gas in place from performance data, such as pressure and production data.

Material balance methods can be used to determine the existence and effectiveness of any natural water drive, and can assist in predicting performance and reserves. Material balance may also verify possible extensions to a partially developed reservoir when gas in place calculated by the material balance equation is much larger than a volumetric estimate, particularly when water influx is thought to be small.

Accurate pressure-production data are essential for reliable material balance calculations. The most likely source of error is incorrect estimates of average reservoir pressure, especially during the early history period when even slight pressure errors have a significant effect on results. Therefore, the material balance equation should not be relied on early in the producing life of the reservoir.

If the gas reservoir has a water drive, then there will be two unknowns in the material balance equation, even though production data, pressure, temperature, and gas gravity are known. These two unknowns are initial gas-in-place, G, and cumulative water influx *vs.* time, $W_e(t)$. To use the material balance equation to calculate initial gas in place, some independent method of estimating W_e must be developed.[15]

The gas material balance equation including water influx and water production is

$$G = \frac{G_p B_g - \left(W_e - W_p B_w\right)}{B_g - B_{gi}} \quad \text{.......} \quad (3)$$

Eq. (3) can be rearranged as

$$G+\frac{W_e}{B_g-B_{gi}}=\frac{G_pB_g+W_pB_w}{B_g-B_{gi}}\,. \quad \text{...} \quad (4)$$

To estimate the value of W_e, a plot of cumulative gas produced (G_p) versus $G+\frac{W_e}{B_g-B_{gi}}$ is made. Extrapolation of the line formed by these points back to the point where G_p = 0 shows the true value of gas in place, G, because when G_p = 0 then $\frac{W_e}{B_g-B_{gi}}$ is also zero.

Material Balance as a Straight Line (After Havlena and Odeh)

The material balance is expressed in reservoir volumes of production, expansion and influx as:

$$\begin{matrix}\text{Underground} & & \text{Gas} & & \text{Water expansion/} & & \text{Water}\\ \text{withdrawal} & = & \text{expansion} & + & \text{pore compaction} & + & \text{influx}\\ \text{(rcf)} & & \text{(rcf)} & & \text{(rcf)} & & \text{(rcf)}\end{matrix} \quad , .. \quad (5)$$

$$\mathrm{G_p\,B_g+W_p\,B_w} \quad = \quad \mathrm{G}\left(\mathrm{B_g}+B_{\mathrm{gi}}\right) \quad + \quad \mathrm{G\,B_{gi}}\,\frac{\left(c_\mathrm{w}S_\mathrm{wc}+c_\mathrm{f}\right)}{1-S_\mathrm{wc}}\Delta p \quad + \quad W_\mathrm{e}\,B_\mathrm{w}$$

Using the nomenclature of Havlena and Odeh [12,13], we can express Eq. 5 in the following form:

$$F=G\left(E_\mathrm{G}+E_\mathrm{f,w}\right)+W_\mathrm{e}\,B_\mathrm{w}\,, \quad \text{...} \quad (6)$$

with the terms F, E_G, and $E_\mathrm{f,w}$ defined as

Underground fluid withdrawal, F (rcf):

$$F=G_p\,B_g+W_pB_w\,, \quad \text{...} \quad (7)$$

Gas expansion term, E_G (rcf/scf):

$$E_G = B_g + B_{gi} \ , \quad \ldots\ldots\ldots\ldots\ldots\ldots\ldots\ldots\ldots\ldots\ldots\ldots \quad (8)$$

Water and rock expansion, $E_{f,w}$ (rcf/scf):

$$E_{f,w} = B_{gi} \frac{\left(c_w \, S_{wi} + c_f\right)}{1 - S_{wi}} \Delta p \ . \quad \ldots\ldots\ldots\ldots\ldots\ldots\ldots\ldots\ldots \quad (9)$$

In most practical cases, $E_{f,w} \langle\langle \ E_g$ and may be eliminated, but we should check to ensure that this simplification is valid throughout the entire range of pressure depletion. The material balance equation then becomes

$$F = G \, E_g + W_e \, B_w \, , \quad \ldots\ldots\ldots\ldots\ldots\ldots\ldots\ldots\ldots\ldots\ldots\ldots \quad (10)$$

Finally, dividing both sides of the equation by E_g gives

$$\frac{F}{E_g} = G + \frac{W_e \, B_w}{E_g} \, , \quad \ldots\ldots\ldots\ldots\ldots\ldots\ldots\ldots\ldots\ldots\ldots\ldots \quad (11)$$

Using production, pressure, and PVT data to calculate individual terms, we should plot the left-hand side of this expression as a function of the cumulative gas production, G_p. This plot is simply for display purposes to inspect its variation during depletion. The plot will have one of the three shapes shown in Fig. 1. If the reservoir is of the volumetric depletion type, $W_e = 0$. Alternatively if the reservoir is affected by natural water influx then the plot of F / E_g will usually produce a concave-downward shaped arc whose exact form is dependent upon the aquifer size and strength and the gas offtake rate. The main advantage of the F / E_g versus G_p plot is that it is much more sensitive than other methods, even a plot of *p/Z* versus the cumulative gas production (G_p), which is a widely accepted method (as shown in Fig. 2), in establishing whether the reservoir is being influenced by natural water influx or not. In the *p/Z* versus G_p plot, the extrapolation of the plot to atmospheric pressure provides a reliable estimate of the original gas in place. If a water drive is present the plot often appears to be linear, but the extrapolation will give an inaccurately high value for original gas in place.

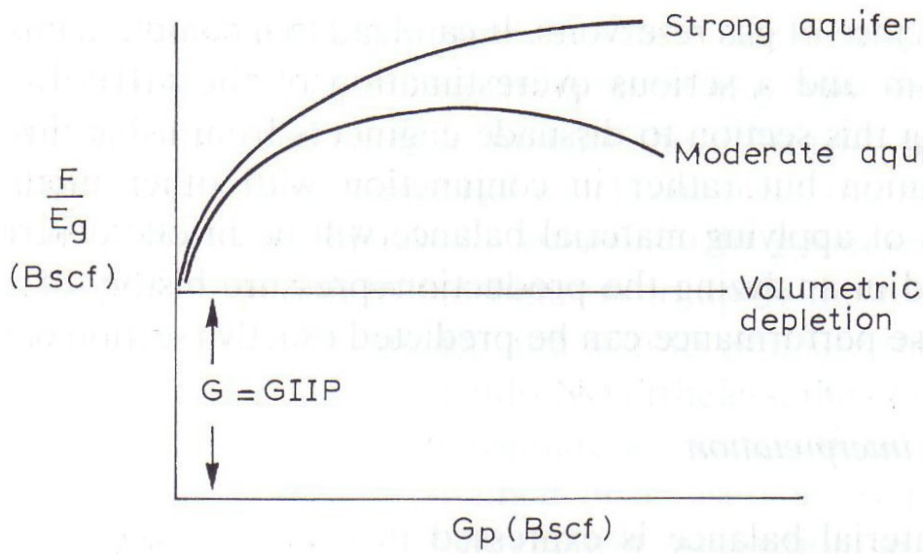

Fig. 1-Diagnostic gas material balance plot (after Dake[11]).

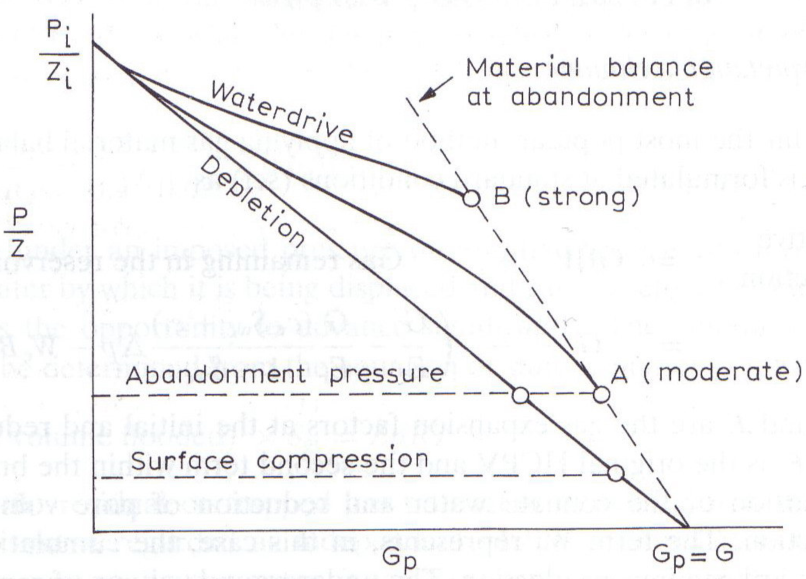

Fig. 2-Conventional p/Z plot (after Dake[11]).

If a reservoir is influenced by water drive, then operators usually try to accelerate the production of gas. The purpose is to reduce the pressure at which the residual gas saturation is trapped behind the advancing flood front.

Water Influx

Water-bearing rocks called aquifers surround nearly all hydrocarbon reservoirs.[17,18] These aquifers may be substantially larger than the gas reservoirs they adjoin and may appear to be infinite in size. They may be so small as to be negligible in their effect on the reservoir performance. As reservoir fluids are produced and reservoir pressure declines, a pressure differential develops from the surrounding aquifer into the reservoir. The result is water influx, commonly called water encroachment, which is attributed to

- expansion of the water in the aquifer,
- compressibility of the aquifer rock, and/or
- artesian flow where the water-bearing formation outcrop is located structurally higher than the pay zone.

In general, reservoir systems are classified as either edge-water or bottom-water drive. In edge-water drive systems, water moves into the flanks of the reservoir as a result of hydrocarbon production and pressure drop at the reservoir-aquifer boundary. Water flow is essentially radial with negligible flow in the vertical direction. Bottom-water drive occurs in a reservoir with large areal extent and a gentle dip where the gas-water contact completely underlies the reservoir. In contrast to the edge-water drive, a bottom-water drive reservoir has significant vertical flow of water.

It should be appreciated that there are usually more uncertainties associated with water influx than with other components of material balance calculations. This is simply because one seldom drills wells into an aquifer to gain the necessary information about the porosity, permeability, thickness, and fluid properties. Instead, these properties frequently have to be inferred from what has been observed in the reservoir. Even more uncertain, however, is the geometry and areal continuity of the aquifer itself.

Several models have been developed for estimating water influx, based on assumptions that describe the characteristics of the aquifer. Due to inherent uncertainties in the aquifer characteristics, all the proposed models require historical reservoir performance data to evaluate constants representing aquifer property parameters, since these are rarely known from exploration and development drilling with sufficient accuracy for direct application.

The mathematical water influx models that are commonly used in the petroleum industry include:

- van Everdingen and Hurst unsteady state:
    - edge-water drive
    - bottom-water drive
- Carter-Tracy unsteady state
- Fetkovich pseudo-steady state
    - radial aquifer
    - linear aquifer

In this work, I will use the Fetkovich pseudo-steady state model because it contains fewer parameters (two) than the other models.

<u>Fetkovich Model</u>

The Fetkovich model is based on the premise that the productivity index concept will adequately describe water influx from a finite aquifer into a hydrocarbon reservoir. Specifically, the water influx rate is directly proportional to the pressure drop between the average aquifer pressure and the pressure at the original reservoir-aquifer boundary. The Fetkovich method is much simpler than the van Everdingen-Hurst method or the

Carter-Tracy method, and does not require the use of superposition. The Fetkovich method neglects the effects of any transient period. Thus, in cases where pressure is changing rapidly at the aquifer-reservoir interface, predicted results may differ somewhat from the van Everdingen-Hurst or Carter-Tracy approaches. The water influx calculated with the Fetkovich method will be less than the values predicted by the other two approaches.

The Fetkovich approach begins with two simple equations. The first is the productivity index (PI) equation for the aquifer, which is analogous to the PI equation used to describe an oil or gas well:

$$q_w = \frac{\mathrm{d}W_e}{\mathrm{d}t} = J\left(\bar{p}_{aq} - p_r\right)^n, \quad \text{(12)}$$

where n = 1 for flow obeying Darcy's law, and n = 0.5 for fully turbulent flow.

The second equation is an aquifer material balance equation for a constant compressibility system, which states that the pressure depletion in the aquifer is directly proportional to the cumulative water influx from the aquifer, or

$$W_e = c_t W_i \left(p_{aq,i} - \bar{p}_{aq}\right), \quad \text{(13)}$$

The following steps describe the methodology of using the Fetkovich model in predicting the cumulative water influx:

a. Calculate the initial volume of water in the aquifer from:

$$W_i = \frac{\pi\left(r_a^2 - r_r^2\right)h\phi}{5.615}\left(\frac{\theta}{360}\right), \quad \text{(14)}$$

where $$r_a = \sqrt{\left(\frac{43{,}560\, A_a}{\pi}\right)\left(\frac{360}{\theta}\right)}, \quad \text{(15)}$$

b. Calculate the maximum water volume, W_{ei}, from the aquifer that could enter the reservoir if the reservoir pressure were reduced to zero:

$$W_{ei} = c_t \, p_{aq,i} \, W_i \, . \quad \text{..} \quad (16)$$

c. Calculate the aquifer productivity index, J, for radial flow with a finite, no-flow outer aquifer boundary:

$$J = \frac{0.00708\,kh(\theta/360)}{\pi[ln(r_a/r_r) - 0.75]} \, . \quad \text{..} \quad (17)$$

d. Calculate the incremental water influx (ΔW_{en}) from the aquifer during the n^{th} time interval:

$$\Delta W_{en} = \frac{W_{ei}}{p_{aq,i}}\left(\bar{p}_{aq,n-1} - \bar{p}_{r,n}\right)\left[1 - exp\left(-\frac{Jp_{aq,i}\Delta t_n}{W_{ei}}\right)\right], \quad \text{.................} \quad (18)$$

where $p_{aq,n}$ is the average aquifer pressure at the end of the n^{th} period.

e. Calculate W_{en} during the n^{th} time interval.

$$W_{en} = \sum_{i=1}^{n} \Delta W_{ei} \, . \quad \text{..} \quad (19)$$

Repeat steps d. and e. for each pressure step.

Usually, the reservoir properties required to estimate J and W_i are unknown. Thus, these two unknown parameters, J and W_i, are usually determined from analysis of performance data.

CHAPTER III
BAYES' THEOREM FOR COMBINING VOLUMETRIC AND MATERIAL BALANCE ANALYSIS

In the Bayesian approach[5] to statistics, an attempt is made to utilize all available information in order to reduce the amount of uncertainty present in a decision-making problem. As new information is obtained, it is combined with previous information to form the basis for statistical procedures. The formal mechanism used to combine the new information with the previously available information is known as *Bayes' theorem*.

The Bayesian approach to statistics allows a parameter to be considered a random variable and involves the use of probabilities for parameters as wells as observations and sample statistics, since probability can be thought of as the mathematical language of uncertainty. At any given point in time, the information about some uncertain quantity can be represented by a set of probabilities. When new information is obtained, these probabilities are revised in order that they may represent all of the available information.

A random variable describes the outcomes of an experiment in terms of numbers. If the only possible outcomes of the experiment are distinct numbers separated from each other (e.g., counts), then the random variable is discrete. When we have a continuous random variable, we believe all values over some range are possible if our measurement device is adequately accurate. There are an infinite number of real numbers in an interval, so the probability of getting any particular value must be zero.

In many problems involving statistical inference and decision, it is realistic and convenient to assume that the random variable (uncertain quantity) of interest is continuous. It should be emphasized that measurement procedures are such that actual observed random variables are never truly continuous.

Suppose that the uncertain quantity of interest in some inferential or decision-making problem is continuous, and call this uncertain quantity *m*. Furthermore, suppose that sample information involving *m* can be summarized by the sample statistics d_{obs}. If d_{obs} contains all the information from the sample that is relevant with regard to the uncertainty about *m*, then d_{obs} is called a sufficient statistic.

If *m* is continuous, the prior and posterior distributions of *m* can be represented by density functions. The posterior distribution is the conditional density of *m*, given the observed values of the sample statistics d_{obs}.

The prior distribution and the likelihood function are assessed. Then the posterior density can be written as follows:

$$\sigma(m|d_{obs}) = \frac{\rho_M(m)\theta(d_{\mathrm{obs}} \mid m)}{\int_{\mathrm{M}} dm\ \rho_M(m)\theta(d_{\mathrm{obs}} \mid m)}, \quad \ldots\ldots\ldots\ldots\ldots\ldots\ldots\ldots\ldots \quad (20)$$

This is Bayes' theorem for continuous random variables. The densities $\sigma(m \mid d_{obs})$ and $\rho_M(m)$ represent the posterior distribution and the prior distribution, respectively, and $\theta(d_{obs} \mid m)$ represents the likelihood function. The prior and posterior distributions must be proper density functions. The denominator of Eq. 21 makes the posterior distribution a probability distribution.

Often we are interested in only relative posterior probabilities. So we often write Bayes' theorem can be written as:

$$posterior \propto prior \times likelihood \quad \ldots\ldots\ldots\ldots\ldots\ldots\ldots\ldots\ldots\ldots\ldots\ldots \quad (21)$$

The posterior distribution is one input to a problem of decision-making under uncertainty, and this is why so much space has been devoted to the revision of prior probabilities and the determination of posterior probabilities. If no sample information is available, then it is the prior distribution that is an input to decision-making problem. It also should be noted that some decision-making problems are directly related to a sample outcome, in which case the predictive distribution is the distribution of interest. Prior, posterior, or predictive, the distribution represents the decision maker's state of uncertainty, or state of information, in a situation in which he or she must make a decision under uncertainty.

Appendix A shows the code in VBA language using the procedure outlined in Fig. 3.

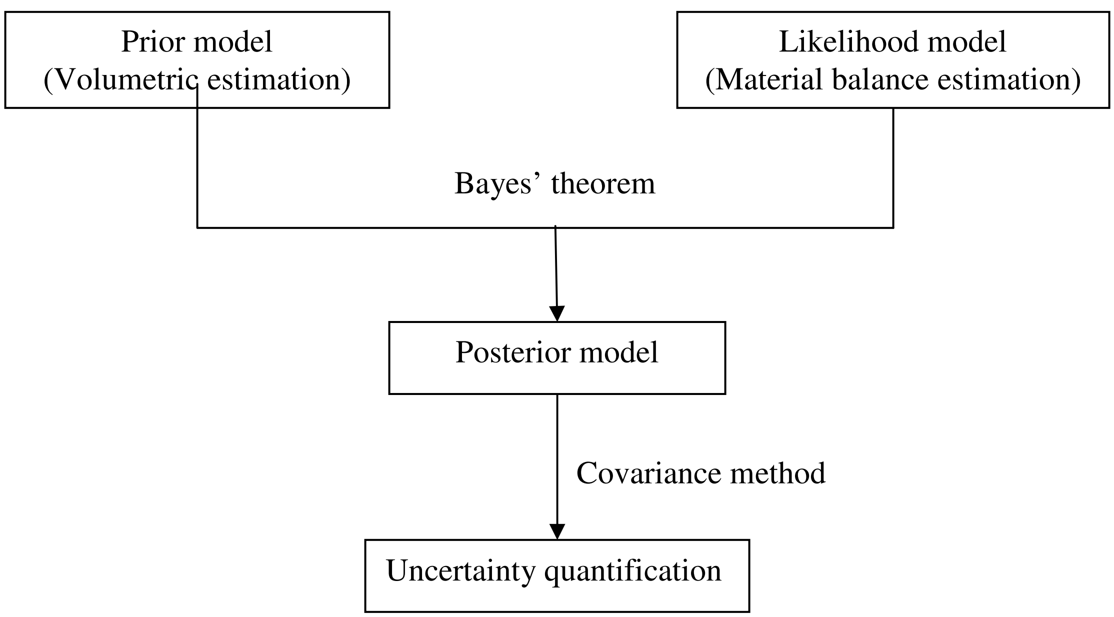

Fig. 3-Procedure to quantify fluids-in-place uncertainty using a Bayesian framework.

<u>*A Priori* Distribution</u>

To build the *a priori* distribution, first I determine the probability distributions of parameters to calculate gas in place (G), aquifer productivity index (J), and aquifer size (W_i) using the volumetric method. Parameters used in this process are area of the gas reservoir (A_r) in acres, pay thickness (h_r) in ft, porosity (ϕ), water saturation (S_w), gas formation volume factor (B_g) in RB/scf, aquifer permeability (k) in darcies, aquifer thickness (h_a) in ft, and aquifer area (A_a) in acres.

Then I use Monte Carlo simulation to calculate the individual probability distributions of G, J, and W_i with Eq. 1, Eq. 17, and Eq. 14, respectively, from Chap. 2. Using the mean and standard deviation for G, J, and W_i, and assuming a multivariate Gaussian distribution, as expressed by Eq. 22, the multivariate prior probability density function can be formed,

$$\rho_M(m) = \left[(2m)^n \, det\, C_{\mathrm{M}}\right]^{-\frac{1}{2}} exp\left[-\frac{1}{2}\left(m - m_{\mathrm{prior}}\right)^t C_M^{-1}\left(m - m_{\mathrm{prior}}\right)\right], \quad \ldots.. \quad (22)$$

where

$$m_{prior} = \begin{bmatrix} G_{prior} \\ J_{prior} \\ W_{i\ prior} \end{bmatrix}, \quad \ldots\ldots\ldots\ldots \quad (23)$$

$$C_M = \begin{bmatrix} \sigma_G^2 & 0 & 0 \\ 0 & \sigma_J^2 & 0 \\ 0 & 0 & \sigma_{W_i}^2 \end{bmatrix}, \quad \ldots\ldots\ldots\ldots \quad (24)$$

G_{prior}, J_{prior}, and $W_{i\ prior}$ are the mean values from the volumetric analysis. G, J, and W_i will be assumed to be independent of each other; i.e., there is no correlation between the parameters. As a result, the covariance matrix in Eq. 24 has zeros for the off-diagonal terms.

Likelihood Distribution

Definition of the Bayesian likelihood function relies on the specification of a model for the uncertainty associated with the observed dynamic data from the reservoir, pressure and production data in this case.

The likelihood function is obtained by incorporating the pressure data (*d*) and a forward model g(m) expressing pressure implicitly as a function of *G*, *J*, and W_i. The vector g(m) consists of the pressures that satisfy the Havlena and Odeh material balance equation for a gas reservoir with water influx, given by Eqs. 7, 8 and 10 in Chap 2.

I use Newton-Rhapson iteration to solve Eq. 10 for pressure given *G*, *J*, and W_i. The equation used in the Newton-Rhapson iteration process is

$$f(p) = F - G\,E_g - W_e\,B_w = 0, \quad \text{...} \quad (25)$$

or

$$f(p) = G_p\,B_g + W_p\,B_w - G\,E_g - W_e\,B_w = 0. \quad \text{..............................} \quad (26)$$

The pressure misfits (data minus forward model) is assumed to follow a normal distribution, which is represented as

$$\theta(d_{\text{obs}}|m) = \left[(2\pi)^n\, det\, C_D\right]^{-\frac{1}{2}}$$
$$\bullet\ exp\left[-\frac{1}{2}\left(g(m) - d_{\text{obs}}\right)^t C_D^{-1}\left(g(m) - d_{\text{obs}}\right)\right], \quad \text{...................} \quad (27)$$

where

$$C_D = \begin{bmatrix} \sigma_{d_1}^2 & 0 & 0 & . & 0 \\ 0 & \sigma_{d_2}^2 & 0 & . & 0 \\ 0 & 0 & \sigma_{d_3}^2 & . & 0 \\ . & . & . & . & . \\ 0 & 0 & 0 & . & \sigma_{d_n}^2 \end{bmatrix}. \quad \text{..} \quad (28)$$

A Posteriori Distribution

The *a posteriori* distribution is the product of the *a priori* distribution with the likelihood distribution, in this case the prior distribution from volumetric analysis and the likelihood distribution from the material balance analysis, as shown in Eq. 20.

Comparison of the Prior and Posterior Parameter Covariance Matrices

The covariance matrix of the posterior distribution is an expression of the uncertainty in the parameter estimates. There are two ways to approximate the covariance matrix, as follows:

1. Linear regression method
2. Numerical method

Linear Regression Method

Because the *a posteriori* distribution is usually non-Gaussian and quite complex, the task we are faced with is that of information reduction. A point that is usually of significant interest is the mode of the *a posteriori* distribution, called the *maximum a posteriori* (MAP) estimate. The MAP is given by the values of G, J, and W_i that maximize the posterior distribution.

After the MAP estimate is found, sensitivities are derived to reconcile the uncertainties associated with the G, J, and W_i. I use the posterior covariance matrix as an indicator of uncertainties associated with the model parameters at the MAP estimate. The covariance matrix of the posterior probability distribution is given by the inverse of the Hessian matrix:

$$C_x = H^{-1}, \quad \text{.........} \quad (29)$$

The Hessian matrix can be obtained by using the following relationship:

$$H = G^T C_D^{-1} G + C_M^{-1}, \quad \text{.........} \quad (30)$$

where G is the sensitivity matrix containing the parameter sensitivities given as follows:

$$G = \begin{bmatrix} \frac{\partial p_1}{\partial G} & \frac{\partial p_1}{\partial J} & \frac{\partial p_1}{\partial W_i} \\ \frac{\partial p_2}{\partial G} & \frac{\partial p_2}{\partial J} & \frac{\partial p_2}{\partial W_i} \\ \frac{\partial p_3}{\partial G} & \frac{\partial p_3}{\partial J} & \frac{\partial p_3}{\partial W_i} \\ \cdot & \cdot & \cdot \\ \frac{\partial p_{nd}}{\partial G} & \frac{\partial p_{nd}}{\partial J} & \frac{\partial p_{nd}}{\partial W_i} \end{bmatrix} . \quad \ldots\ldots\ldots\ldots\ldots\ldots\ldots\ldots\ldots\ldots\ldots\ldots\ldots\ldots \quad (31)$$

Comparing the diagonal elements of the covariance matrix at the MAP with the diagonal elements of the prior covariance matrix will give an indication of the change in uncertainties of G, J, and W_i after applying material balance analysis.

Numerical Method

In this method, we calculate the expected value of joint distributions of two or more random variables. By calculating the covariance of the posterior, we can quantify the uncertainties of G, J, and W_i from the posterior distribution. The covariance matrix for the posterior distribution is given by:

$$C_x = \begin{bmatrix} \mathrm{cov}(G,G) & \mathrm{cov}(G,J) & \mathrm{cov}(G,W_i) \\ \mathrm{cov}(J,G) & \mathrm{cov}(J,J) & \mathrm{cov}(J,W_i) \\ \mathrm{cov}(W_i,G) & \mathrm{cov}(W_i,J_i) & \mathrm{cov}(W_i,W_i) \end{bmatrix}, \quad \ldots\ldots\ldots\ldots\ldots\ldots\ldots \quad (32)$$

where cov(G,G) can be calculated using the expectation rules for the joint probability functions follows:

$$\mathrm{cov}(G,G) = E(G^2) - E(G)\cdot E(G), \quad \ldots\ldots\ldots\ldots\ldots\ldots\ldots\ldots\ldots\ldots\ldots\ldots\ldots \quad (33)$$

$$E(G^2) = \sum_G \sum_J \sum_{W_i} G^2 \cdot \sigma(m|d_{\mathrm{obs}}), \quad \ldots\ldots\ldots\ldots\ldots\ldots\ldots\ldots\ldots\ldots\ldots\ldots\ldots \quad (34)$$

$$E(G)=\sum_{G}\sum_{J}\sum_{W_i} G\cdot\sigma(m|d_{\text{obs}}). \quad\ldots\ldots\ldots\ldots\ldots\ldots\ldots\ldots\ldots\ldots\ldots\ldots\ldots\ldots \quad (35)$$

Similarly,

$$\text{cov}(J,J)=E(J^2)-E(J)\cdot E(J), \quad\ldots\ldots\ldots\ldots\ldots\ldots\ldots\ldots\ldots\ldots\ldots\ldots \quad (36)$$

$$\text{cov}(W_i,W_i)=E(W_i^{\;2})-E(W_i)\cdot E(W_i), \quad\ldots\ldots\ldots\ldots\ldots\ldots\ldots\ldots\ldots\ldots\ldots \quad (37)$$

$$\text{cov}(G,J)=E(G\cdot J)-E(G)\cdot E(J), \quad\ldots\ldots\ldots\ldots\ldots\ldots\ldots\ldots\ldots\ldots\ldots\ldots \quad (38)$$

$$\text{cov}(G,W_i)=E(G\cdot W_i)-E(G)\cdot E(W_i), \quad\ldots\ldots\ldots\ldots\ldots\ldots\ldots\ldots\ldots\ldots\ldots \quad (39)$$

$$\text{cov}(J,W_i)=E(J\cdot W_i)-E(J)\cdot E(W_i), \quad\ldots\ldots\ldots\ldots\ldots\ldots\ldots\ldots\ldots\ldots\ldots \quad (40)$$

where

$$E(J^2)=\sum_{G}\sum_{J}\sum_{W_i} J^2\cdot\sigma(m|d_{\text{obs}}), \quad\ldots\ldots\ldots\ldots\ldots\ldots\ldots\ldots\ldots\ldots\ldots\ldots\ldots \quad (41)$$

$$E(J)=\sum_{G}\sum_{J}\sum_{W_i} J\cdot\sigma(m|d_{\text{obs}}), \quad\ldots\ldots\ldots\ldots\ldots\ldots\ldots\ldots\ldots\ldots\ldots\ldots\ldots\ldots \quad (42)$$

$$E(W_i^{\;2})=\sum_{G}\sum_{J}\sum_{W_i} W_i^{\;2}\cdot\sigma(m|d_{\text{obs}}), \quad\ldots\ldots\ldots\ldots\ldots\ldots\ldots\ldots\ldots\ldots\ldots\ldots \quad (43)$$

$$E(W_i)=\sum_{G}\sum_{J}\sum_{W_i} W_i\cdot\sigma(m|d_{\text{obs}}), \quad\ldots\ldots\ldots\ldots\ldots\ldots\ldots\ldots\ldots\ldots\ldots\ldots\ldots \quad (44)$$

$$E(G\cdot J)=\sum_{G}\sum_{J}\sum_{W_i} G\cdot J\cdot\sigma(m|d_{\text{obs}}), \quad\ldots\ldots\ldots\ldots\ldots\ldots\ldots\ldots\ldots\ldots\ldots \quad (45)$$

$$E(G\cdot W_i)=\sum_{G}\sum_{J}\sum_{W_i} G\cdot W_i\cdot\sigma(m|d_{\text{obs}}), \quad\ldots\ldots\ldots\ldots\ldots\ldots\ldots\ldots\ldots\ldots \quad (46)$$

$$E(J\cdot W_i)=\sum_{G}\sum_{J}\sum_{W_i} J\cdot W_i\cdot\sigma(m|d_{\text{obs}}), \quad\ldots\ldots\ldots\ldots\ldots\ldots\ldots\ldots\ldots\ldots \quad (47)$$

CHAPTER IV
APPLICATIONS

The proposed methodology is applied in the gas-in-place (G) estimation of two cases: Lagan gas field case and a synthetic field case study reported in Dake, Chap. 6.[11] Both cases have water drive, with weak water drive for the Lagan gas field case and strong water drive for the synthetic case.

Lagan Gas Field

Table 1–Performance Data from BB Sand

Time (days)	Pressure (psia)	G_p (MMscf)	W_p (Bbl)	Z
	1335.35	0	0	0.765976
803	1287.6	1713.51	710	0.774323
1052	1294.6	2435.45	1040	0.773094
1109	1200.6	2822.87	1180	0.789708
1392	1216.92	4327.34	1840	0.786808
1522	1180.6	5036.65	2170	0.79327
1778	1170.6	5734.07	2480	0.795053
1822	1168.6	5756.75	2500	0.79541
2087	1151.6	6966.77	3030	0.798447
2519	1090.6	8174.12	3950	0.809374
2920	997.6	9604.47	9220	0.826093
5448	978.6	17742.43	16790	0.829512
5859	942.27	18920.56	17210	0.836049

Lagan gas field was discovered in 1941, but the development of this field was started after 1986. This field has 15 different sands, but only six sands are producing - P sand, AA sand, A sand, BB sand, B sand, and D sand. There are 5 active producing wells. Thus, the production of some sands is commingled. All of these sands are known to have weak water drive. From the six sands that are producing, I applied the proposed methodology to the BB sand, since it is not being commingled with other sands.

Performance data and PVT data from the BB sand are presented in Table 1. The initial formation volume factor, B_{gi}, is 1.9178 bbl/scf.

Fig. 4 shows the conventional p/Z plot for this sand. Weak water drive is indicated in this plot, since the line deviates later in the life of the sand.

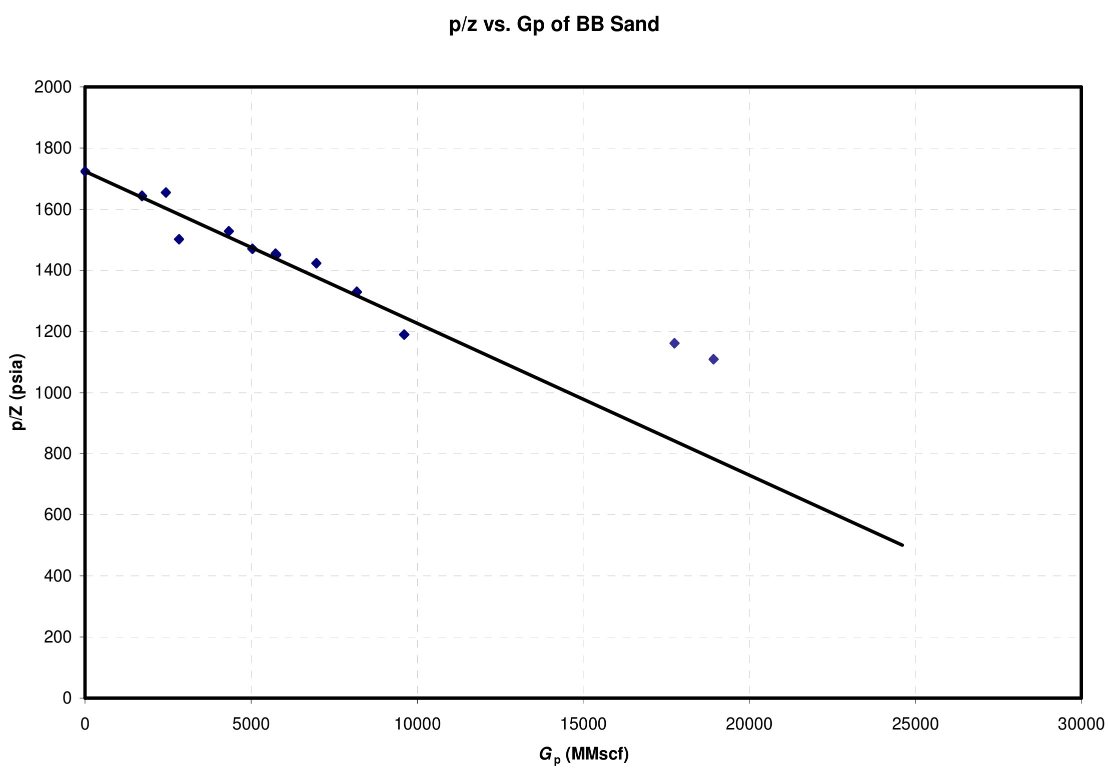

Fig. 4-p/Z versus Gp for BB sand.

Using volumetric calculations and Monte Carlo simulation, I calculated mean and standard deviation of G, J, and W_i (Table 2). I used 100 evenly-spaced values for each of G, J, and W_i to calculate the prior distributions. A total of 100 x 100 x 100 = 1,000,000 combinations were required to obtain the prior distributions.

Table 2–Mean and Standard Deviation of G, J, and W_i from Volumetric Analysis, BB Sand

Parameter	Mean	Standard Deviation
G (Mscf)	31,920,343.89	6,101,753.79
J (STB/D-psi)	264.33	194.986
W_i (RB)	167,357.656	54,146.76

Since this work involves three unknown parameters, to visualize each probability distribution, I use three different plots:

1. Plot of probability distribution of G versus J for particular value of W_i.
2. Plot of probability distribution of G versus W_i for particular value of J.
3. Plot of probability distribution of W_i versus J for particular value of G.

The *a priori* distribution of BB sand for the 50% of maximum value for each parameter is presented in Figs. 5-7.

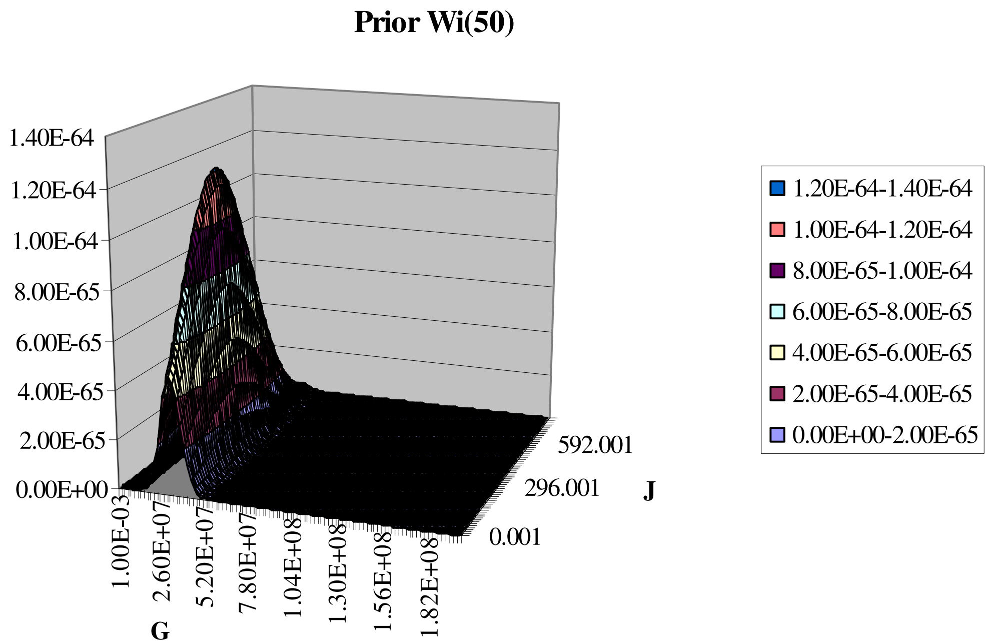

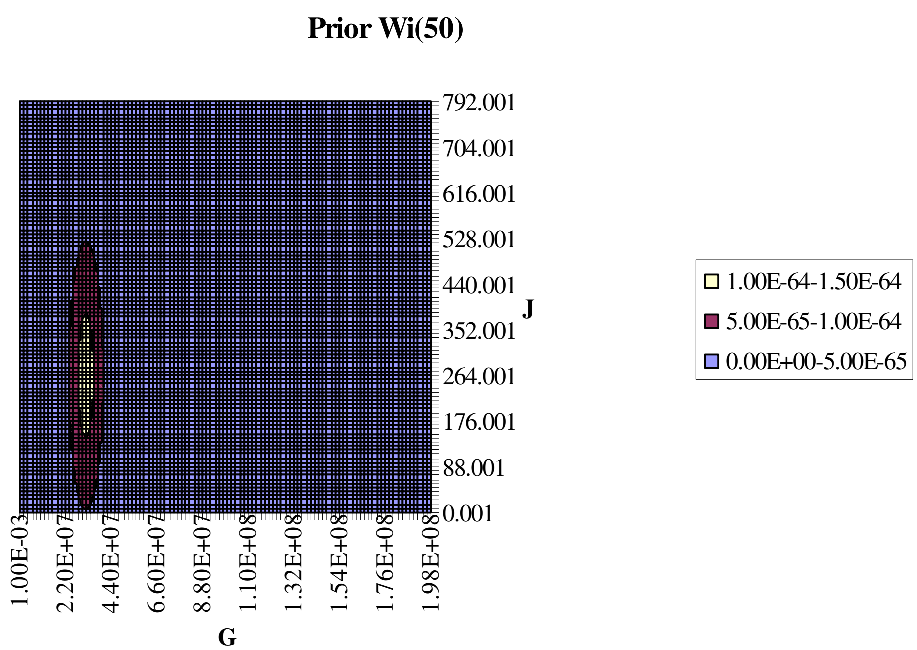

Fig. 5-Prior distribution of *G* versus *J* for $W_i = 0.5\ W_{i\,\max}$, BB sand.

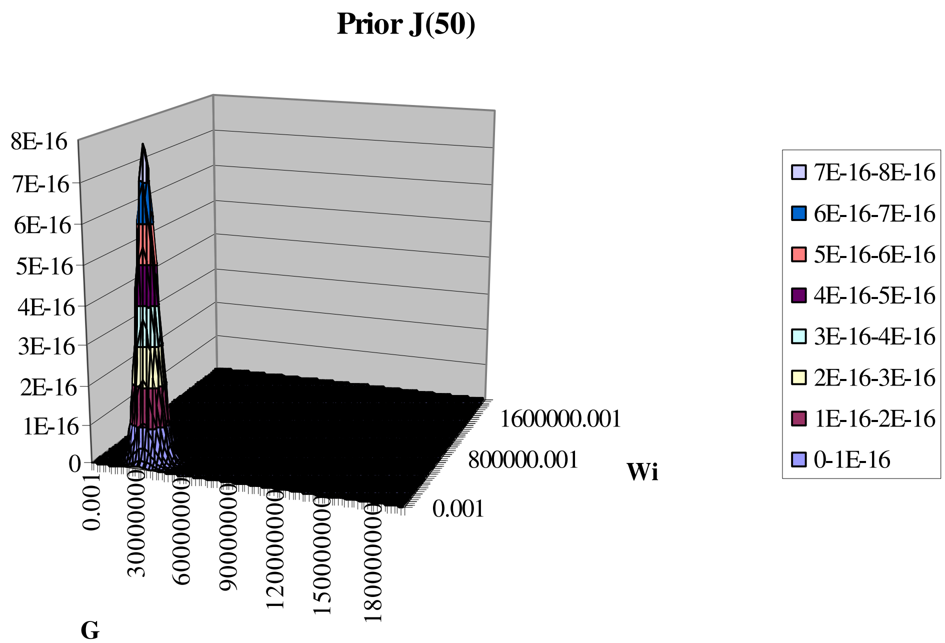

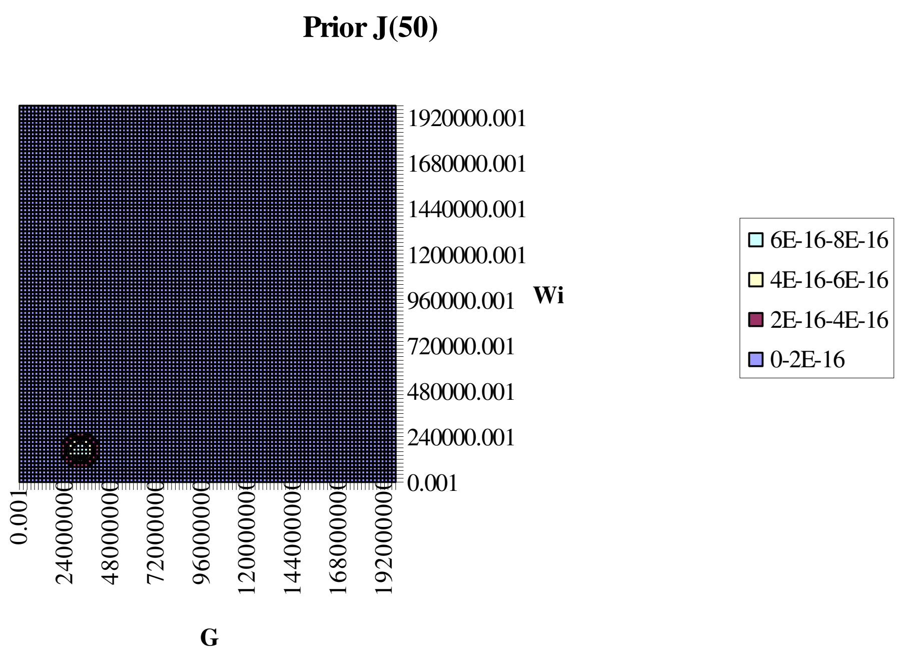

Fig. 6-Prior distribution of *G* versus W_i for J = 0.5 J_{max}, BB sand.

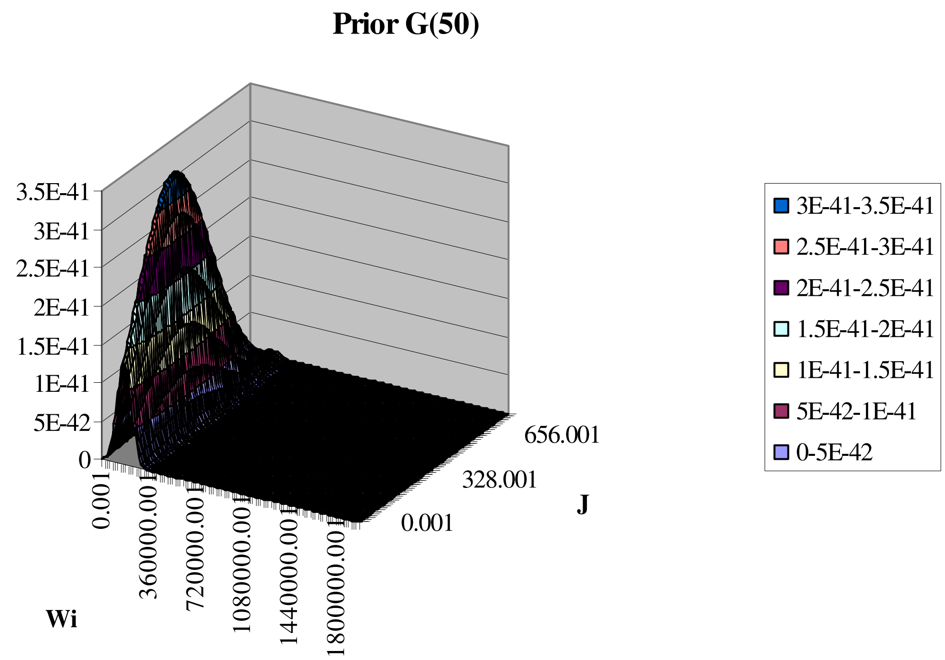

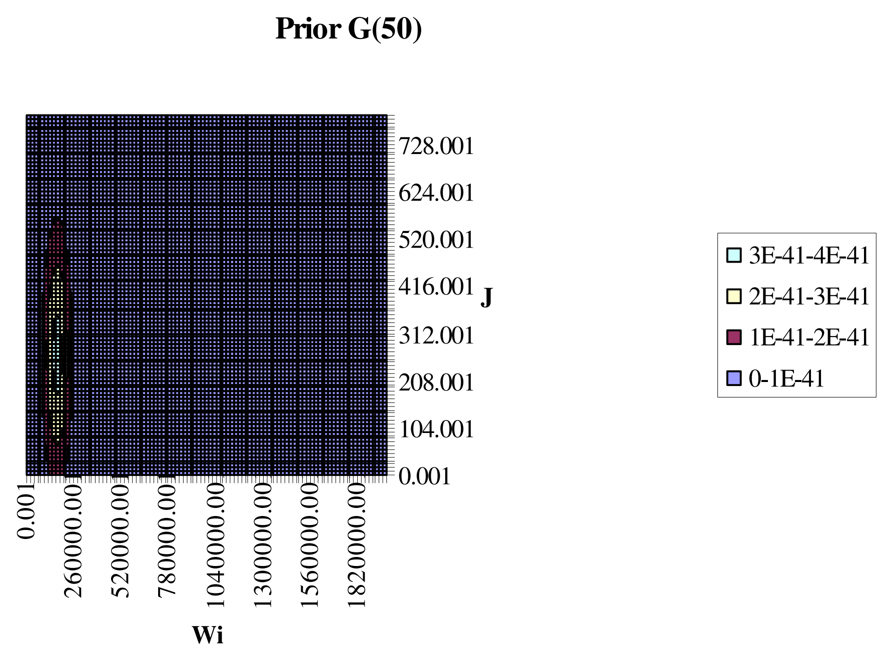

Fig. 7-Prior distribution of W_i versus J for G = 0.5 G_{max}, BB sand.

For building the likelihood distributions, I only use six data points from Table 1 in order to obtain faster running times. The data used to build likelihood distribution are presented in Table 3. A pressure standard deviation of 100 psia has been assumed in this case, representing the error due to short shut-in times and/or gauge error.

Table 3–Observed Data Used in Analysis, BB sand

Days	Pressure (psia)	G_p	W_p (RB)	Z
1052	1294.6	2,435,450	1040	0.7731
1552	1180.6	5,036,650	2170	0.7932
1822	1168.6	5,756,750	2500	0.7954
2519	1090.6	8,174,120	3950	0.8094
5448	978.6	17,742,430	5448	0.8295
5859	942.27	18,920,560	5859	0.836

The likelihood distribution for the 50% of maximum value for each parameter is presented in Figs. 8-10.

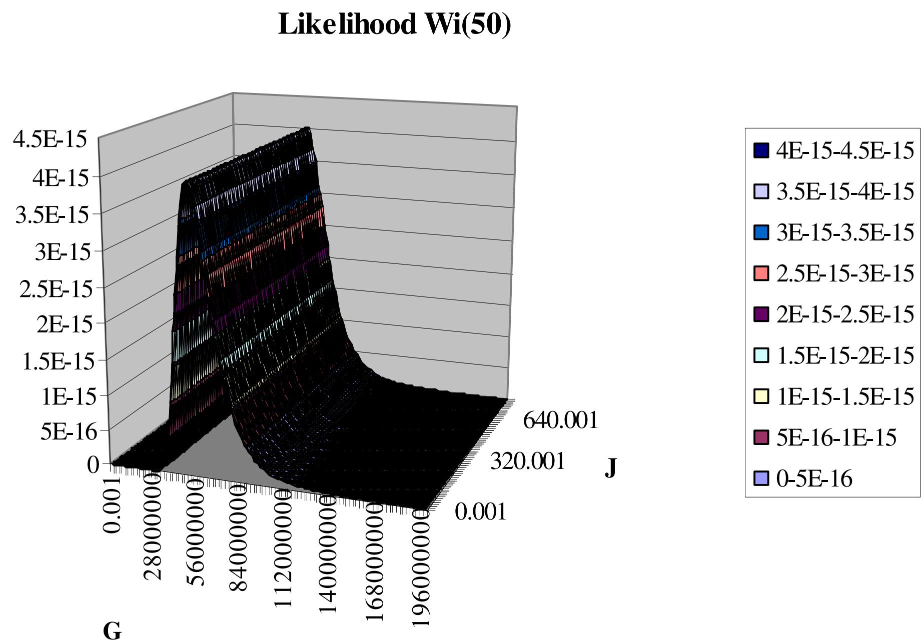

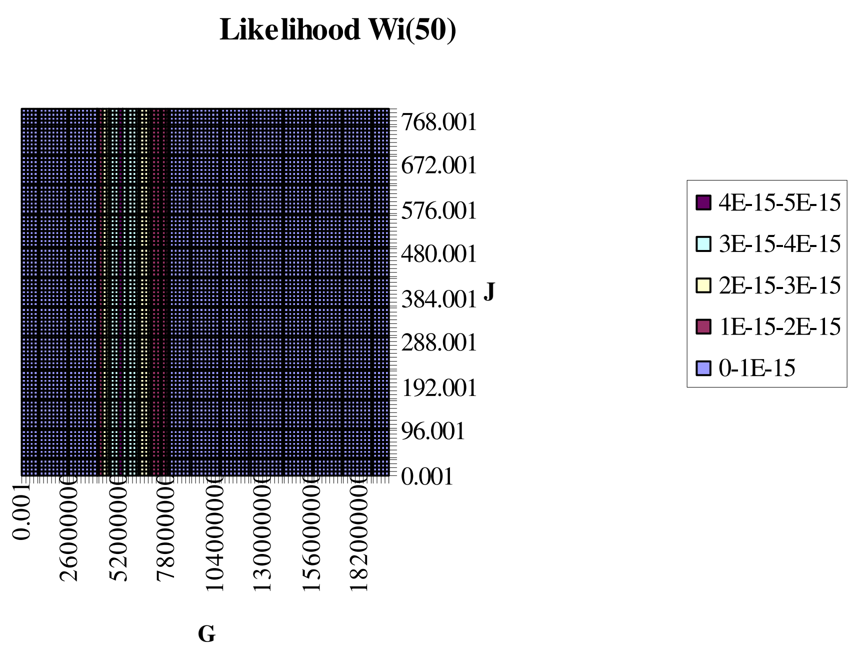

Fig. 8-Likelihood distribution of *G* versus *J* for $W_i = 0.5\ W_{i\,max}$, BB sand.

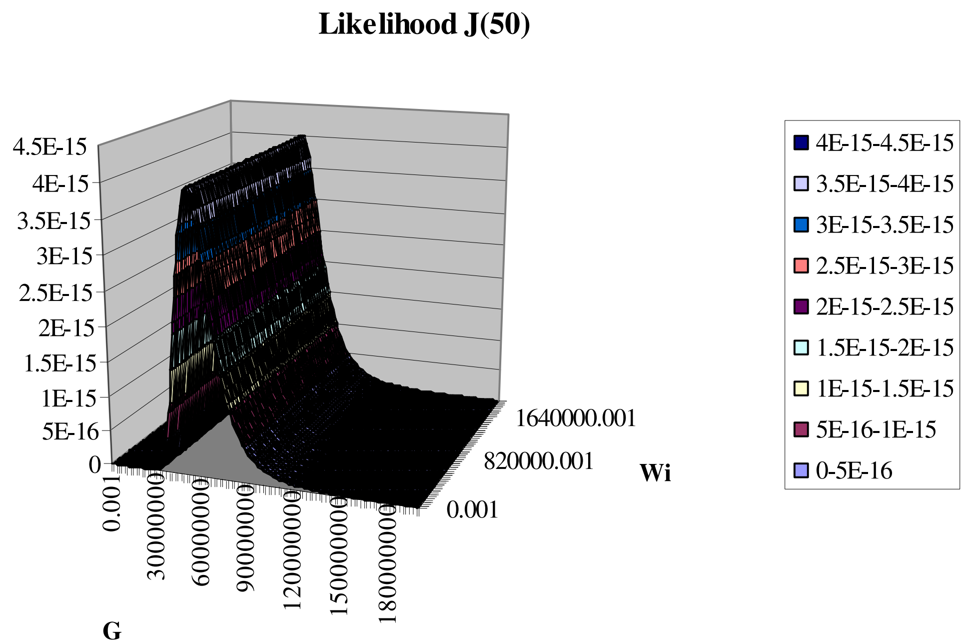

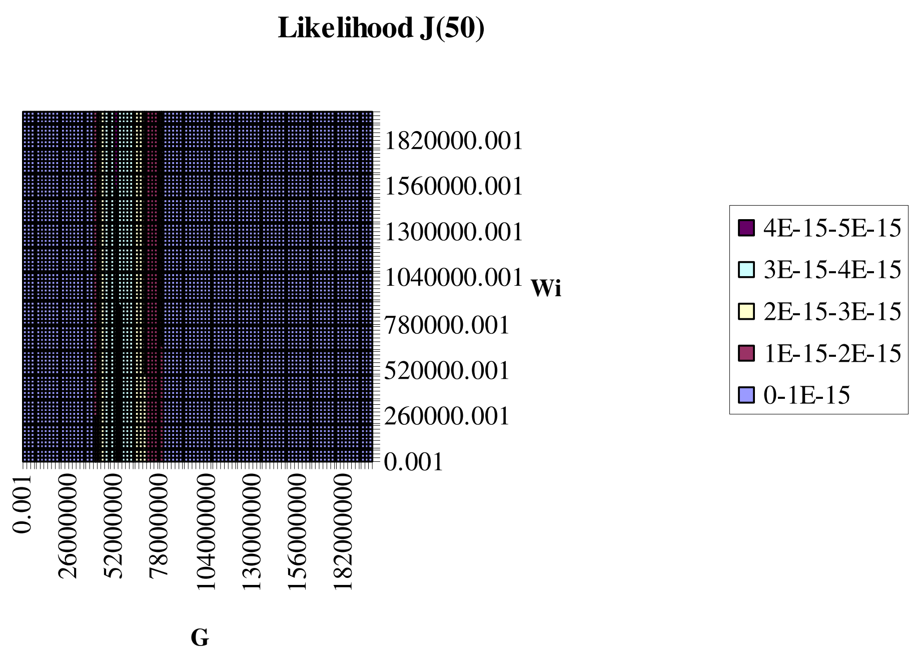

Fig. 9-Likelihood distribution of G versus W_i for J = 0.5 J_{max}, BB sand.

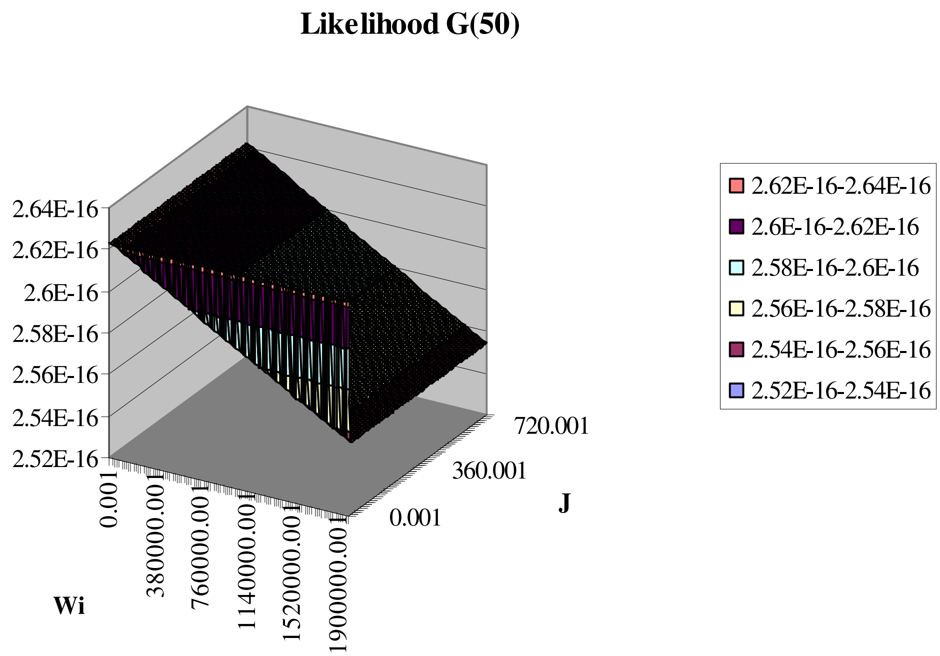

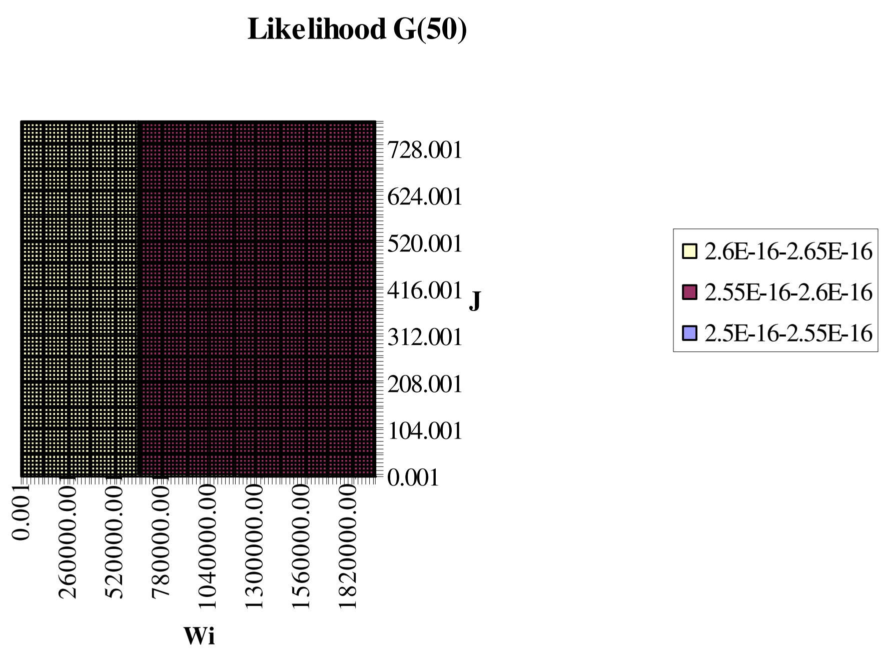

Fig. 10-Likelihood distribution of W_i versus J for $G = 0.5\ G_{max}$, BB sand.

In Fig. 8, although probability increases slightly with increasing J, the likelihood distribution runs parallel to the J axis and is not bounded within the range of J displayed. In other words, many values of J yield similar matches to the pressure and production data. Similarly in Fig. 9, the likelihood distribution also runs parallel to the W_i axis, indicating a non-unique value for aquifer volume. Fig. 10 echoes these results, showing that the probability distribution as a function of W_i and J for constant G is essentially a plane over wide ranges of both W_i and J. These results indicate that the material balance analysis does not uniquely characterize properties of the aquifer and, most likely, defines a minimum aquifer size and strength.

In both Figs. 8 and 9, significant probability is restricted to a specific range for G. This indicates that, unlike aquifer size and strength, the original gas is place is defined to be within a specific and reasonable range of values. The range in G on Figs. 8 and 9 defines the uncertainty in original gas in place from the material balance analysis.

The posterior distribution is the product of the prior and likelihood distributions. The posterior probability for this case is shown in Figs. 11-13.

As shown in Fig. 13, the posterior distribution of W_i versus J for $G = 0.5\ G_{max}$ for the BB sand has a very similar shape as its prior probability distribution (Fig. 7). This indicates that the likelihood distribution for W_i and J is so broad (i.e., the material balance analysis is so non-unique for W_i and J) that the shape of the probability distribution from the prior is changed little when multiplied by the likelihood distribution. These results also indicate that uncertainty in aquifer size and strength were underestimated severely in the prior, volumetric analysis.

Uncertainties in the prior volumetric analysis should be considered carefully, particularly for aquifer parameters. Usually, there will be very large uncertainties in aquifer parameters from volumetric analysis. If the uncertainties in aquifer parameters are underestimated in the prior volumetric analysis, this may result in a corresponding underestimation of uncertainty in the posterior distribution if the material balance solution is non-unique (i.e., has large uncertainty) for aquifer parameters.

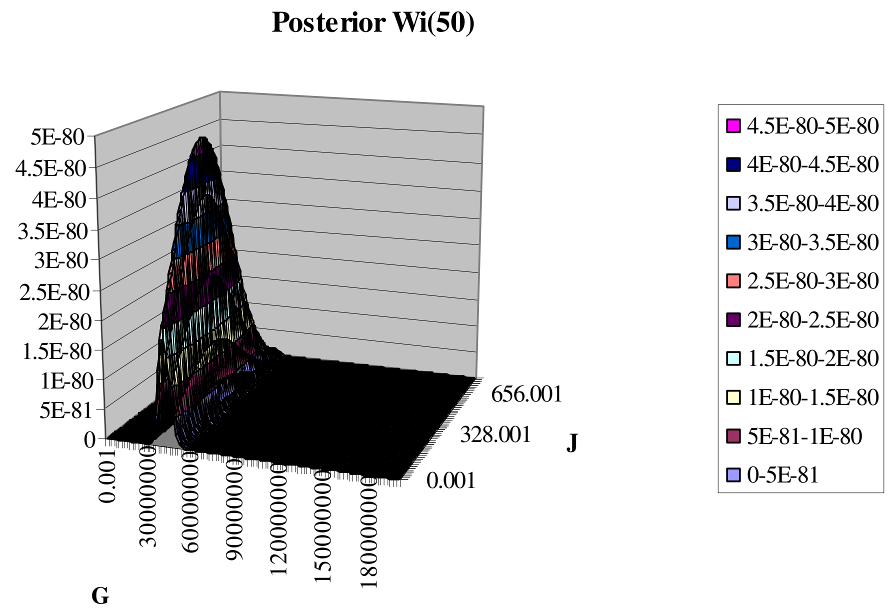

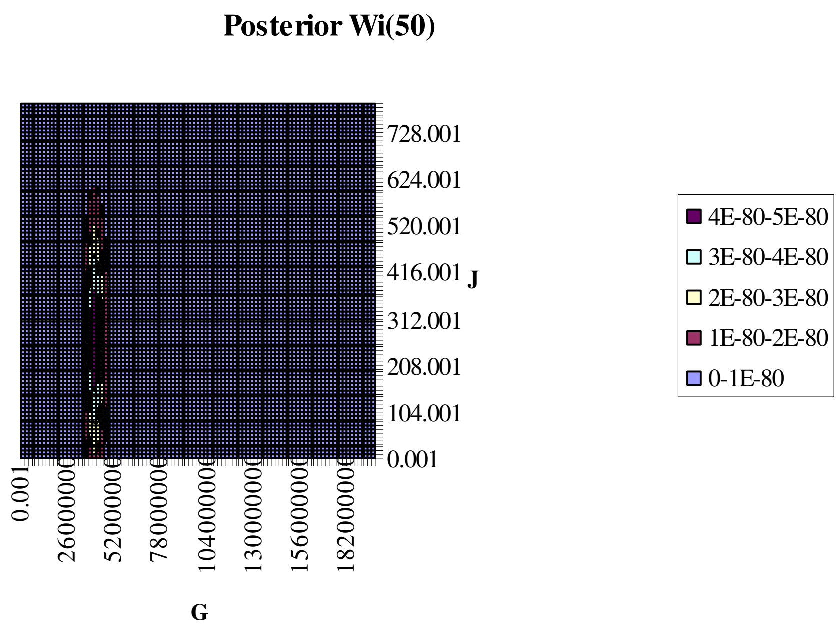

Fig. 11–Posterior distribution of G versus J for $W_i = 0.5\ W_{i\ max}$, BB sand.

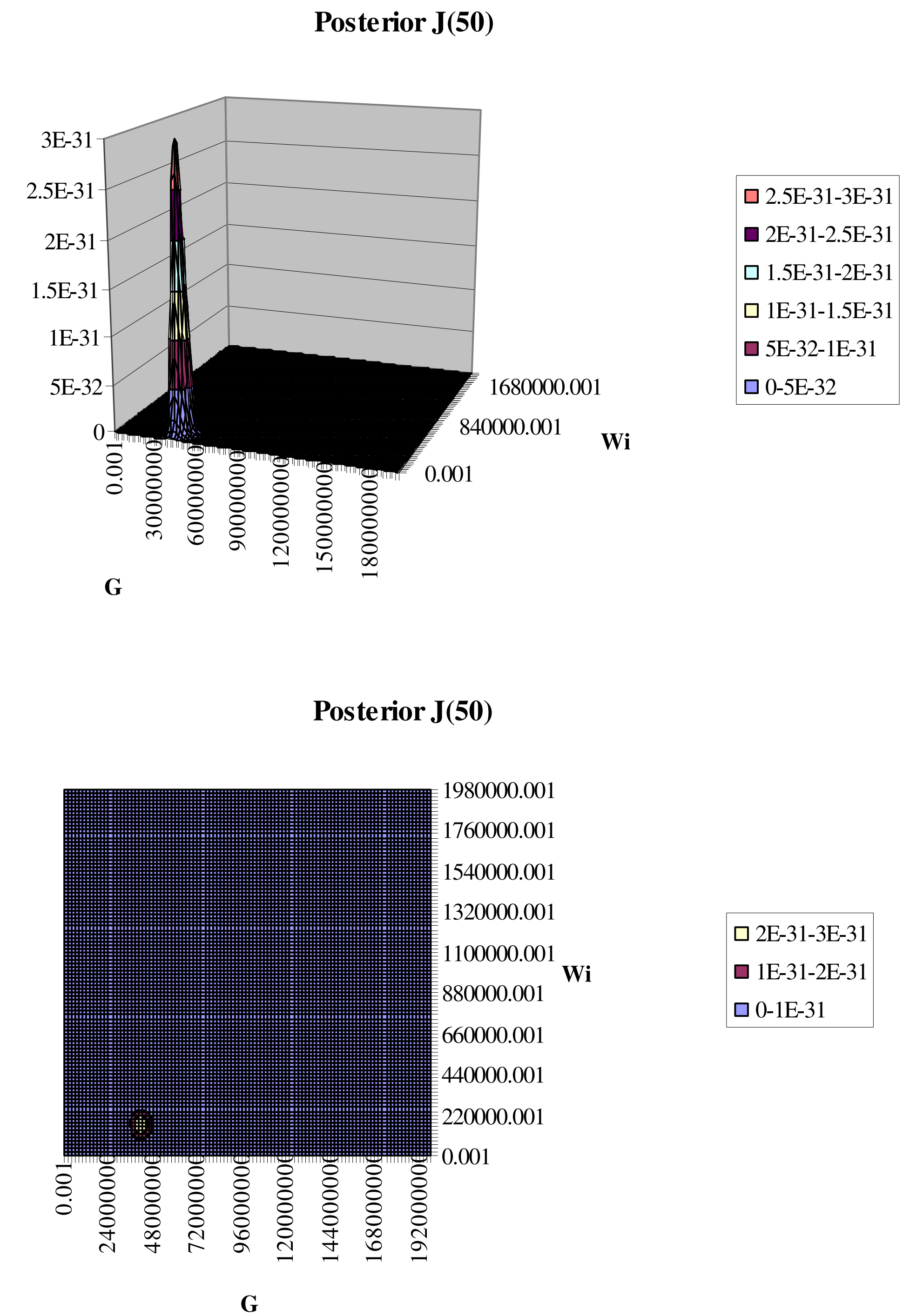

Fig. 12-Posterior distribution of G versus W_i for J = 0.5 J_{max}, BB sand.

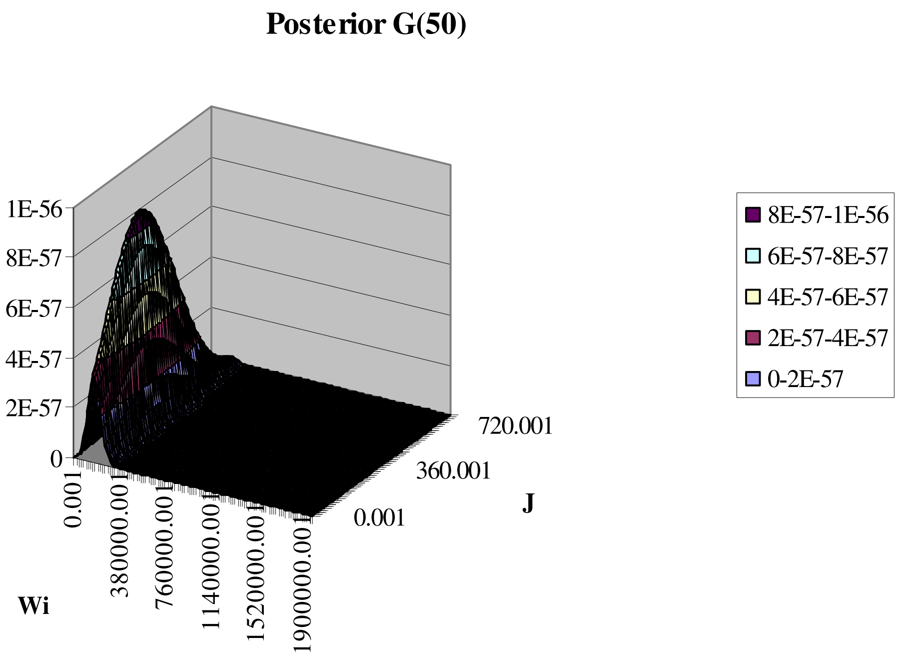

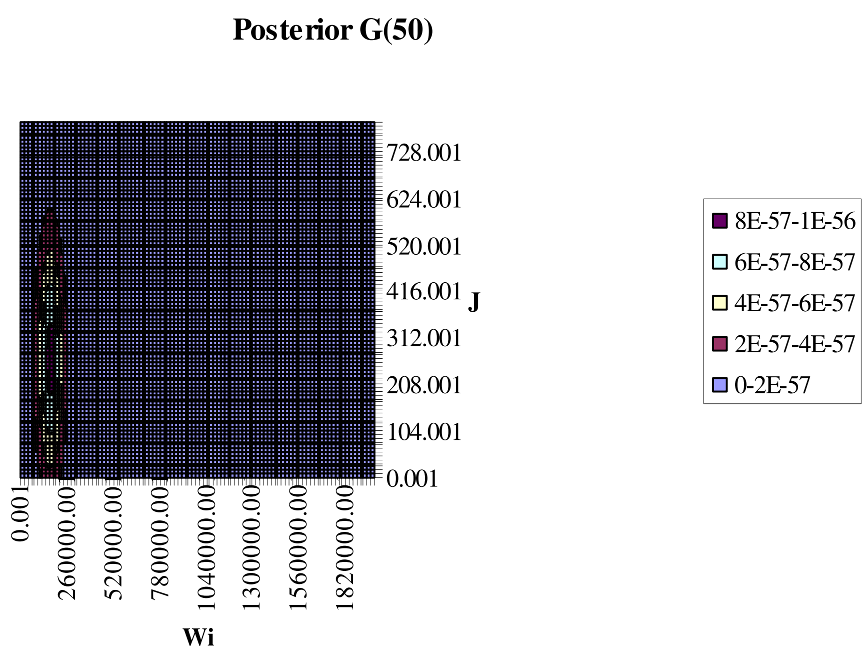

Fig. 13-The posterior distribution of W_i versus J for G = 0.5 G_{max}, BB sand.

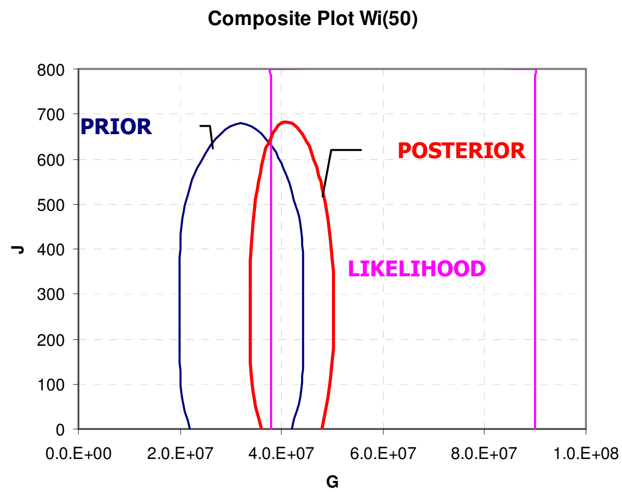

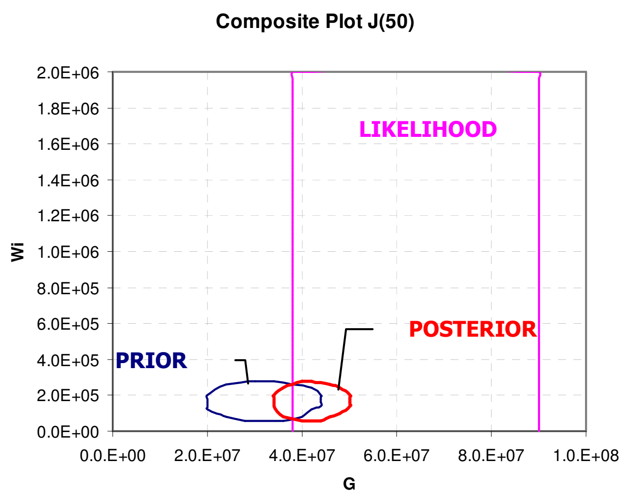

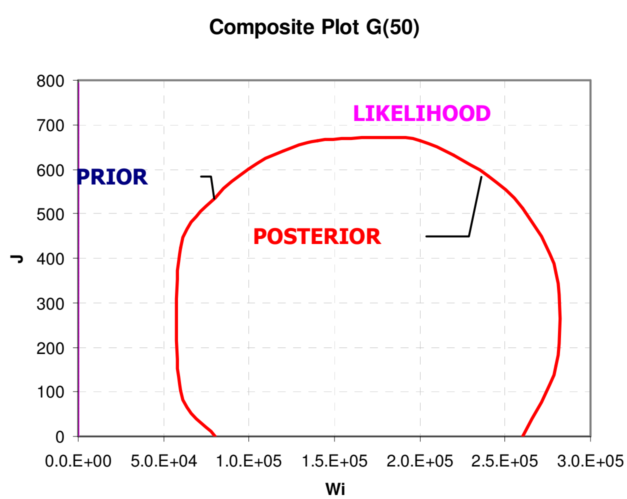

Fig. 14-Composite plot for 50% of the maximum values of each parameter, BB Sand.

The relationships between the prior, likelihood and posterior distributions for the 50% of maximum value for each parameter are better illustrated in Fig. 14.

The MAP estimate is G = 42 Bscf, J = 264 STB/D-psi, and W_i = 160,000 RB. The diagonal elements of the covariance matrix give us the variances of G, J, and W_i. The posterior variances of G, J, and W_i using the numerical method are:

$$\sigma_G^2 = 1.604 \times 10^{13} \qquad \sigma_J^2 = 27{,}708.75 \qquad \sigma_{W_i}^2 = 2{,}914{,}833{,}162$$

Finally, the prior and posterior standard deviations are compared in the following table:

Table 4–Standard Deviations of *G*, *J*, and W_i from Prior and Posterior, BB Sand

	Prior	Posterior (numerical)
σ_G	6,101,753.79	4,002,694.39
σ_J	194.99	164.56
σ_{Wi}	54,146.76	53,989.19

Table 4 shows that the uncertainty in G has been reduced by combining volumetric and material balance analyses, although G still has significant uncertainty. Table 4 also shows that the prior uncertainties in J and W_i are not significantly reduced by integrating the volumetric and material balance analysis. The results for J and W_i are misleading, however, because the unrealistically small uncertainty in the prior carries over to the posterior, even though the material balance solution indicates that there is considerable uncertainty in aquifer properties. The method should be used with care, particularly in the evaluation of prior uncertainties in aquifer properties.

A Synthetic Case by Dake

Problem statement: A gas field and its radial aquifer are described and its performance is then predicted exactly for a prescribed offtake result. The system is described below:

GIIP	= 823 Bscf	k	= 120 mD
p_i	= 3200 psia	c_w	$= 3 \times 10^{-6}$ psi^{-1}
h	= 120 ft	c_f	$= 8 \times 10^{-6}$ /psi^{-1}
ϕ	= 0.22	f	= 1
S_{wc}	= 0.23 PV	r_r	= 8350 ft
S_{gr}	= 0.30 PV	r_{eD}	= 10
γ_g	= 0.67	T	= 210 °F
μ_w	= 0.4 cp	B_w	= 1.0 rb/stb

Table 5–PVT Data, Synthetic Gas Field Case

p (psia)	Z	p/Z (psia)	Bg (rcf/scf)
3200	0.9315	3503.0	5.408×10^{-3}
3000	0.9070	3307.6	5.727×10^{-3}
2750	0.9008	3052.8	6.205×10^{-3}
2500	0.8968	2787.7	6.795×10^{-3}
2250	0.8955	2512.6	7.539×10^{-3}
2000	0.8968	2230.2	8.494×10^{-3}
1750	0.9010	1942.3	9.753×10^{-3}
1500	0.9080	1652.0	11.466×10^{-3}
1250	0.9178	1362.0	13.908×10^{-3}
1000	0.9302	1075.0	17.621×10^{-3}
750	0.9449	793.7	23.866×10^{-3}
500	0.9616	520.0	36.428×10^{-3}

The gas PVT properties are listed in Table 5 and the gas offtake-rate schedule and pressure data are listed in Table 6.

Table 6–Field Performance Data, Synthetic Gas Field Case

Time (years)	p (psia)	Q (MMscf/d)	G_p (Bscf)
0	3200	0	0
0.25	3173	59.0	5.384
0.5	3156	59.0	10.768
0.75	3138	59.0	16.152
1	3110	59.0	21.535
2	2990	115.5	63.693
3	2760	203.0	137.788
4	2540	225.0	219.913
5	2360	217.0	299.118
6	2170	225.0	381.243
7	2020	195.0	452.418
8	1875	180.0	518.118
9	1730	175.0	581.993
10	1590	160.0	640.393

This problem did not specify the uncertainties in the volumetric estimates of G, J and W_i, so I created these myself. I assumed a uniform distribution for r_{eD} and normal distributions for the other parameters listed above. Using Monte Carlo analysis and the @Risk software application, I quantified the means and standard deviations of G, J and W_i.

Fig. 15 shows us the conventional p/z plot for this case. Based on the linearity of this plot, it appears that this reservoir does not have a water drive mechanism. However, extrapolation of the straight line yields a gas-in-place estimate of 1260 Bscf, which is 53% in excess of the reported volumetric estimate of 823 Bscf.

Alternatively, we can use the Havlena-Odeh plot of F / E_g versus G_p, as shown in Fig. 16. This plot indicates that the reservoir has a strong water drive.

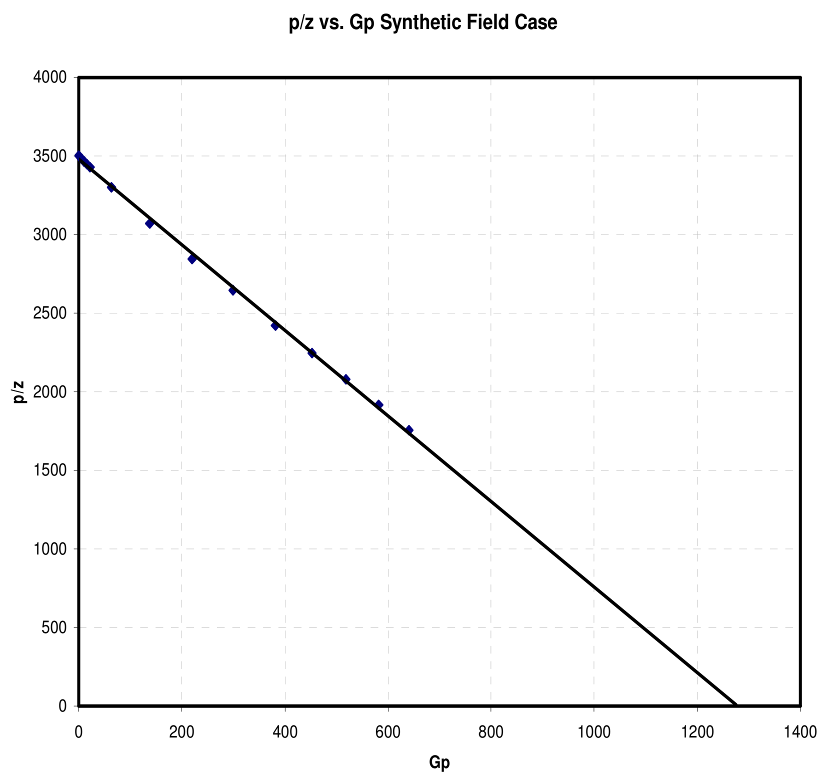

Fig. 15-p/Z plot of synthetic gas field case (data from Dake[11]).

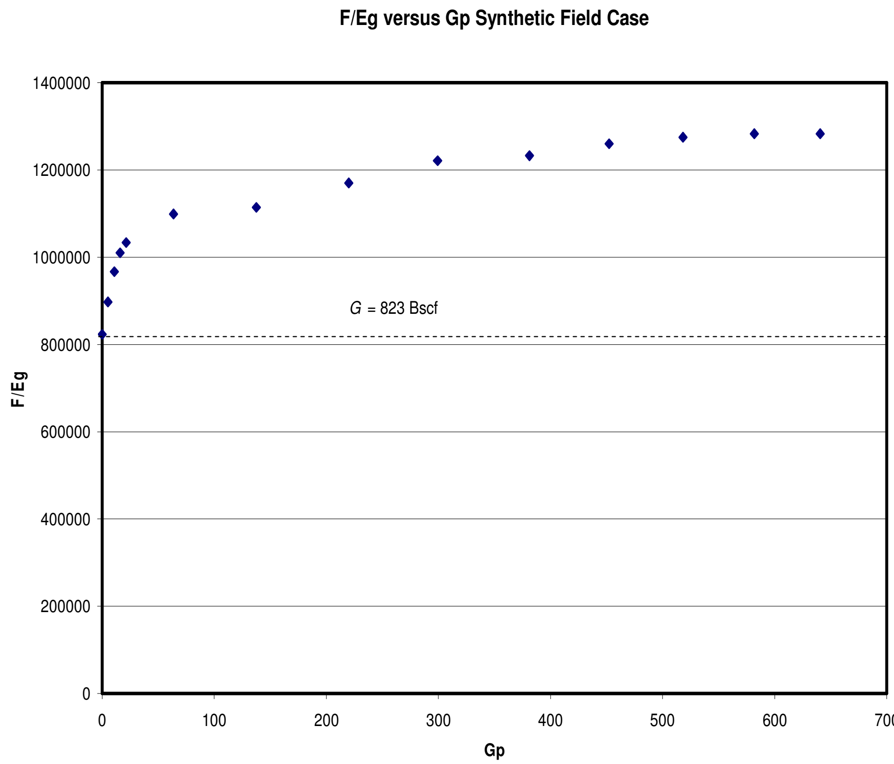

Fig. 16-F/E_g versus G_p for synthetic gas field case (data from Dake[11]).

This problem, as presented by Dake, did not specify the uncertainty in the pressure data. I will compare results of this case analyzed under two sets of conditions:

A. Without noise added to the pressure data, and

B. With noise added to the pressure data

A. Synthetic Field Case Without Noise Added to Pressure Data

Using volumetric calculations and Monte Carlo simulation, and assuming uncertainties for intermediate reservoir parameters, I obtained means and standard deviations for G, J, and W_i (Table 7).

Table 7–Means and Standard Deviations of *G*, *J*, and W_i from Volumetric Analysis, Synthetic Field A

Parameter	Mean	Standard Deviation
G (Mscf)	827,210,521.28	370,224,075.35
J	48.43	459.00
W_i (RB)	3.46×10^{14}	3.71×10^{14}

The multivariate prior distribution consists of a 100x100x100 mesh (1,000,000 total) of values for *G*, *J*, and W_i. As with the Lagan field case, I will use three different 2D plots to visualize the 3D probability distribution. The prior distribution for this synthetic field A case for every 50% of the maximum values of each parameter is presented in Figs. 17-19.

Actually, the distributions of *G*, *J* and W_i, resulting from Monte Carlo simulation are not normal distributions. However, in my work I assume a multivariate normal distribution for the prior (Eq. 22). For future work, the combinations of *G*, *J* and W_i resulting directly from the Monte Carlo simulation should be used for the prior.

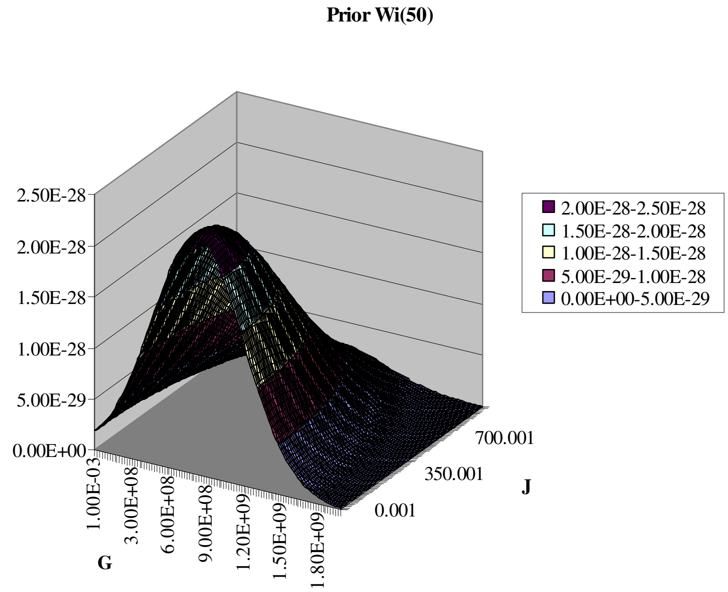

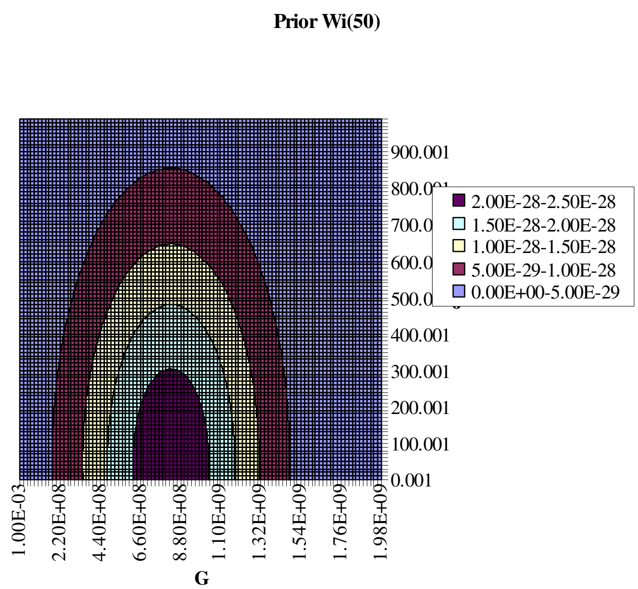

Fig. 17-Prior distribution of *G* versus *J* for $W_i = 0.5\ W_{i\ max}$, synthetic field A.

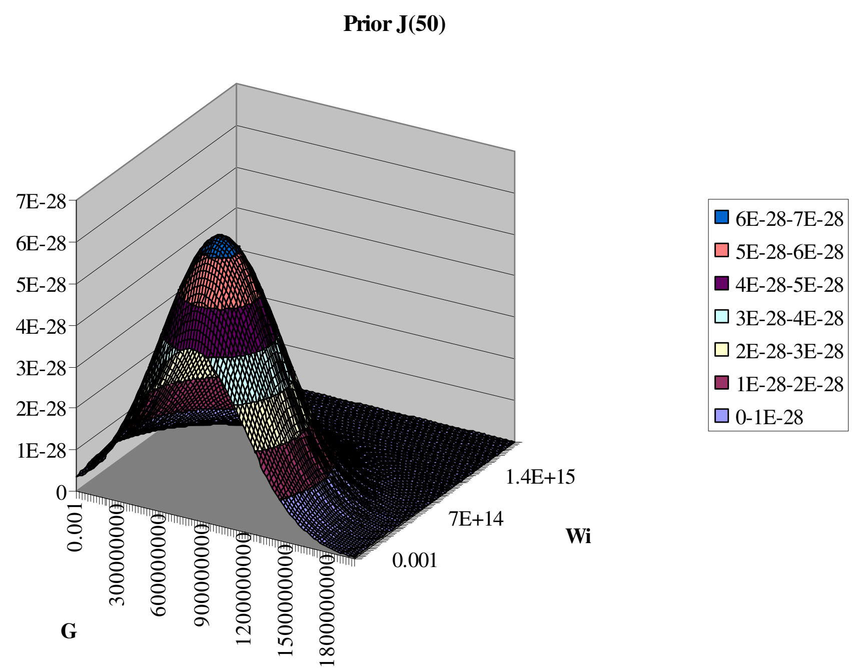

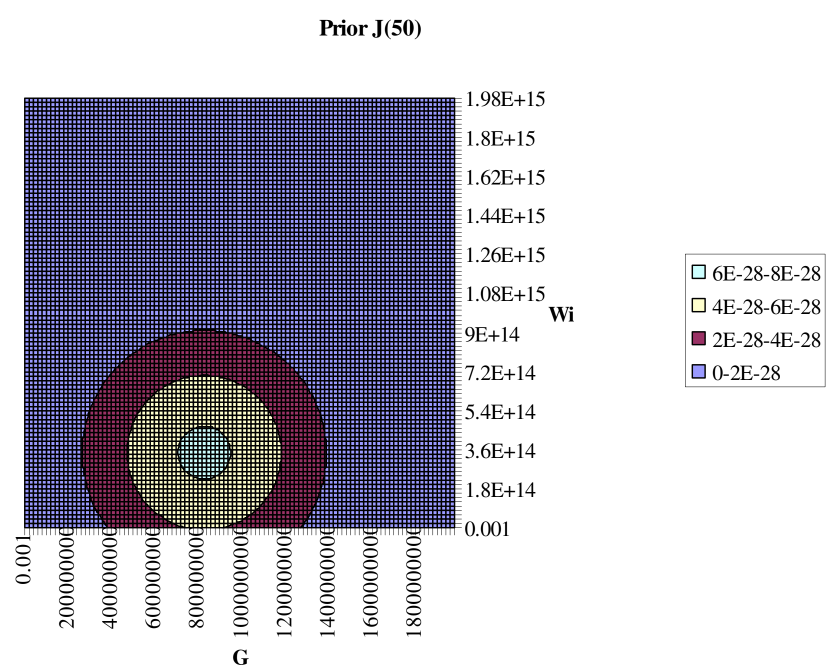

Fig. 18-Prior distribution of G versus W_i for $J = 0.5\ J_{max}$, synthetic field A.

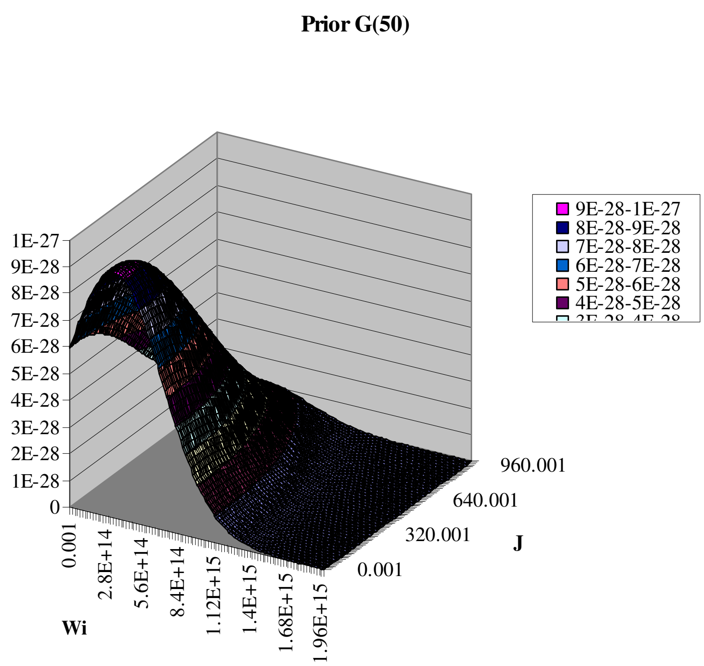

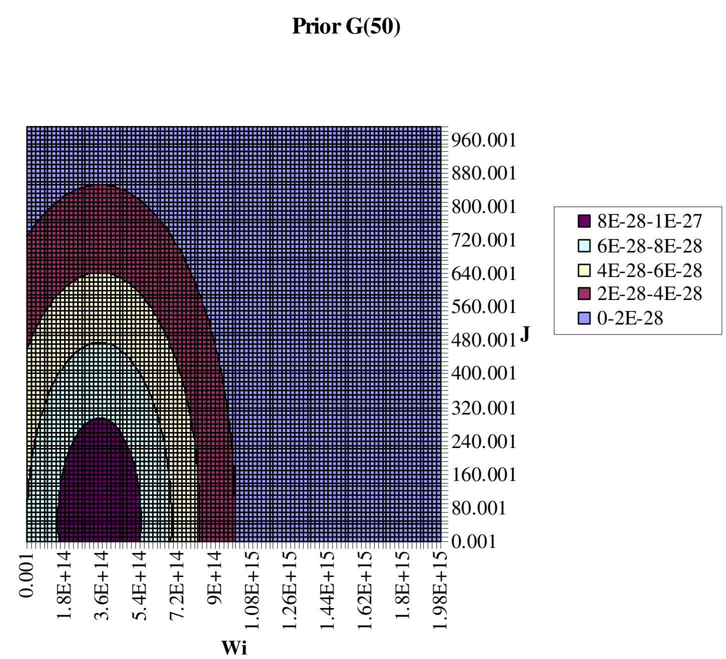

Fig. 19-Prior distribution of W_i versus J for G = 0.5 G_{max}, synthetic field A.

As in the Lagan field case, for building the likelihood distribution I only use six data points from Tables 5 and 6. This is done to obtain faster run times. The data used to build the likelihood distribution is presented in Table 8. Pressure standard deviation of 100 psia has been assumed in this case.

Table 8–Observed Data Used in Analysis, Synthetic Field A

Days	Pressure (psia)	G_p (Mscf)	W_p (RB)	Z
91.25	3173	5,384,000	0	0.911258
365	3110	21,535,000	0	0.906706
1095	2760	137,788,000	0	0.899023
1825	2360	299,118,000	0	0.89225
2555	2020	452,418,000	0	0.899777
3285	1730	581,883,000	0	0.903394

The likelihood distribution for synthetic field A for 50% of the maximum values of each parameter is presented in Figs. 20-22.

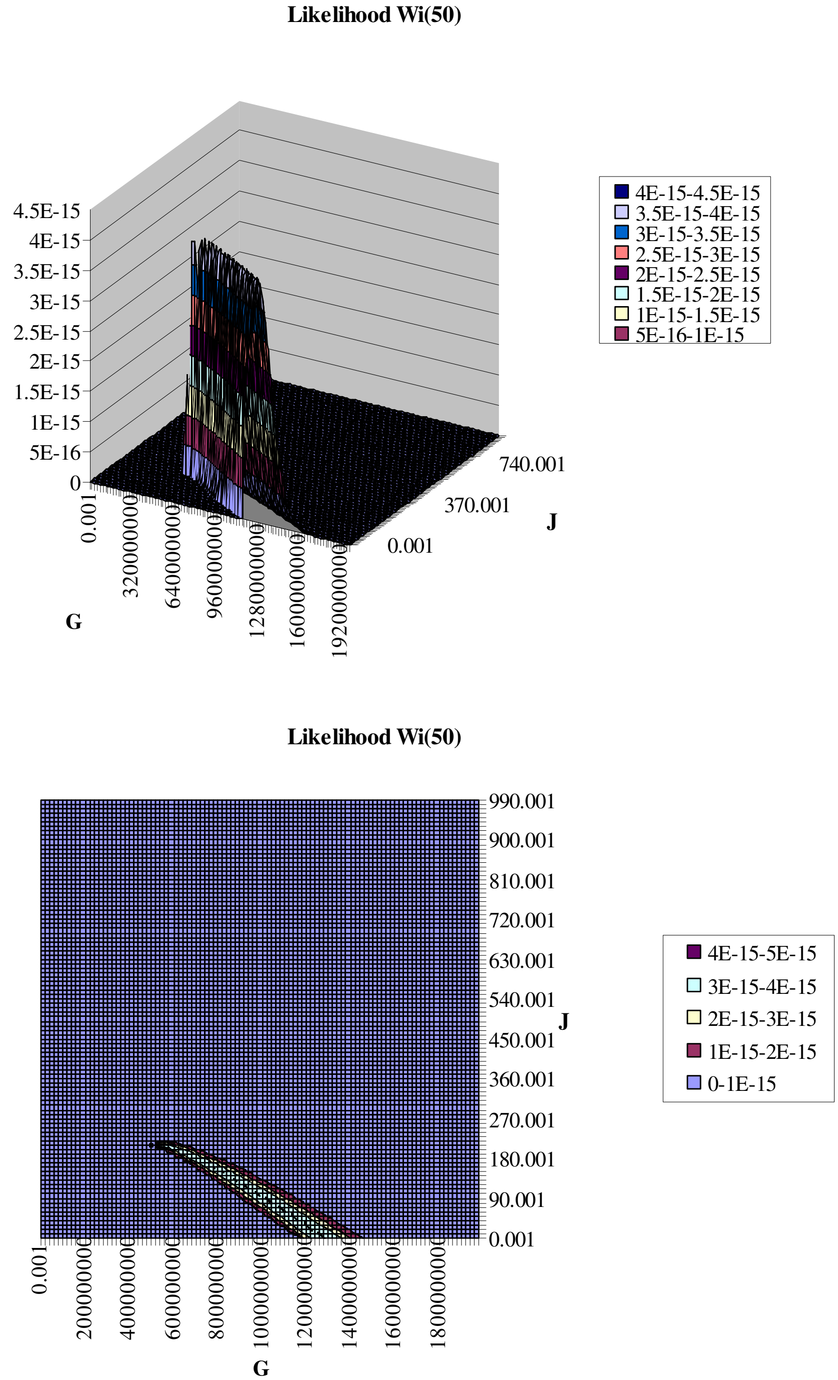

Fig. 20-Likelihood distribution of *G* versus *J* for W_i = 0.5 $W_{i\ max}$, synthetic field A.

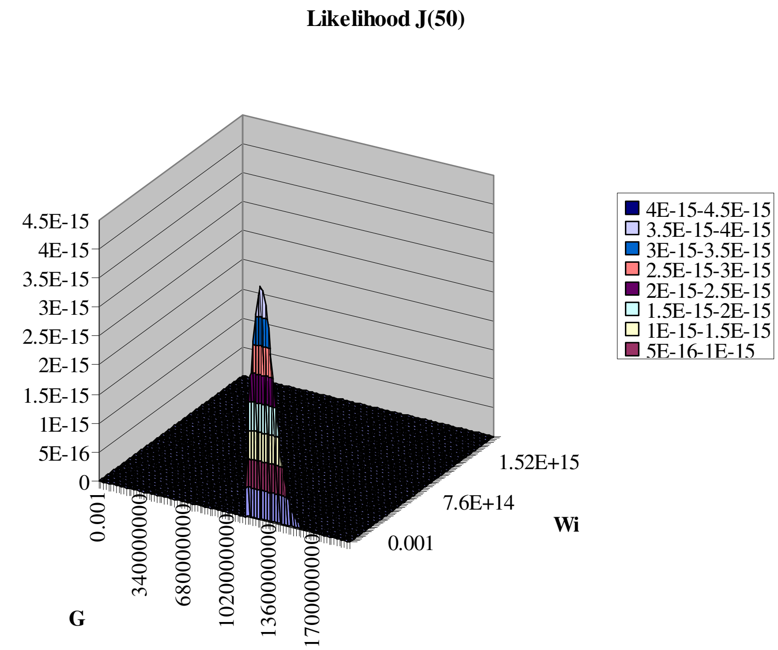

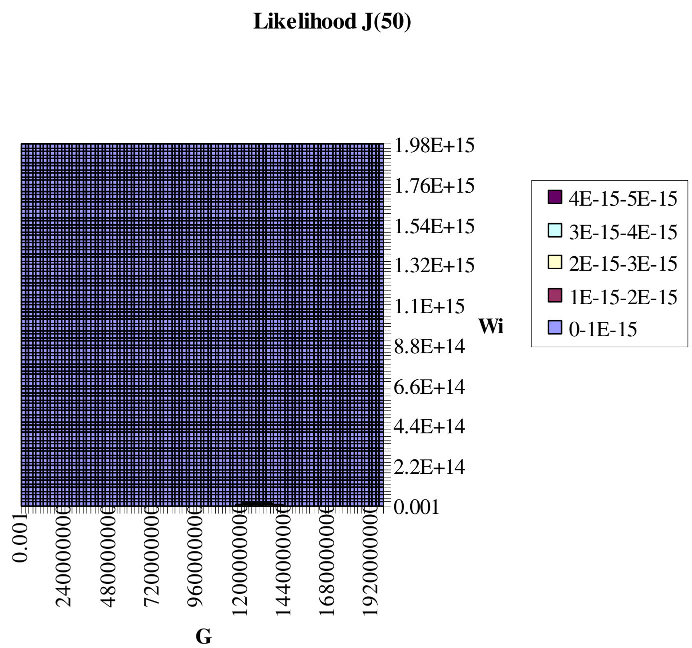

Fig. 21-Likelihood distribution of G versus W_{i} for J = 0.5 J_{max}, synthetic field A.

Likelihood G(50)

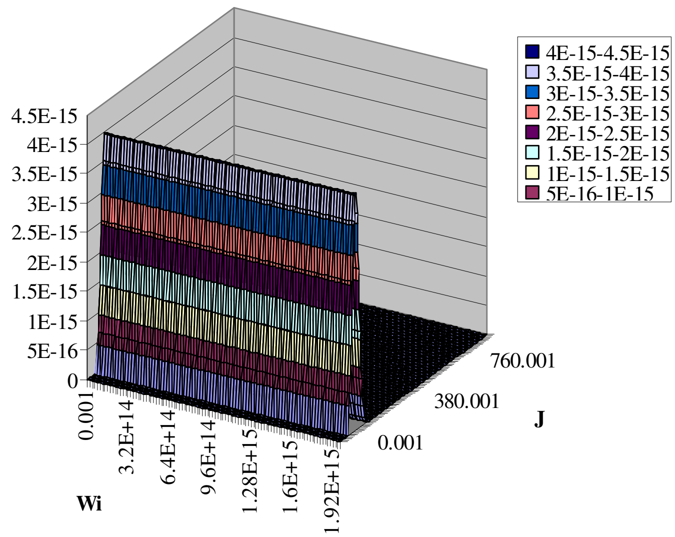

Likelihood G(50)

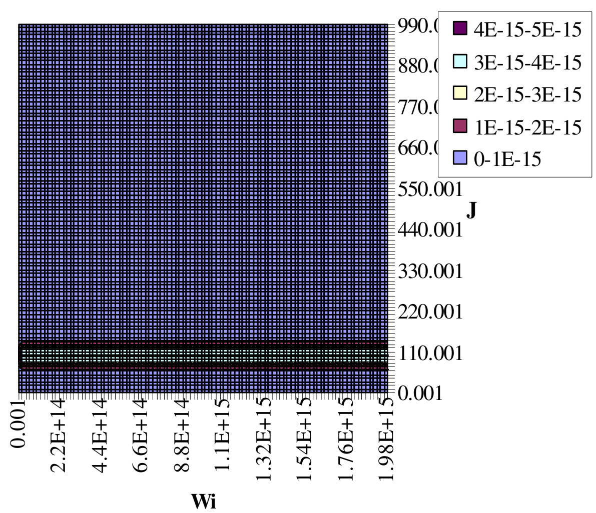

Fig. 22-Likelihood distribution of W_i versus J for $G = 0.5\ G_{max}$, synthetic field A.

From Fig. 20, we can see that, from material balance estimates for $W_i = 0.5\ W_{i\ max}$, many combinations of parameter G and J have significant probability. In Fig. 22, the likelihood distribution of W_i and J for $G = 0.5\ G_{max}$ runs parallel to the W_i axis over a significant range for W_i. This indicates that material balance analysis cannot uniquely determine the aquifer size in this case and, most likely, is indicating only a minimum aquifer size.

The most-likely (ML) parameter estimates for this case are G = 660 Bscf, J = 190 STB/D-psi, and $W_i = 1.98 \times 10^{15}$ RB. The estimate of G from the material balance solution is smaller than the volumetric solution, which may be another indicator of strong water drive. However, this is not conclusive evidence.

The ratio of cumulative water influx to gas in place after 10 years of production is:

$$\frac{W_e}{G} = \frac{441\times10^6\ \text{RB}\times5.615\,\text{rcf/RB}}{823\times10^9\ \text{scf}\times5.408\times10^{-3}\,\text{rcf/scf}} = 0.556 = \underline{\underline{55.6\%}}$$

This calculation also shows that this reservoir has a strong water influx, since 55.6% of reservoir pore volume has already filled with water from the aquifer after 10 years of production.

The posterior distributions are shown in Figs. 23-25. We can see from these figures that the extent of the posterior distribution is smaller than either the prior or likelihood distributions, indicating the reduced uncertainty in the combined volumetric and material balance solution. The relationships between the prior, likelihood and posterior distributions for 50%, 25% and 75% of the maximum values of each parameter are illustrated in Figs. 26, 27 and 28, respectively.

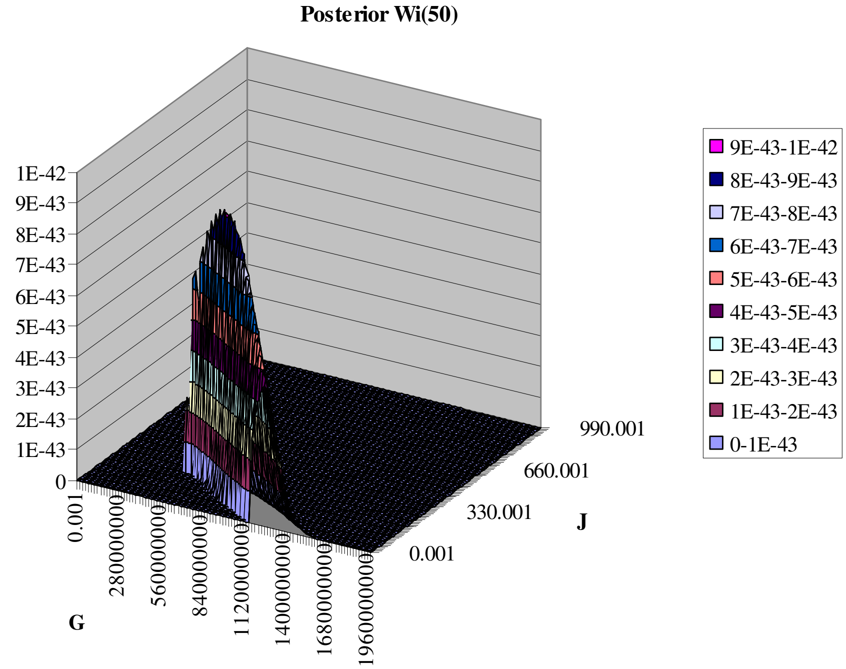

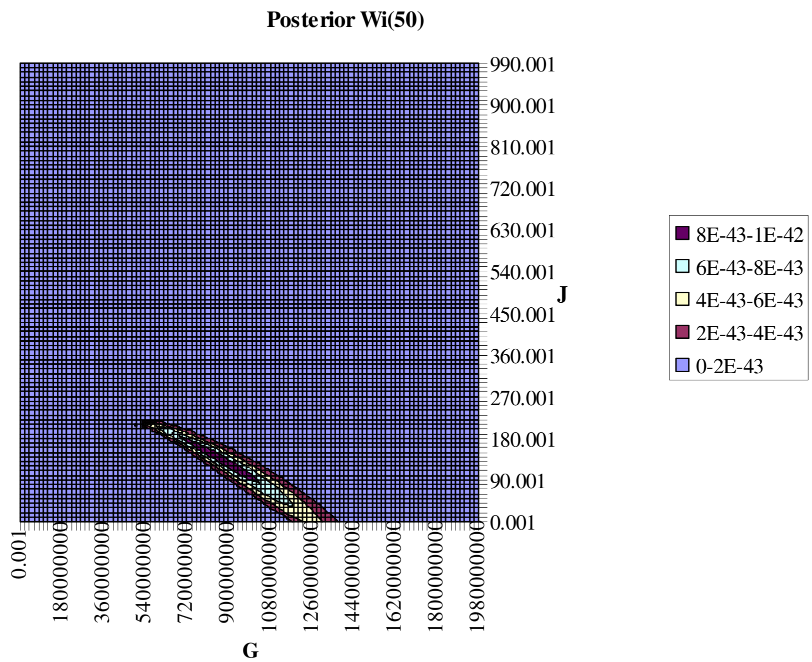

Fig. 23-Posterior distribution of G versus J for $W_i = 0.5\ W_{i\ max}$, synthetic field A.

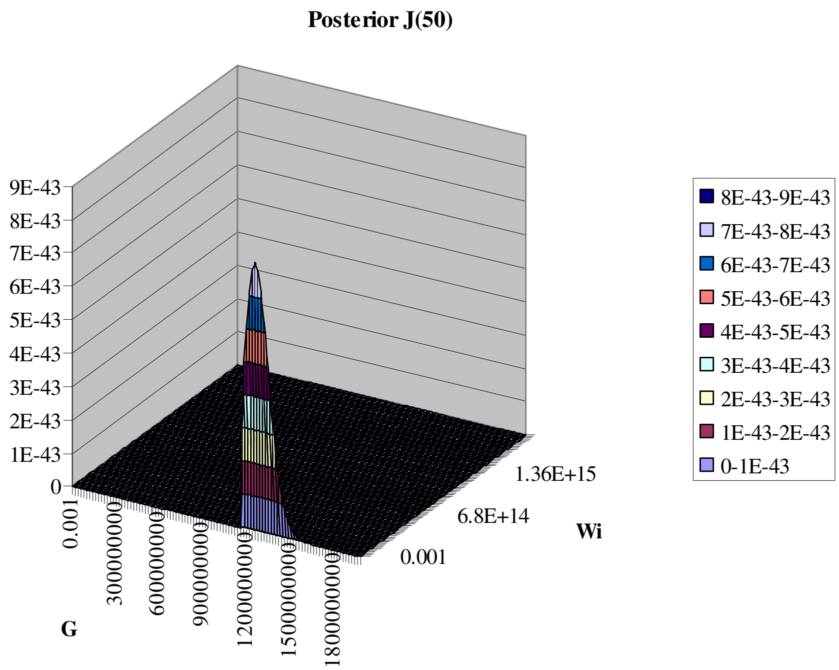

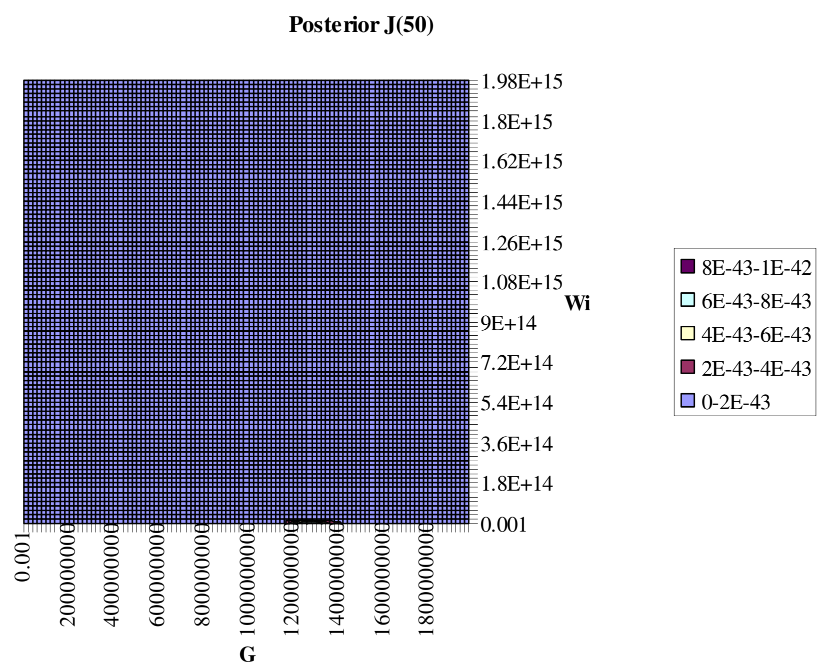

Fig. 24-Posterior distribution of G versus W_i for $J = 0.5\ J_{max}$, synthetic field A.

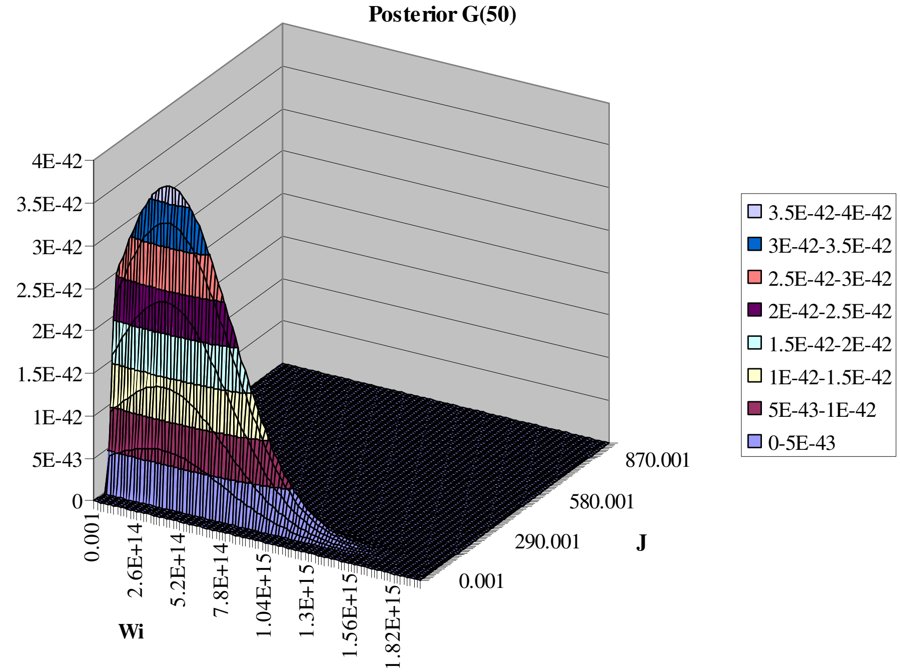

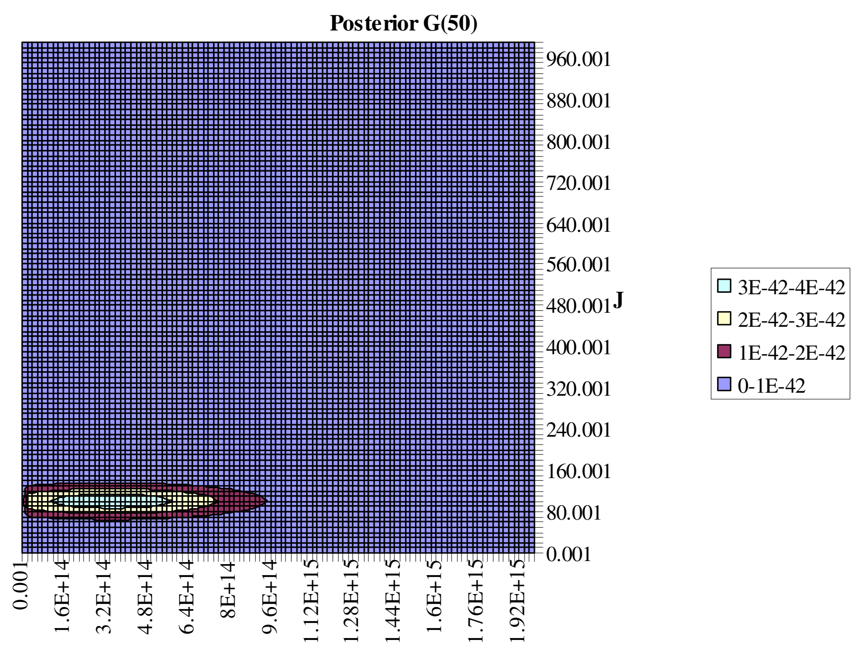

Fig. 25-Posterior distribution of W_i versus J for $G = 0.5\ G_{max}$, synthetic field A.

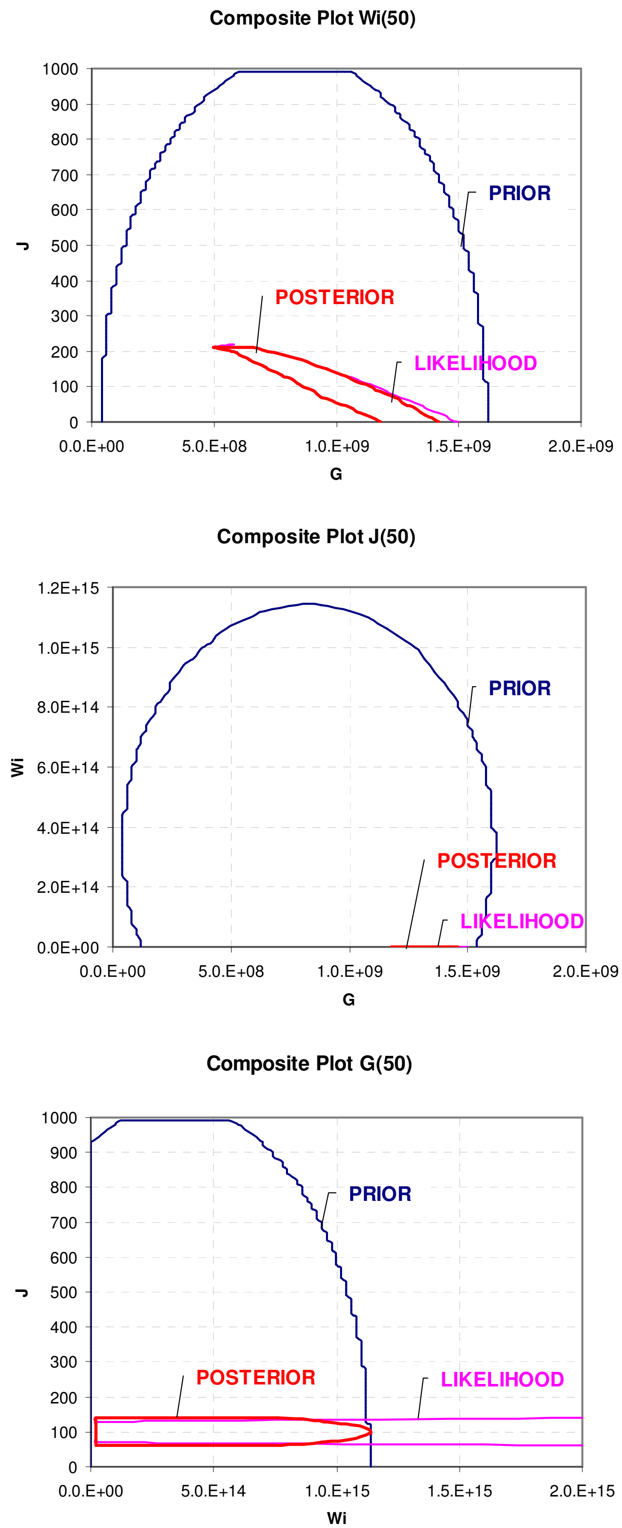

Fig. 26-Composite plot for 50% of the maximum values of each parameter, synthetic field A.

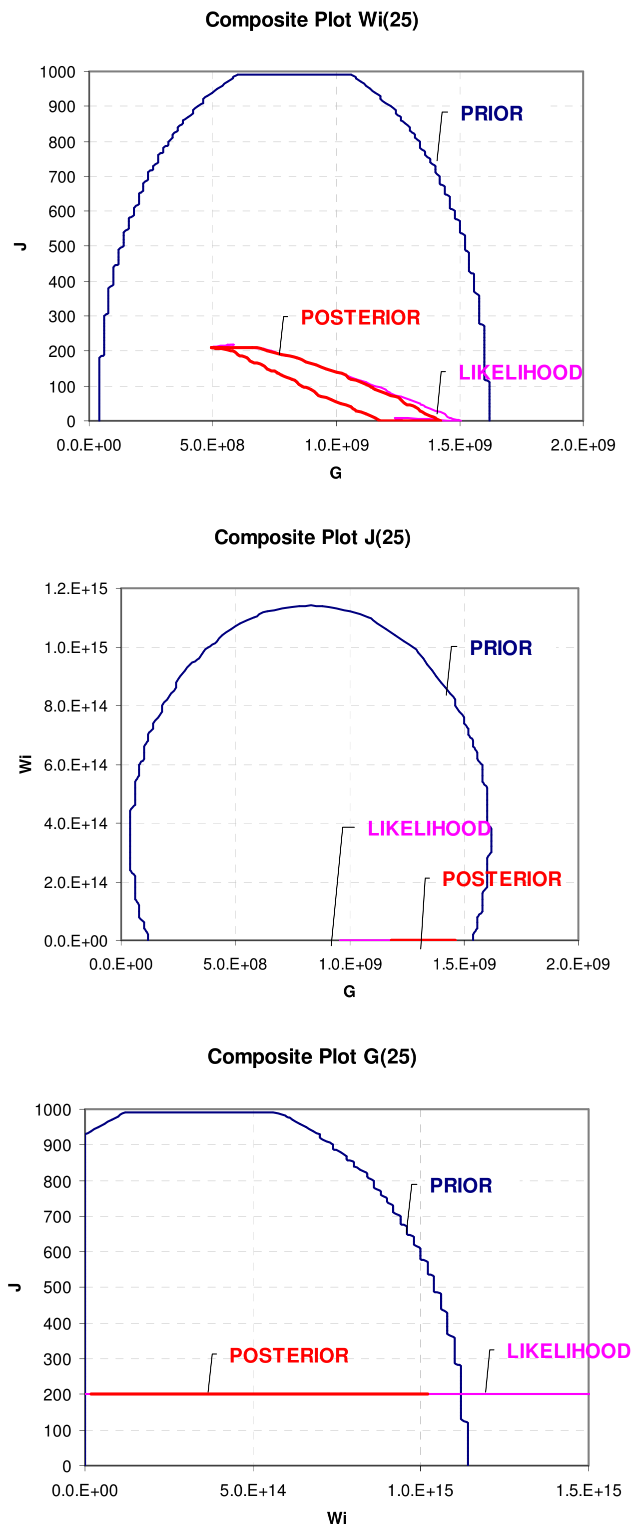

Fig. 27-Composite plot for 25% of the maximum values of each parameter, synthetic field A.

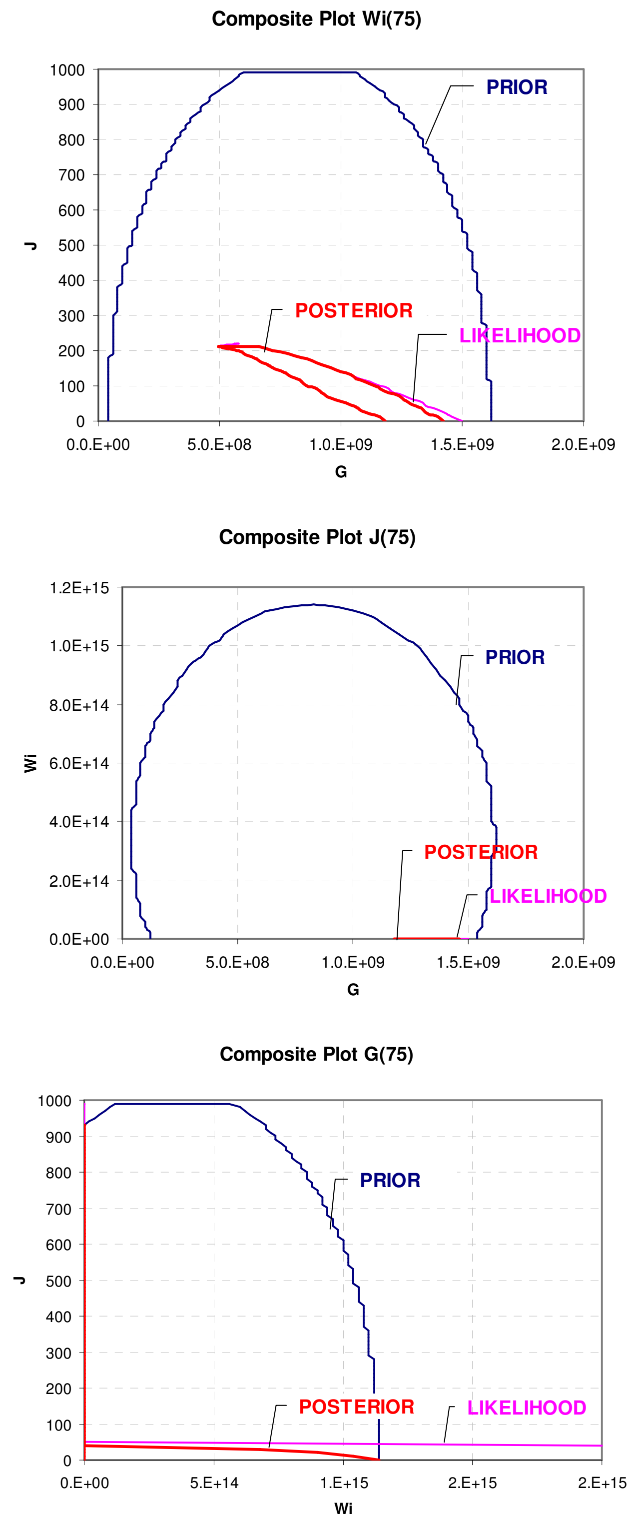

Fig. 28-Composite plot for 75% of the maximum values of each parameter, synthetic field A.

The MAP solution for this case is G = 880 Bscf, J = 130 STB/D-psi, and $W_i = 3.4 \times 10^{14}$ RB. The posterior covariance matrix for the numerical method is:

$$C_x = \begin{bmatrix} 4.14\times10^{16} & -7{,}928{,}455{,}581.07 & -4.68\times10^{21} \\ -7{,}928{,}455{,}581.07 & 7{,}180.28 & -3.67\times10^{15} \\ -4.68\times10^{21} & -3.67\times10^{15} & 8.71\times10^{28} \end{bmatrix}$$

The diagonal elements of the covariance matrix give us the variances of G, J, and W_i. Thus, the posterior variances of G, J, and W_i from the numerical method are:

$$\sigma_G^2 = 4.143\times10^{16} \qquad \sigma_J^2 = 7{,}180.28 \qquad \sigma_{W_i}^2 = 8.71\times10^{28}$$

Finally, the prior and posterior standard deviations are compared in the following table:

Table 9– Prior and Posterior Standard Deviations of *G*, *J*, and *W*i, Synthetic Field A

	Prior	Posterior (numerical)
σ_G	370,224,075.35	203,535,471.00
σ_J	459.00	84.74
σ_{Wi}	3.713×10^{14}	2.951×10^{14}

Table 9 shows that all posterior standard deviations are less than the respective prior standard deviations, as expected. Incorporating the material balance analysis has reduced the uncertainties in G, J, and W_i from the prior volumetric analysis.

Note that the off-diagonal elements of the posterior covariance matrix are non-zero, indicating that the parameters have some degree of correlation. This is contrary to the assumption of no correlation that I made in the prior volumetric analysis. Correlation between parameters should be investigated in the future work.

B. Synthetic Field Case With Noise Added to Pressure Data

Illustrations of the prior distribution for this case can be seen in Figs. 17-19, since the prior is the same as for the previous case.

In this case, I added noise to the pressure data that will be used for building the likelihood probability distribution. These "noisy" pressure data are shown in Fig. 29.

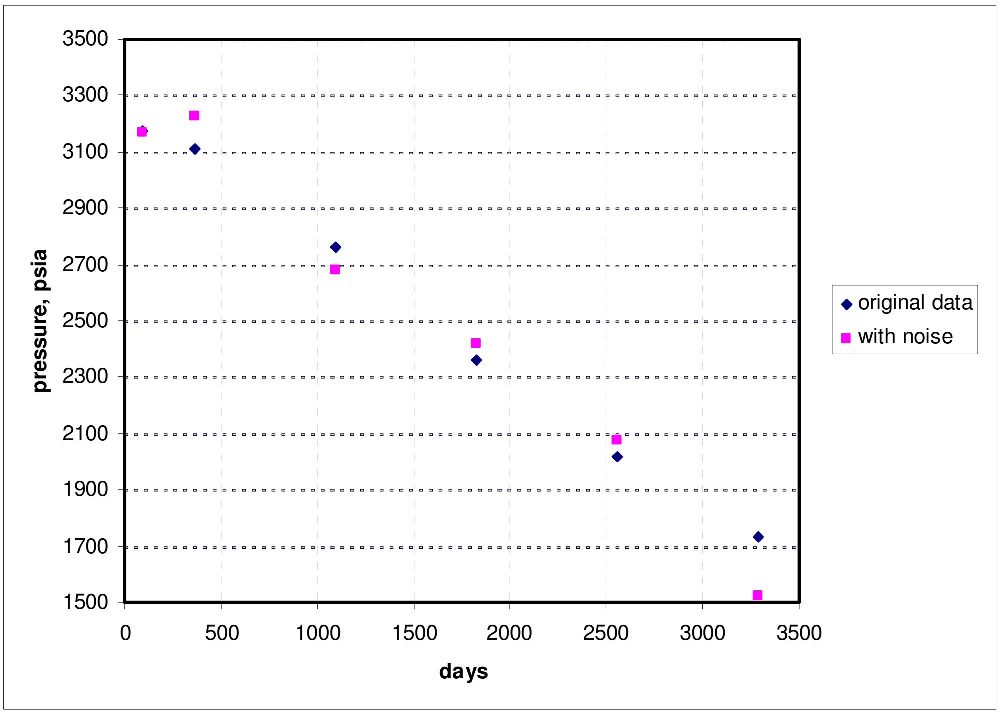

Fig. 29-Pressure data with noise added.

As with the Lagan field case and the synthetic field A case, I used only six data points from Tables 5 and 6 to build the likelihood probability distribution. The data used to build the likelihood distribution are presented in Table 10. A pressure standard deviation of 100 psia has been assumed in this case as well.

Table 10–Observed Data Used in Analysis, Synthetic Field B.

Days	Pressure (psia)	G_p	W_p (RB)	Z
91.25	3167.2364	5,384,000	0	0.911258
365	3226.4386	21,535,000	0	0.906706
1095	2677.8782	137,788,000	0	0.899023
1825	2417.1217	299,118,000	0	0.89225
2555	2078.4749	452,418,000	0	0.899777
3285	1521.0818	581,883,000	0	0.903394

The likelihood distribution for the synthetic field B case for 50% of the maximum values of each parameter is presented in Figs. 30-32.

Similarly to synthetic field A case, we can see that, from material balance estimates for $W_i = 0.5\ W_{i\ max}$, many combinations of parameters G and J have significant probability (Fig. 30). In Fig. 32, the likelihood distribution of W_i and J for $G = 0.5\ G_{max}$ runs parallel to the W_i axis over a significant range for W_i. This indicates that material balance analysis cannot uniquely determine the aquifer size in this case and, most likely, is indicating only a minimum aquifer size.

The ML parameter estimates for this case are G = 720 Bscf, J = 150 STB/D-psi, and $W_i = 6 \times 10^{13}$ RB.

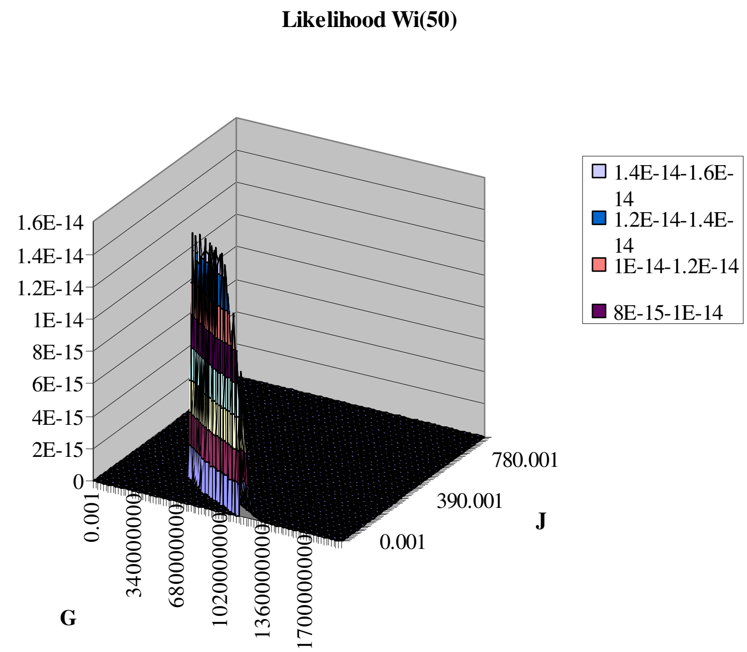

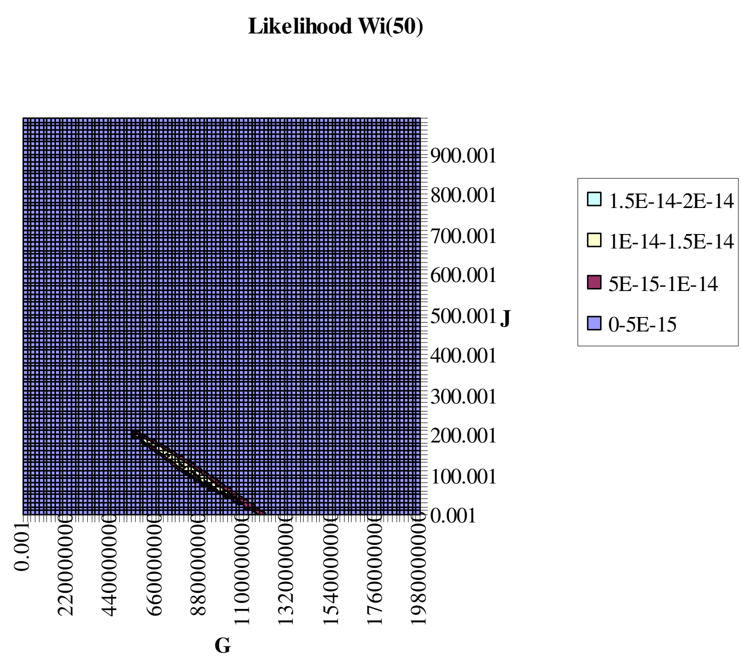

Fig. 30-Likelihood distribution of G versus J for $W_i = 0.5\ W_{i\ max}$, synthetic Field B.

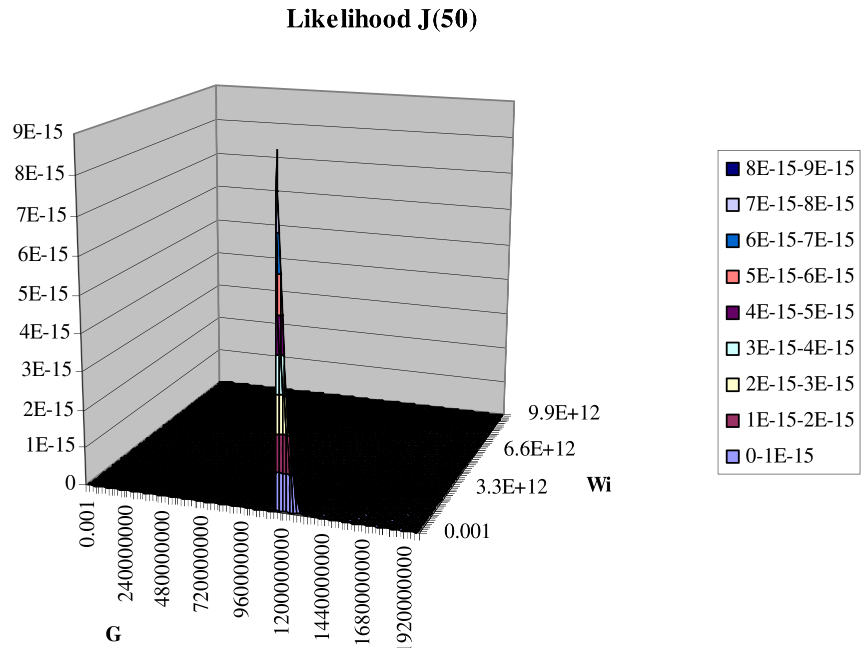

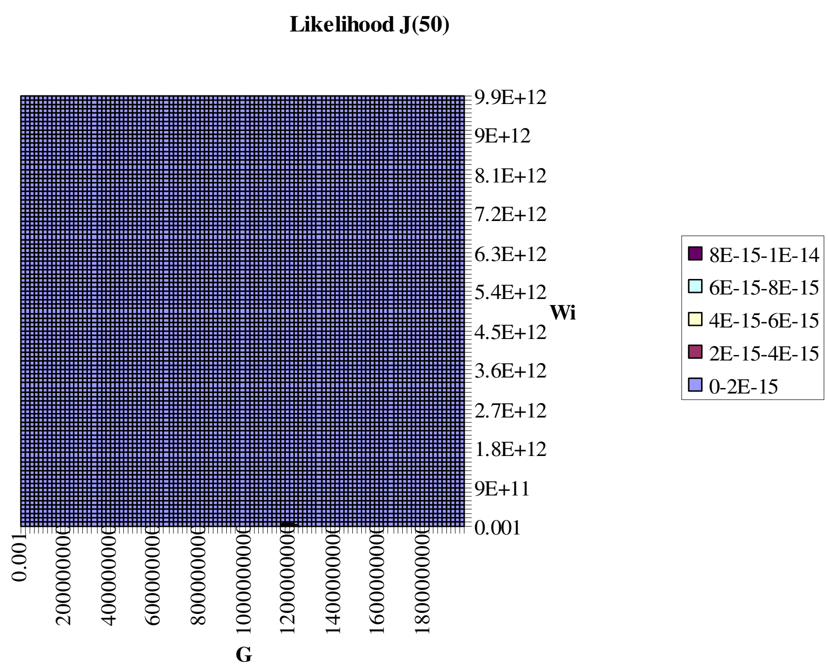

Fig. 31-Likelihood distribution of G versus W_i for $J = 0.5\ J_{max}$, synthetic field B.

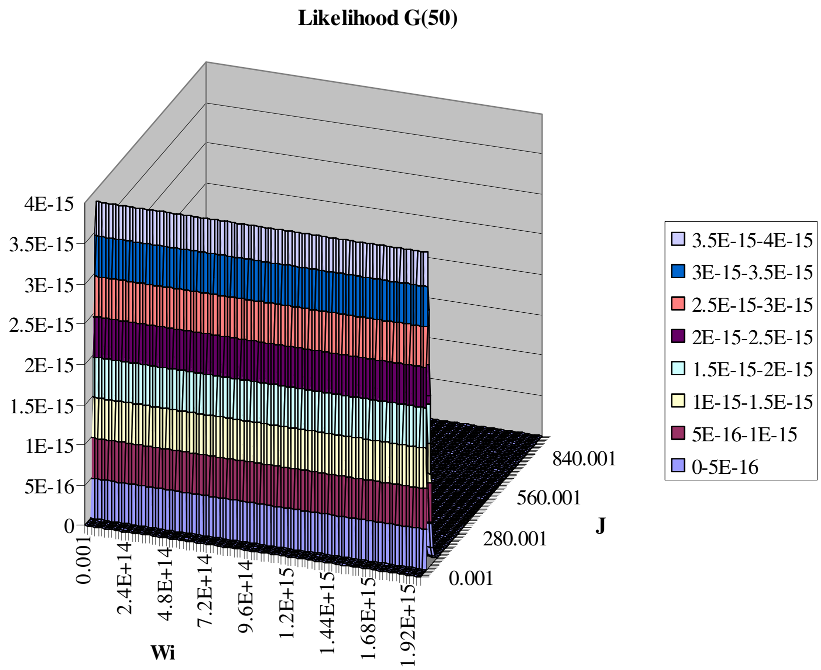

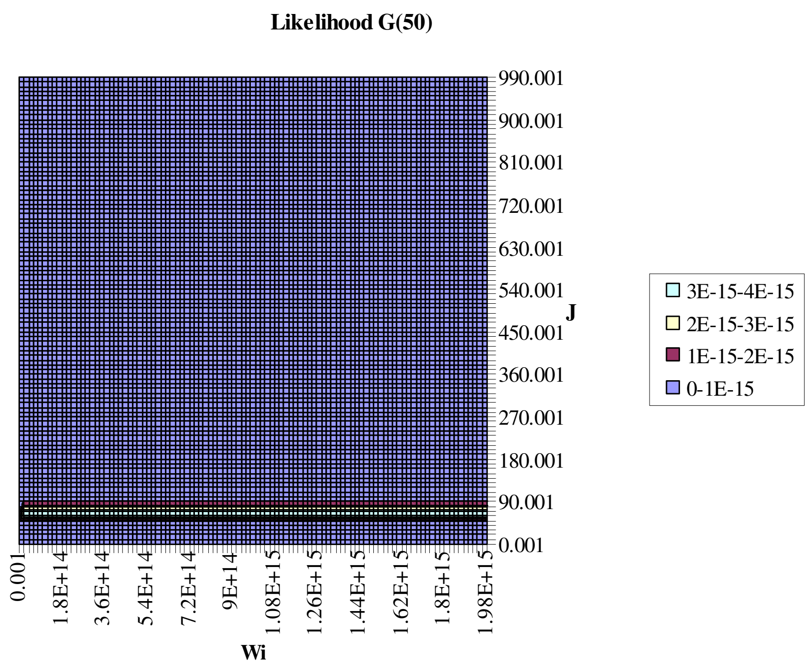

Fig. 32-Likelihood distribution of W_i versus J for $G = 0.5\ G_{max}$, synthetic field B.

The posterior distributions are shown in Figs. 33-35. We can see from these figures that the extent of the posterior distribution is considerable smaller than either the prior or likelihood distributions, indicating the reduced uncertainty in the combined volumetric and material balance solution.

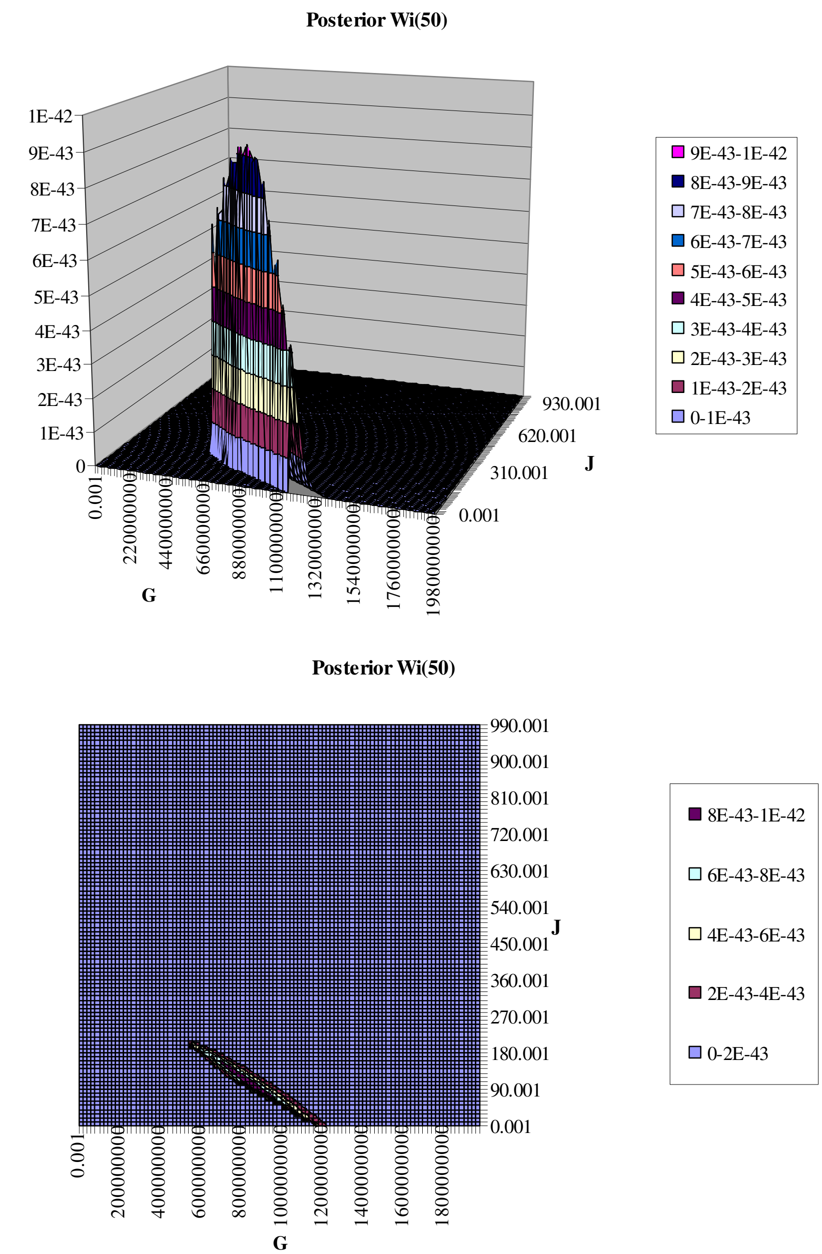

Fig. 33-Posterior distribution of *G* versus *J* for $W_i = 0.5\ W_{i\ max}$, synthetic field B.

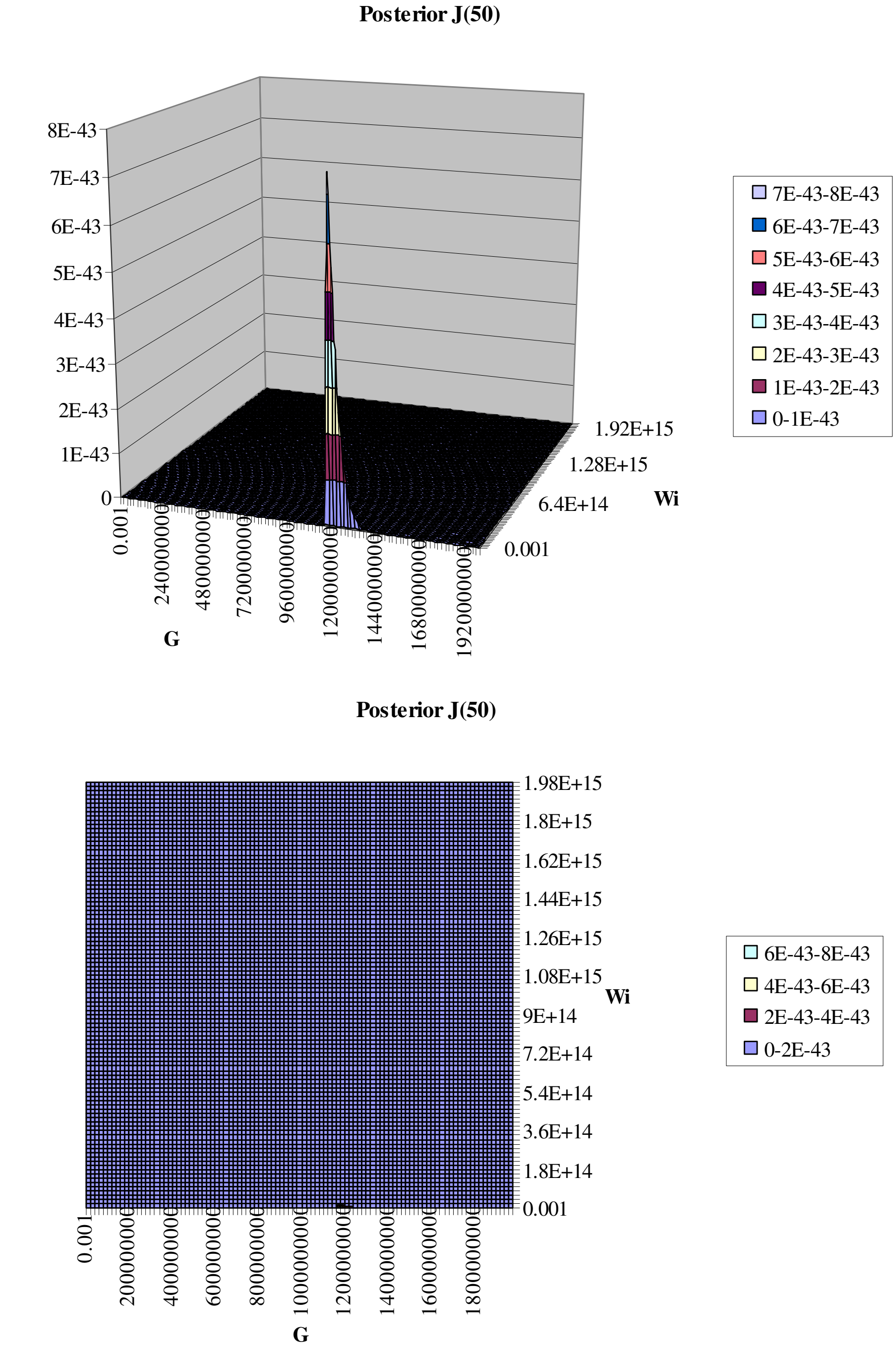

Fig. 34-Posterior distribution of G versus W_i for J = 0.5 J_{max}, synthetic field B.

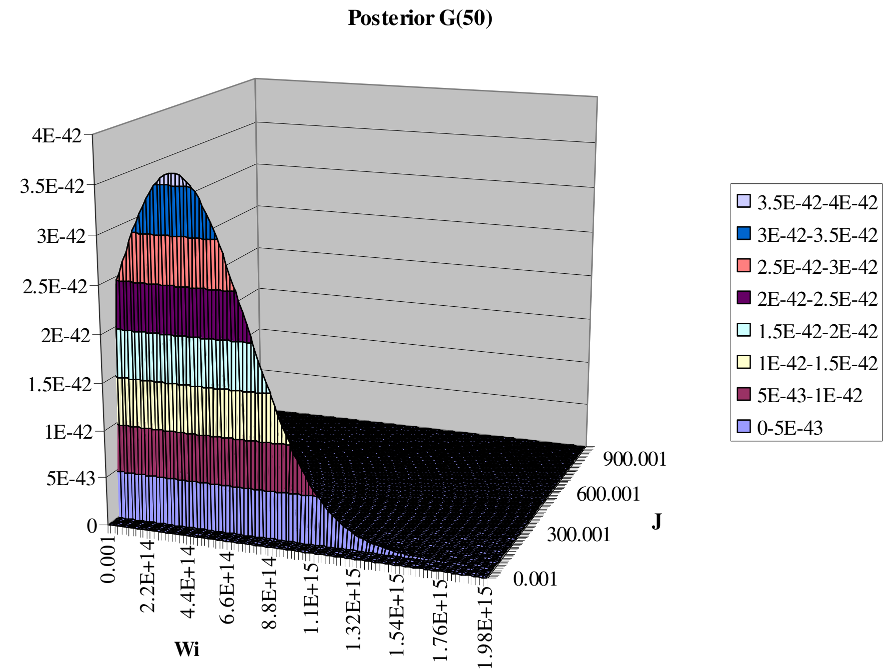

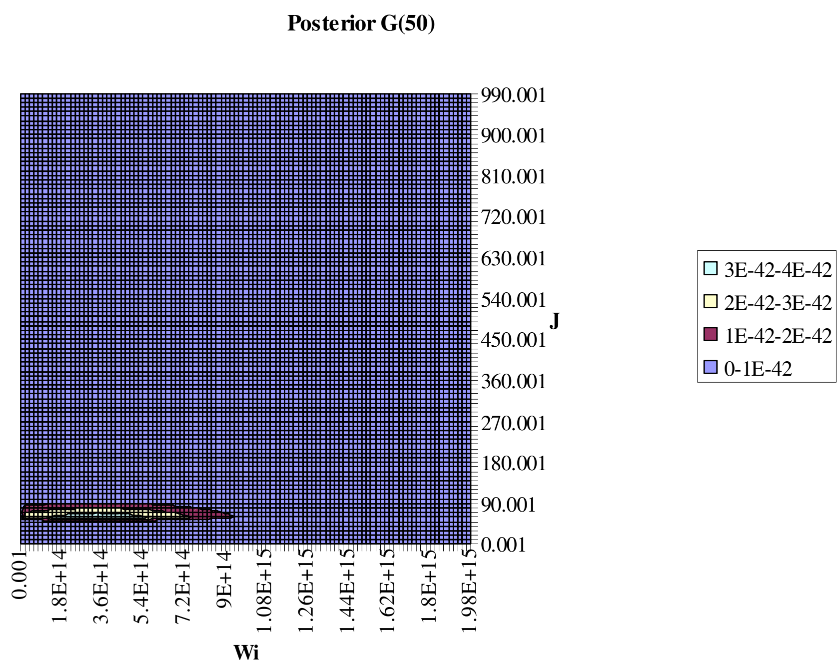

Fig. 35-Posterior distribution of W_i versus J for $G = 0.5G_{max}$, synthetic field B.

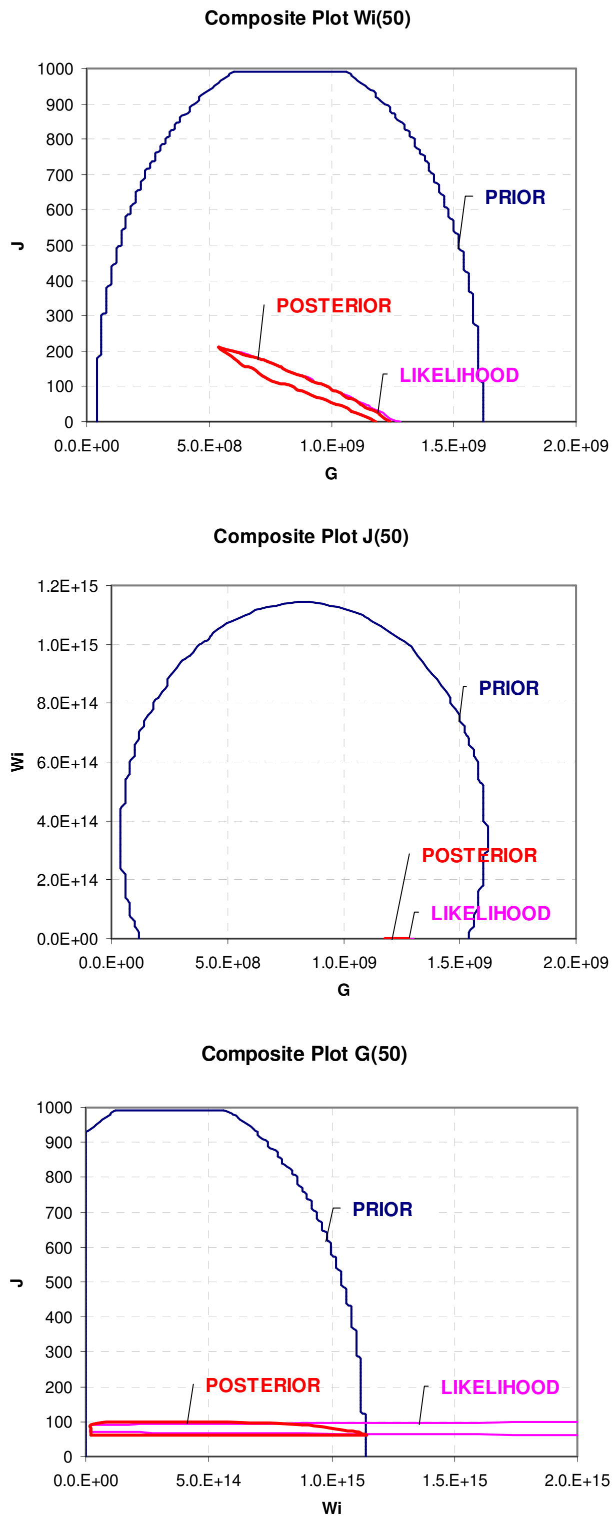

Fig. 36-Composite plot for 50% of the maximum values of each parameter, synthetic field B.

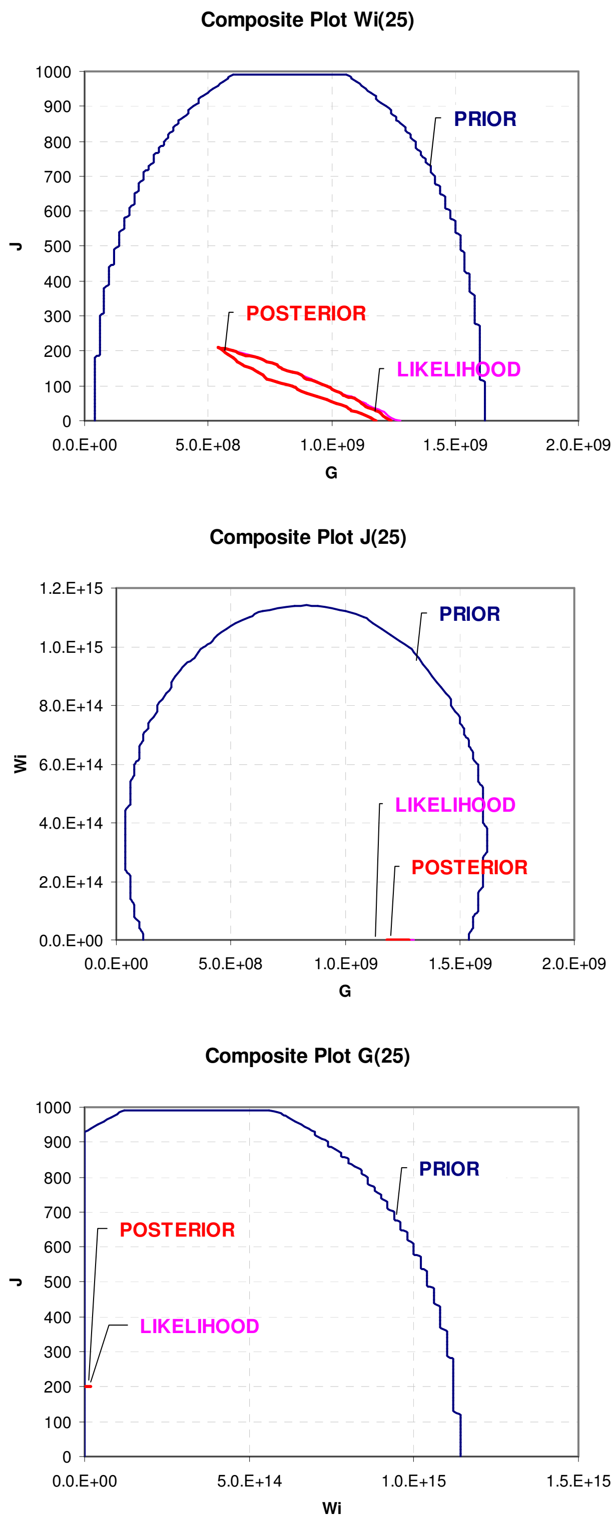

Fig. 37-Composite plot for 25% of the maximum values of each parameter, synthetic field B.

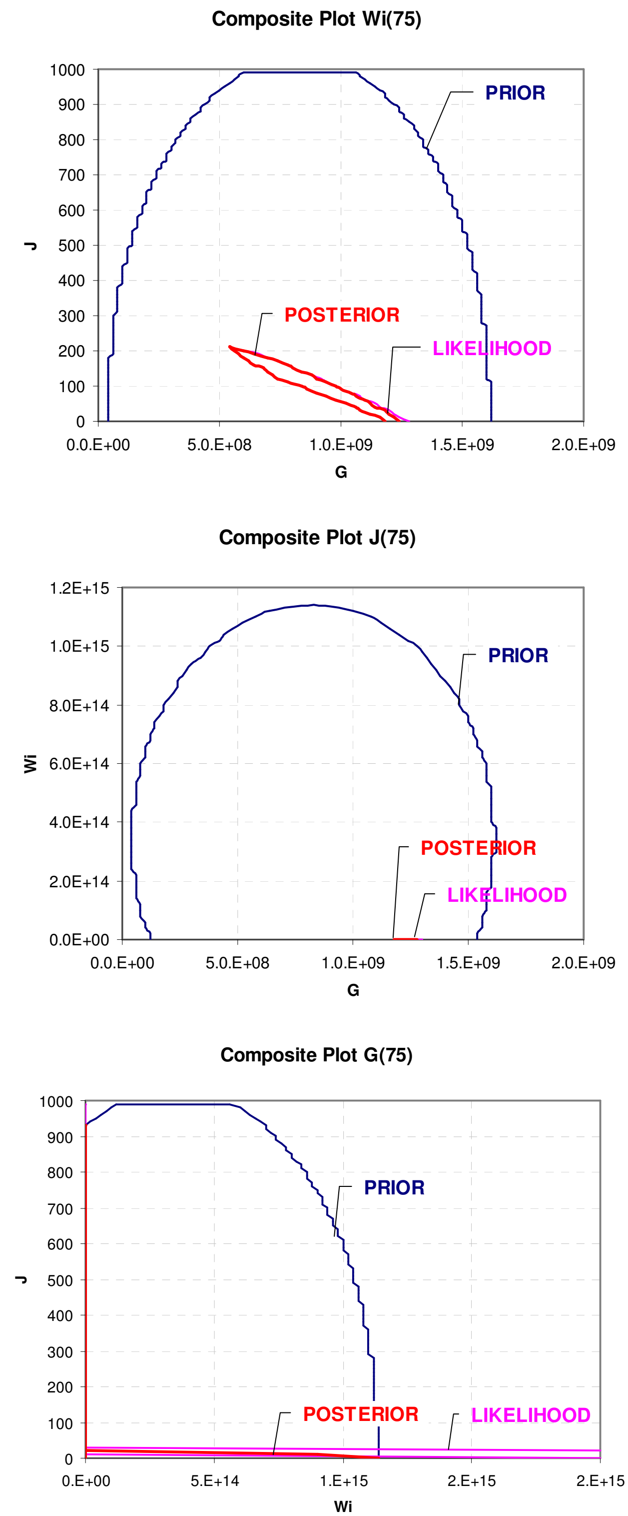

Fig. 38-Composite plot for 75% of the maximum values of each parameter, synthetic field B.

The relationships between the prior, likelihood and posterior distributions for 50%, 25% and 75% of the maximum values of each parameter are illustrated in Figs. 36, 37 and 38, respectively. From these plots, we can also see that uncertainty is reduced in the combined volumetric and material balance analysis.

The MAP solution for this case is G = 860 Bscf, J = 100 STB/D-psi, and $W_i = 3.4\times10^{14}$ RB. The covariance matrix obtained from the numerical method is:

$$C_x = \begin{bmatrix} 2.51\times10^{16} & -5.7\times10^{9} & -2.6\times10^{21} \\ -5.7\times10^{9} & 4{,}145.138 & -1.8\times10^{15} \\ -2.6\times10^{21} & -1.8\times10^{15} & 8.5\times10^{28} \end{bmatrix}$$

The diagonal elements of the covariance matrix give us the variances of G, J, and W_i. Thus, the posterior variances of G, J, and W_i from the numerical method are:

$$\sigma_G^2 = 2.51\times10^{16} \qquad \sigma_J^2 = 4{,}145.138 \qquad \sigma_{W_i}^2 = 8.5\times10^{28}$$

Finally, the prior and posterior standard deviations for the synthetic field B case are compared in the following table:

Table 11– Prior and Posterior Standard Deviations of *G*, *J*, and W_i, Synthetic Field B

	Prior	Posterior (numerical)
σ_G	370,224,075.35	158,393,333.13
σ_J	459.00	64.38
σ_{Wi}	3.71×10^{14}	2.92×10^{14}

Table 11 shows that all posterior standard deviations for synthetic field B are less than prior standard deviations, as expected. The material balance analysis reduces the uncertainty from the prior volumetric analysis by 57% for G, 85.97% for J and 21.29% for W_i.

Similar to synthetic field case A, the off-diagonal elements of the posterior covariance matrix are non-zero, indicating correlation between parameters. Again, correlation between parameters should be investigated in future work.

Higher Uncertainty in Prior

In this section, I investigate how the posterior and its covariance behave with greater uncertainty in the prior volumetric analysis for synthetic field case B. To obtain this case, I increased the uniform distribution of r_{eD} from 1–1,000 to 1–10,000. The parameter means and standard deviations for this revised case are listed in Table 12.

Table12–Mean and Standard Deviation of G, J, and W_i from Volumetric Analysis, Synthetic Field B, with Higher Uncertainty in Prior

Parameter	Mean	Standard Deviation
G (Mscf)	826,453,714.05	368,254,942.24
J (STB/D-psi)	35.85	31.23
W_i (RB)	3.42×10^{16}	3.69×10^{16}

Fig. 39 shows the composite plots of the prior, likelihood, and posterior distributions for 50% of the maximum values of each parameter for synthetic field case B with more uncertainty in the prior.

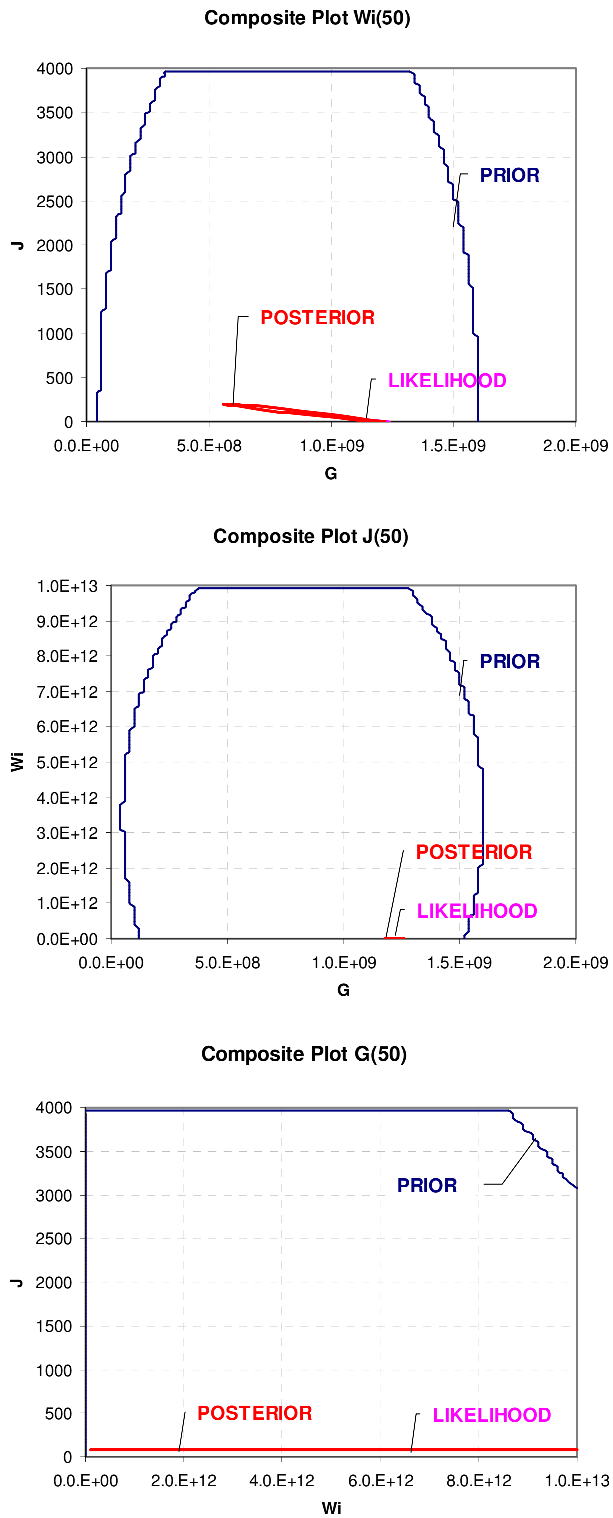

Fig. 39-Composite plot for 50% of the maximum value of each parameter, synthetic field B, with higher uncertainty in prior.

The prior and posterior standard deviations for the synthetic field case B with more uncertainty in the prior are compared in the following table:

Table 13– Prior and Posterior Standard Deviations of *G*, *J*, and W_i, Synthetic Field B, with Higher Uncertainty in Prior

	Prior	Posterior (numerical)
σ_G	368,254,942.24	96,275,944.10
σ_J	31.23	27.00
σ_{Wi}	3.69×10^{16}	2.49×10^{16}

Table 13 shows that, for this case with higher uncertainty in prior, we can reduce the uncertainty of *G* as much as 73.86 %, *J* as much as 13.54 % and W_i as much as 32.52%. The posterior standard deviations for *G* and *J* are greater than those for the original prior distribution (Table 11), as expected. However, the posterior standard deviation for W_i for this case with higher uncertainty in the prior is lower than the previous case.

<u>Lower Uncertainty in Prior</u>

This example is similar to the previous, except I reduce the uncertainty in the prior. To obtain this case, I decreased the uniform distribution of r_{eD} from 1–1,000 to 1–100. Using Monte Carlo analysis, I obtained the mean and standard deviation of each parameter as shown in Table 14.

Table 14–Mean and Standard Deviation of G, J, and W_i from Volumetric Analysis, Synthetic Field B, with Less Uncertainty in Prior		
Parameter	Mean	Standard Deviation
G (Mscf)	825,656,139.04	366,514,689.78
J (STB/D-psi)	90.53	2,375.80
W_i (RB)	3.46×10^{12}	3.70×10^{12}

Fig. 40 shows the composite plot of prior, likelihood, and posterior distributions for 50% of the maximum values of each parameter for the case with reduced uncertainty in the prior for synthetic field case B. The prior and posterior standard deviations are compared in the following table:

Table 15– Prior and Posterior Standard Deviations of G, J, and W_i from, Synthetic Field B, with Less Uncertainty in Prior		
	Prior	Posterior (numerical)
σ_G	366,514,689.78	173,788,546.75
σ_J	2,375.80	339.11
σ_{Wi}	3.70×10^{12}	2.57×10^{12}

Table 15 shows that, with lower uncertainty in the prior, we can reduce the uncertainty of G as much as 52.58 %, J as much as 85.72 % and W_i as much as 30.54 %. The posterior standard deviations for G and J are lower than those for the original prior distribution (Table 11), as expected. However, the posterior standard deviation for W_i for this case with lower uncertainty in the prior is higher than the original case.

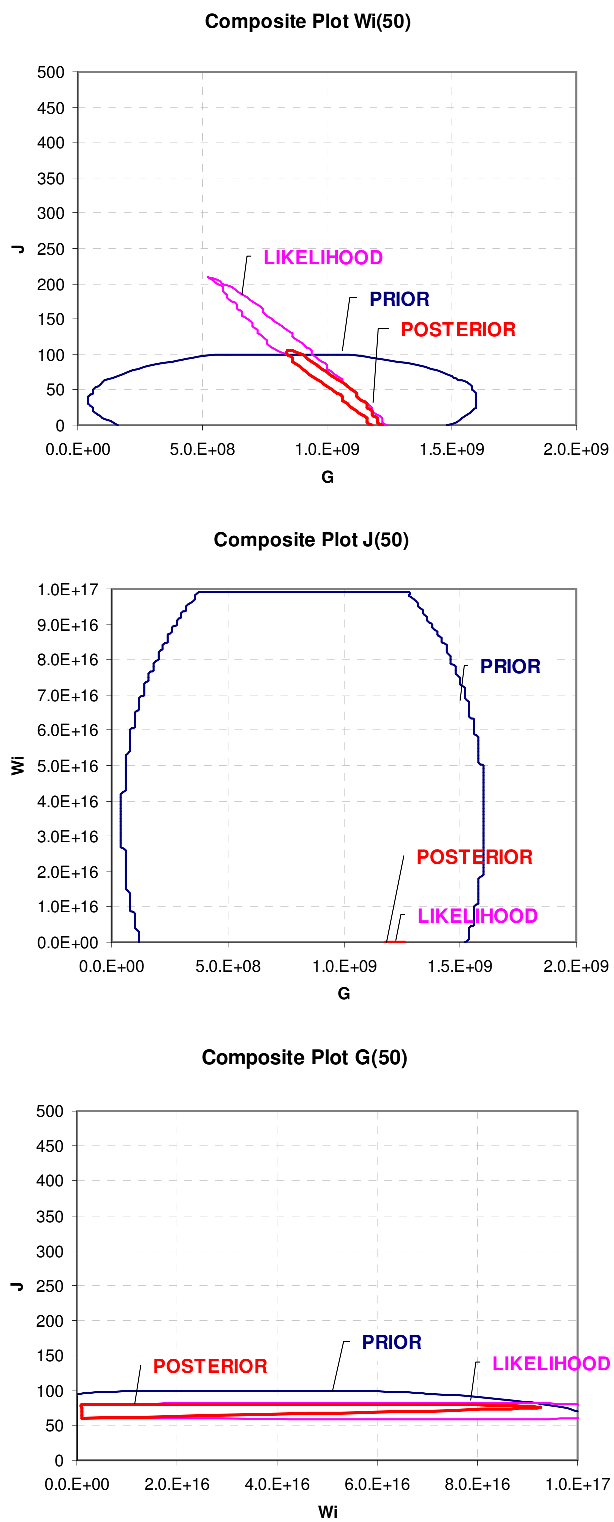

Fig. 40-Composite plot for 50% of the maximum values of each parameter, synthetic field B, with less uncertainty in prior.

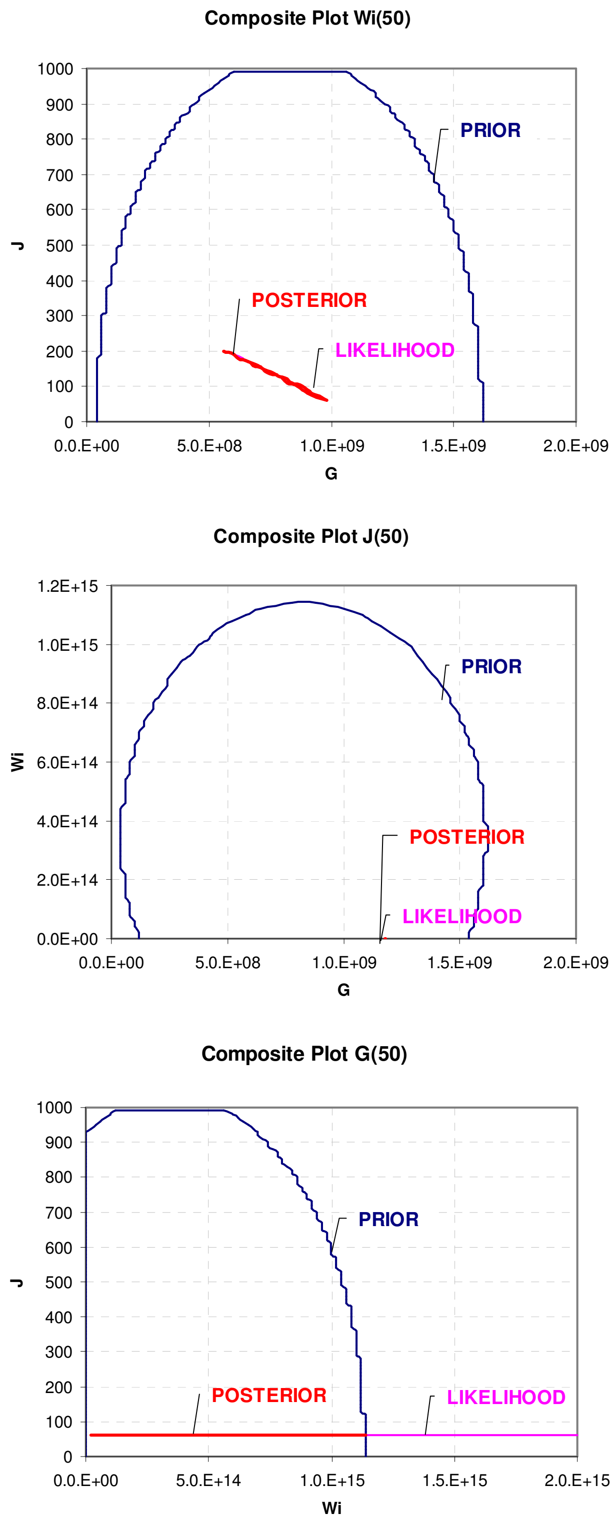

Fig. 41-Composite plot for 50% of the maximum value of each parameter, pressure SD = 20 psia.

Less Uncertainty in the Pressure Data

In synthetic field case B, a standard deviation in pressure data of 100 psia was assumed. Fig. 41 shows the composite plot of prior, likelihood, and posterior distributions for 50% of the maximum values of each parameter if I assume a standard deviation of 20 psia for the pressure data.

We can see from Fig. 41 that, by assuming 20 psia pressure standard deviation, the extent of likelihood distribution becomes smaller than if we assume 100 psia pressure standard deviation. Because the likelihood distribution is smaller, the posterior distribution also becomes smaller, since the posterior distribution is the product of the prior and likelihood distributions. So I can conclude that the smaller the standard deviation of pressure data, the more certain the posterior distribution will be.

CHAPTER V
CONCLUSIONS

In this thesis I have combined volumetric and material balance analysis using Bayes' theorem and have applied it to gas fields with water influx. From the results of these analyses, I conclude:

1. Use of a Bayesian approach to combine volumetric and material balance analyses can reduce uncertainties in gas in place, aquifer volume, and aquifer productivity index resulting from a prior volumetric analysis.
2. Uncertainties in the prior volumetric analysis should be considered carefully, particularly for aquifer parameters. Usually, there will be very large uncertainties in aquifer parameters from volumetric analysis. If the uncertainties in aquifer parameters are underestimated in the prior volumetric analysis, this may result in a corresponding underestimation of uncertainty in the posterior distribution if the material balance solution is non-unique (i.e., has large uncertainty) for aquifer parameters.
3. Material balance solutions can have considerable non-uniqueness (i.e., large uncertainty) in gas in place as well as aquifer parameters. If uncertainties in the volumetric analysis can be determined reliably, then the approach proposed in this thesis can be used to reduce the non-uniqueness of the material balance solution.

Future Work

1. In this work I assume a multivariate normal distribution for the prior, with no correlation between parameters. For future work, it would be better to determine the multivariate prior distribution of G, J and W_i directly from Monte Carlo

analysis. This would provide for the possibility of a non-normal distribution and correlation between parameters.

2. The off-diagonal elements of the posterior covariance matrix turn out to be non-zero. This indicates correlation between parameters, although I assumed no correlation in the prior distribution. Correlation between parameters should be investigated in future work.

NOMENCLATURE

A_a	= aquifer area, acres
A_r	= reservoir area, acres
B_g	= gas formation volume factor, bbl/scf
B_{gi}	= initial gas formation volume factor, bbl/scf
C_D	= covariance matrix for likelihood parameter
C_M	= covariance matrix for prior parameter
c_t	= total aquifer compressibility, psia^{-1}
d_{obs}	= vector of observed pressure
E_g	= $B_g - B_{gi}$ = gas expansivity, bbl/scf
$g(m)$	= vector of pressure from the Newton-Rhapson iteration
G	= original gas in place, scf
G_p	= cumulative gas production, scf
h_a	= aquifer thickness, ft
h_r	= net pay thickness, ft
J	= aquifer productivity index, STB/d-psi
k	= aquifer permeability, darcies
m	= vector of model parameter
m_{prior}	= vector of model parameter from prior distribution
p	= pressure, psia
$\bar{p}_{aq}$	= aquifer pressure, psia
$p_{aq,i}$	= initial aquifer pressure, psia
$\bar{p}_r$	= pressure at original aquifer/reservoir interface, psia
r_a	= radius of aquifer, ft
r_r	= radius to aquifer/reservoir interface, ft
S_w	= water saturation
t	= time, days

W_e = cumulative water influx, RB

W_{ei} = maximum water volume, RB

W_{i} = initial volume of water in aquifer, RB

W_p = cumulative water production, RB

ΔW_{en} = incremental water influx, RB

θ = angle encompassed by aquifer, degrees

$\theta(d_{\mathrm{obs}}|m)$ = likelihood probability distributions

μ = viscosity, cp

ϕ = porosity

$\rho_M(m)$ = prior probability distributions

$\sigma((m|d_{\mathrm{obs}})$ = posterior probability distributions

REFERENCES

1. Bradley, J.: *Petroleum Engineering Handbook*, SPE, Richardson, Texas (1987) Chap. 40.
2. Mian M.A.: *Project Economic and Decision Analysis Volume II: Probabilistic Method*, Penn Well Corporation, Tulsa (1992) Chap. 1.
3. Tarantola, A.: *Inverse Problem Theory and Methods for Model Parameter Estimation*, Siam, Paris (2005) Chap. 1
4. Winkler R.L.: *An Introduction to Bayesian Inference and Decision*, Holt Rinehart and Winston, Bloomington, Indiana (1972)
5. Bolstad, W.M.: *Introduction of Bayesian Statistics*, Wiley, Hoboken, New Jersey (2004) Chap 1.
6. Floris F.J.T., Bush M.D, Cuypers M., Roggero F., and Syversveen A-R.: "Methods for Quantifying the Uncertainty of Production Forecasts: A Comparative Study," *Petroleum Geoscience* **7** (2001) S87-S96.
7. Glimm J., Hou S., Lee Y., Sharp D., and Ye K.: "Prediction of Oil Production with Confidence Intervals," paper SPE 66350 presented at the 2001 SPE Reservoir Simulation Symposium, Houston, 11-14 February.
8. Daoud A., Ogele C. and McVay D.: "Integration and Quantification of Uncertainty of Volumetric and Material Balance Analysis Using a Bayesian Framework," manuscript submitted to AAPG for publication, 2005.
9. Galli A., Armstrong, M., and Dias, M.A.: "The Value of Information: A Bayesian Real Option Approach," paper SPE 90418 presented at the 2004 SPE Annual Technical Conference and Exhibition, Houston, 26-29 September.
10. Jensen J., Corbett P.W., Lake L.W., and Goggin D.J,: *Statistics for Petroleum Engineers and Geoscientist*, second edition, Elsevier, Amsterdam (2000) 169-170.
11. Dake, L.P.: *The Practice of Reservoir Engineering (Revised Edition)*, Elsevier, Amsterdam (2001) Chap. 6.

12. Havlena, D. and Odeh, A.S.: "The Material Balance as an Equation of a Straight Line," paper SPE 559 presented at the 1980 SPE Production Research Symposium, Norman, Oklahoma, 29-30 April.
13. Havlena, D. and Odeh, A.S.: "The Material Balance as an Equation of a Straight Line-Part II, Field Cases," *JPT* (July 1964) 815-822.
14. Lee, W.J. and Wattenbarger R.: *Gas Reservoir Engineering,* SPE textbook, SPE, Richardson, Texas (2002) 242-244.
15. Fetkovich, M.J.: "A Simplified Approach to Water Influx Calculations – Finite Aquifer Systems," *JPT* (July 1971) 814-828.
16. Ikoku, C.U.: *Natural Gas Reservoir Engineering*, Krieger Pub. Co., Malabar, Florida (1984) Chap. 1.
17. Ahmed, T.: *Reservoir Engineering Handbook*, second edition, Gulf Professional Publishing, Houston, Texas (2001) Chap. 11 and Chap. 13.
18. Ahmed, T.: *Advanced Reservoir Engineering*, Elsevier, Oxford (2005) Chap 2, 3.

APPENDIX A
BAYESIAN CODE IN VBA LANGUANGE

```
Option Explicit

Private aG() As Double      'gas in place
Private aJ() As Double      'aquifer productivity index
Private aWi() As Double     'aquifer size
Private days() As Double
Private d() As Double       'pressure data
Private aGp() As Double     'gas production data
Private aWp() As Double     'water production
Private az() As Double
Private gm() As Double      'pressure data matching
Private pprior() As Double
Private pdata() As Double
Private ppost() As Double
Private Gsen() As Double
Private Cd() As Double
Private invCd() As Double
Private Cm() As Double
Private invCm() As Double
Private Gt() As Double
Private CdGs() As Double
Private GtCdGs() As Double
Private Cmapinv() As Double
Private Cmap() As Double

Private n As Integer
Private nd As Integer
Private m As Integer
Private i As Integer
Private j As Integer
Private k As Integer
Private l As Integer
Private d1 As Double
Private Gs1 As Double
Private Gs2 As Double
Private Gs3 As Double
Private phi As Double
Private rr As Double
Private miu As Double
Private perm As Double
Private teta As Double
```

```
Private ct As Double
Private h As Double
Private Temp As Double
Private sumpost As Double
Private sumGpost As Double
Private sumJpost As Double
Private sumWipost As Double
Private sumGGpost As Double
Private sumJJpost As Double
Private sumWiWipost As Double
Private sumGJpost As Double
Private sumGWipost As Double
Private sumJWipost As Double

Private aGavg As Double
Private aJavg As Double
Private aWiavg As Double
Private sdaG As Double
Private sdaJ As Double
Private sdaWi As Double
Private sdd As Double
Private Bgi As Double
Private Bw As Double

Private amaxl As Double
Private amax As Double

Private sum As Double
Private sum1 As Double
Private sum2 As Double

Private dfpdp As Double
Private aGmaxl As Double
Private aJmaxl As Double
Private aWimaxl As Double
Private aGmax As Double
Private aJmax As Double
Private aWimax As Double
Private dfpdpmax As Double
Private Gs() As Double
Private aG1 As Double
Private aJ1 As Double
Private aWi1 As Double
Private dfpdp1() As Double

Private constprior As Double
Private constdata As Double
Private Pi As Double
```

```
'Program to Calculate the Prior, Likehood, and the Posterior Distribution
Sub program()

'Read input data
With ThisWorkbook.Sheets("Data")
  n = .Cells(2, 3)
  m = .Cells(3, 3)
  nd = .Cells(4, 3)
  aGavg = .Cells(5, 3)
  aJavg = .Cells(6, 3)
  aWiavg = .Cells(7, 3)
  sdaG = .Cells(8, 3)
  sdaJ = .Cells(9, 3)
  sdaWi = .Cells(10, 3)
  sdd = .Cells(11, 3)
  Bgi = .Cells(12, 3)
  d1 = .Cells(13, 3)
  Temp = .Cells(6, 6)
End With

'Dimension of arrays
ReDim aG(1 To n)
ReDim aJ(1 To n)
ReDim aWi(1 To n)
ReDim aGp(1 To nd)
ReDim days(1 To nd)
ReDim d(1 To nd)
ReDim az(1 To nd)
ReDim aWp(1 To nd)
ReDim gm(1 To nd)
ReDim pprior(1 To n, 1 To n, 1 To n)
ReDim pdata(1 To n, 1 To n, 1 To n)
ReDim ppost(1 To n, 1 To n, 1 To n)
ReDim Gsen(1 To nd, 1 To m)
ReDim Cd(1 To nd, 1 To nd)
ReDim invCd(1 To nd, 1 To nd)
ReDim Cm(1 To m, 1 To m)
ReDim invCm(1 To m, 1 To m)
ReDim Gt(1 To m, 1 To nd)
ReDim CdGs(1 To nd, 1 To m)
ReDim GtCdGs(1 To m, 1 To m)
ReDim Cmapinv(1 To m, 1 To m)
ReDim Cmap(1 To m, 1 To m)
ReDim objinv(1 To n, 1 To n, 1 To n)

Dim summ() As Double
```

```
Dim summ1() As Double
Dim aG0 As Double
Dim aJ0 As Double
Dim aWi0 As Double
Dim aG2 As Double
Dim aJ2 As Double
Dim aWi2 As Double
Dim aG3 As Double
Dim aJ3 As Double
Dim aWi3 As Double
Dim ppriormax As Double
Dim pdatamax As Double
Dim ppostmax As Double
Dim x0 As Integer, y0 As Integer, z0 As Integer
Dim x As Integer, y As Integer, z As Integer
Dim x1 As Integer, y1 As Integer, z1 As Integer


'read pressure data, gas production data, water production data, gas in place, aquifer productivity index and aquifer size
With ThisWorkbook.Worksheets("Data")
  For j = 1 To nd
    days(j) = .Cells(j + 17, 1)
    d(j) = .Cells(j + 17, 2)
    aGp(j) = .Cells(j + 17, 3)
    aWp(j) = .Cells(j + 17, 4)
    az(j) = .Cells(j + 17, 5)
  Next j

  For i = 1 To n
    aG(i) = .Cells(i + 17, 7)
  Next i

  For k = 1 To n
    aJ(k) = .Cells(k + 17, 8)
  Next k

  For l = 1 To n
    aWi(l) = Cells(l + 17, 9)
    Debug.Print aWi(l)
  Next l
End With


'For calculating 2x2 diagonal matrix of Cm and Cd
constprior = (1 / (((2 * 22 / 7) ^ (m / 2)) * (((sdaG ^ 2) * (sdaJ ^ 2) * (sdaWi ^ 2)) ^ (0.5))))
constdata = (1 / (((2 * 22 / 7) ^ (nd / 2)) * (((sdd ^ 2) ^ nd) ^ (0.5))))
```

```
Debug.Print constprior; constdata

'-----------------------------------PDF for the Prior-Likehood-Posterior-----------------------------------
----------------'

'Save the maximum of the likelihood and the posterior in array amaxl, amax

ReDim Gs(1 To nd, 1 To m)
ReDim dfpdp1(1 To nd)
ReDim summ(1 To n, 1 To n, 1 To n)
ReDim summ1(1 To n, 1 To n, 1 To n)

'Clear contents of worksheets
ThisWorkbook.Worksheets("Prior").Cells.ClearContents
ThisWorkbook.Worksheets("Likelihood").Cells.ClearContents
ThisWorkbook.Worksheets("Posterior").Cells.ClearContents
ThisWorkbook.Worksheets("Posterior_norm").Cells.ClearContents
ThisWorkbook.Worksheets("Check").Cells.ClearContents
ThisWorkbook.Worksheets("Check_sensitivity").Cells.ClearContents
ThisWorkbook.Worksheets("sheet1").Cells.ClearContents
'ThisWorkbook.Worksheets("maximum value1").Cells.ClearContents
'ThisWorkbook.Worksheets("maximum value2").Cells.ClearContents

For i = 1 To n
  For k = 1 To n
    For l = 1 To n
    pprior(i, k, l) = constprior * (Exp(-0.5 * ((((aG(i) - aGavg) ^ 2) / (sdaG ^ 2)) + (((aJ(k) - aJavg)
^ 2) / (sdaJ ^ 2)) + (((aWi(l) - aWiavg) ^ 2) / (sdaWi ^ 2)))))
    Next l
  Next k
Next i

For l = 25 To 75 Step 25
  For k = 1 To n
    For i = 1 To n
      With ThisWorkbook.Worksheets("Prior")
        .Cells(((l / 25) + ((l / 25) - 1) * 102), 1).Value = "J \ G"
        .Cells(((l / 25) + ((l / 25) - 1) * 102), 4).Value = "Wi = " & aWi(l)
        .Cells((2 + ((l / 25) - 1) * 103), i + 1).Value = aG(i)
        .Cells((k + 2 + ((l / 25) - 1) * 103), 1).Value = aJ(k)
        .Cells((k + 2 + ((l / 25) - 1) * 103), i + 1).Value = pprior(i, k, l)
      End With
    Next i
  Next k
Next l

For k = 25 To 75 Step 25
  For i = 1 To n
```

```
    For l = 1 To n
      With ThisWorkbook.Worksheets("Prior")
        .Cells(((k / 25) + 309 + ((k / 25) - 1) * 102), 1).Value = "Wi \ G"
        .Cells(((k / 25) + 309 + ((k / 25) - 1) * 102), 4).Value = "J = " & aJ(k)
        .Cells((311 + ((k / 25) - 1) * 103), i + 1).Value = aG(i)
        .Cells((l + 311 + ((k / 25) - 1) * 103), 1).Value = aWi(l)
        .Cells((l + 311 + ((k / 25) - 1) * 103), i + 1).Value = pprior(i, k, l)
      End With
    Next l
  Next i
Next k

For i = 25 To 75 Step 25
  For l = 1 To n
    For k = 1 To n
      With ThisWorkbook.Worksheets("Prior")
        .Cells(((i / 25) + 618 + ((i / 25) - 1) * 102), 1).Value = "J \ Wi"
        .Cells(((i / 25) + 618 + ((i / 25) - 1) * 102), 4).Value = "G = " & aG(i)
        .Cells((620 + ((i / 25) - 1) * 103), l + 1).Value = aWi(l)
        .Cells((k + 620 + ((i / 25) - 1) * 103), 1).Value = aJ(k)
        .Cells((k + 620 + ((i / 25) - 1) * 103), l + 1).Value = pprior(i, k, l)
      End With
    Next k
  Next l
Next i

sumpost = 0
sumGpost = 0
sumJpost = 0
sumWipost = 0
sumGGpost = 0
sumJJpost = 0
sumWiWipost = 0
sumGJpost = 0
sumGWipost = 0
sumJWipost = 0

For i = 1 To n
  For k = 1 To n
    For l = 1 To n
    aG1 = aG(i)
    aJ1 = aJ(k)
    aWi1 = aWi(l)

    Call iterate(i, k, l, j, aG1, aJ1, aWi1, aGp(), aWp(), days(), az(), Bgi, d(), sdd, summ(), Temp,
d1)

    pdata(i, k, l) = constdata * Exp(-0.5 * summ(i, k, l))
```

```
        ppost(i, k, l) = pprior(i, k, l) * pdata(i, k, l)

        sumpost = sumpost + ppost(i, k, l)

        sumGpost = sumGpost + (aG1 * ppost(i, k, l))

        sumJpost = sumJpost + (aJ1 * ppost(i, k, l))

        sumWipost = sumWipost + (aWi1 * ppost(i, k, l))

        sumGGpost = sumGGpost + (aG1 * aG1 * ppost(i, k, l))

        sumJJpost = sumJJpost + (aJ1 * aJ1 * ppost(i, k, l))

        sumWiWipost = sumWiWipost + (aWi1 * aWi1 * ppost(i, k, l))

        sumGJpost = sumGJpost + (aG1 * aJ1 * ppost(i, k, l))

        sumGWipost = sumGWipost + (aG1 * aWi1 * ppost(i, k, l))

        sumJWipost = sumJWipost + (aJ1 * aWi1 * ppost(i, k, l))
      Next l
    Next k
Next i

sumGpost = sumGpost / sumpost
sumJpost = sumJpost / sumpost
sumWipost = sumWipost / sumpost
sumGGpost = (sumGGpost / sumpost) - (sumGpost * sumGpost)
sumJJpost = (sumJJpost / sumpost) - (sumJpost * sumJpost)
sumWiWipost = (sumWiWipost / sumpost) - (sumWipost * sumWipost)
sumGJpost = (sumGJpost / sumpost) - (sumGpost * sumJpost)
sumGWipost = (sumGWipost / sumpost) - (sumGpost * sumWipost)
sumJWipost = (sumJWipost / sumpost) - (sumJpost * sumWipost)

ThisWorkbook.Worksheets("check").Cells(21, 1).Value = "sum_posterior ="
ThisWorkbook.Worksheets("check").Cells(21, 3).Value = sumpost
ThisWorkbook.Worksheets("check").Cells(35, 1).Value = "Mean Gpost ="
ThisWorkbook.Worksheets("check").Cells(35, 3).Value = sumGpost
ThisWorkbook.Worksheets("check").Cells(36, 1).Value = "Mean Jpost ="
ThisWorkbook.Worksheets("check").Cells(36, 3).Value = sumJpost
ThisWorkbook.Worksheets("check").Cells(37, 1).Value = "Mean Wipost ="
ThisWorkbook.Worksheets("check").Cells(37, 3).Value = sumWipost
ThisWorkbook.Worksheets("check").Cells(38, 1).Value = "Cov GGpost ="
ThisWorkbook.Worksheets("check").Cells(38, 3).Value = sumGGpost
ThisWorkbook.Worksheets("check").Cells(39, 1).Value = "Cov JJpost ="
ThisWorkbook.Worksheets("check").Cells(39, 3).Value = sumJJpost
```

```
ThisWorkbook.Worksheets("check").Cells(40, 1).Value = "Cov WiWipost ="
ThisWorkbook.Worksheets("check").Cells(40, 3).Value = sumWiWipost
ThisWorkbook.Worksheets("check").Cells(41, 1).Value = "Cov GJpost ="
ThisWorkbook.Worksheets("check").Cells(41, 3).Value = sumGJpost
ThisWorkbook.Worksheets("check").Cells(42, 1).Value = "Cov GWipost ="
ThisWorkbook.Worksheets("check").Cells(42, 3).Value = sumGWipost
ThisWorkbook.Worksheets("check").Cells(43, 1).Value = "Cov JWIpost ="
ThisWorkbook.Worksheets("check").Cells(43, 3).Value = sumJWipost


For l = 25 To 75 Step 25
  For k = 1 To n
    For i = 1 To n
      With ThisWorkbook.Worksheets("Likelihood")
        .Cells(((l / 25) + ((l / 25) - 1) * 102), 1).Value = "J \ G"
        .Cells(((l / 25) + ((l / 25) - 1) * 102), 4).Value = "Wi = " & aWi(l)
        .Cells((2 + ((l / 25) - 1) * 103), i + 1).Value = aG(i)
        .Cells((k + 2 + ((l / 25) - 1) * 103), 1).Value = aJ(k)
        .Cells((k + 2 + ((l / 25) - 1) * 103), i + 1).Value = pdata(i, k, l)
      End With
    Next i
  Next k
Next l

For k = 25 To 75 Step 25
  For i = 1 To n
    For l = 1 To n
      With ThisWorkbook.Worksheets("Likelihood")
        .Cells(((k / 25) + 309 + ((k / 25) - 1) * 102), 1).Value = "Wi \ G"
        .Cells(((k / 25) + 309 + ((k / 25) - 1) * 102), 4).Value = "J = " & aJ(k)
        .Cells((311 + ((k / 25) - 1) * 103), i + 1).Value = aG(i)
        .Cells((l + 311 + ((k / 25) - 1) * 103), 1).Value = aWi(l)
        .Cells((l + 311 + ((k / 25) - 1) * 103), i + 1).Value = pdata(i, k, l)
      End With
    Next l
  Next i
Next k

For i = 25 To 75 Step 25
  For l = 1 To n
    For k = 1 To n
      With ThisWorkbook.Worksheets("Likelihood")
        .Cells(((i / 25) + 618 + ((i / 25) - 1) * 102), 1).Value = "J \ Wi"
        .Cells(((i / 25) + 618 + ((i / 25) - 1) * 102), 4).Value = "G = " & aG(i)
        .Cells((620 + ((i / 25) - 1) * 103), l + 1).Value = aWi(l)
        .Cells((k + 620 + ((i / 25) - 1) * 103), 1).Value = aJ(k)
        .Cells((k + 620 + ((i / 25) - 1) * 103), l + 1).Value = pdata(i, k, l)
      End With
```

```
    Next k
  Next l
Next i

For l = 25 To 75 Step 25
  For k = 1 To n
    For i = 1 To n
      With ThisWorkbook.Worksheets("Posterior")
        .Cells(((l / 25) + ((l / 25) - 1) * 102), 1).Value = "J \ G"
        .Cells(((l / 25) + ((l / 25) - 1) * 102), 4).Value = "Wi = " & aWi(l)
        .Cells((2 + ((l / 25) - 1) * 103), i + 1).Value = aG(i)
        .Cells((k + 2 + ((l / 25) - 1) * 103), 1).Value = aJ(k)
        .Cells((k + 2 + ((l / 25) - 1) * 103), i + 1).Value = ppost(i, k, l)
      End With
    Next i
  Next k
Next l

For k = 25 To 75 Step 25
  For i = 1 To n
    For l = 1 To n
      With ThisWorkbook.Worksheets("Posterior")
        .Cells(((k / 25) + 309 + ((k / 25) - 1) * 102), 1).Value = "Wi \ G"
        .Cells(((k / 25) + 309 + ((k / 25) - 1) * 102), 4).Value = "J = " & aJ(k)
        .Cells((311 + ((k / 25) - 1) * 103), i + 1).Value = aG(i)
        .Cells((l + 311 + ((k / 25) - 1) * 103), 1).Value = aWi(l)
        .Cells((l + 311 + ((k / 25) - 1) * 103), i + 1).Value = ppost(i, k, l)
      End With
    Next l
  Next i
Next k

For i = 25 To 75 Step 25
  For l = 1 To n
    For k = 1 To n
      With ThisWorkbook.Worksheets("Posterior")
        .Cells(((i / 25) + 618 + ((i / 25) - 1) * 102), 1).Value = "J \ Wi"
        .Cells(((i / 25) + 618 + ((i / 25) - 1) * 102), 4).Value = "G = " & aG(i)
        .Cells((620 + ((i / 25) - 1) * 103), l + 1).Value = aWi(l)
        .Cells((k + 620 + ((i / 25) - 1) * 103), 1).Value = aJ(k)
        .Cells((k + 620 + ((i / 25) - 1) * 103), l + 1).Value = ppost(i, k, l)
      End With
    Next k
  Next l
Next i

For l = 25 To 75 Step 25
  For k = 1 To n
```

```
    For i = 1 To n
      With ThisWorkbook.Worksheets("Posterior_norm")
        .Cells(((l / 25) + ((l / 25) - 1) * 102), 1).Value = "J \ G"
        .Cells(((l / 25) + ((l / 25) - 1) * 102), 4).Value = "Wi = " & aWi(l)
        .Cells((2 + ((l / 25) - 1) * 103), i + 1).Value = aG(i)
        .Cells((k + 2 + ((l / 25) - 1) * 103), 1).Value = aJ(k)
        .Cells((k + 2 + ((l / 25) - 1) * 103), i + 1).Value = ppost(i, k, l) / sumpost
      End With
    Next i
  Next k
Next l

For k = 25 To 75 Step 25
  For i = 1 To n
    For l = 1 To n
      With ThisWorkbook.Worksheets("Posterior_norm")
        .Cells(((k / 25) + 309 + ((k / 25) - 1) * 102), 1).Value = "Wi \ G"
        .Cells(((k / 25) + 309 + ((k / 25) - 1) * 102), 4).Value = "J = " & aJ(k)
        .Cells((311 + ((k / 25) - 1) * 103), i + 1).Value = aG(i)
        .Cells((l + 311 + ((k / 25) - 1) * 103), 1).Value = aWi(l)
        .Cells((l + 311 + ((k / 25) - 1) * 103), i + 1).Value = ppost(i, k, l) / sumpost
      End With
    Next l
  Next i
Next k

For i = 25 To 75 Step 25
  For l = 1 To n
    For k = 1 To n
      With ThisWorkbook.Worksheets("Posterior_norm")
        .Cells(((i / 25) + 618 + ((i / 25) - 1) * 102), 1).Value = "J \ Wi"
        .Cells(((i / 25) + 618 + ((i / 25) - 1) * 102), 4).Value = "G = " & aG(i)
        .Cells((620 + ((i / 25) - 1) * 103), l + 1).Value = aWi(l)
        .Cells((k + 620 + ((i / 25) - 1) * 103), 1).Value = aJ(k)
        .Cells((k + 620 + ((i / 25) - 1) * 103), l + 1).Value = ppost(i, k, l) / sumpost
      End With
    Next k
  Next l
Next i

Call Find_max0(aG0, aJ0, aWi0, ppriormax, x0, y0, z0, n)
Call Find_max(aG2, aJ2, aWi2, pdatamax, x, y, z, n)
Call Find_max1(aG3, aJ3, aWi3, ppostmax, x1, y1, z1, n)

amaxl = pdatamax
aGmaxl = aG2
aJmaxl = aJ2
aWimaxl = aWi2
```

```
amax = ppostmax
aGmax = aG3
aJmax = aJ3
aWimax = aWi3

With ThisWorkbook.Worksheets("check")
  .Cells(24, 1).Value = "aG_ML ="
  .Cells(24, 3).Value = aGmaxl
  .Cells(24, 5).Value = "i ="
  .Cells(24, 6).Value = x
  .Cells(24, 8).Value = "pdatamax =" & amaxl
  .Cells(25, 1).Value = "aJ_ML ="
  .Cells(25, 3).Value = aJmaxl
  .Cells(25, 5).Value = "k ="
  .Cells(25, 6).Value = y
  .Cells(26, 1).Value = "aWi_ML ="
  .Cells(26, 3).Value = aWimaxl
  .Cells(26, 5).Value = "l ="
  .Cells(26, 6).Value = z
  .Cells(27, 1).Value = "aG_MAP ="
  .Cells(27, 8).Value = "ppostmax =" & amax
  .Cells(27, 3).Value = aGmax
  .Cells(27, 5).Value = "i ="
  .Cells(27, 6).Value = x1
  .Cells(28, 1).Value = "aJ_MAP ="
  .Cells(28, 3).Value = aJmax
  .Cells(28, 5).Value = "k ="
  .Cells(28, 6).Value = y1
  .Cells(29, 1).Value = "aWi_MAP ="
  .Cells(29, 3).Value = aWimax
  .Cells(29, 5).Value = "l ="
  .Cells(29, 6).Value = z1
  .Cells(30, 1).Value = "aG_P ="
  .Cells(30, 3).Value = aG0
  .Cells(30, 5).Value = "i ="
  .Cells(30, 6).Value = x0
  .Cells(30, 8).Value = "ppriormax =" & ppriormax
  .Cells(31, 1).Value = "aJ_P ="
  .Cells(31, 3).Value = aJ0
  .Cells(31, 5).Value = "k ="
  .Cells(31, 6).Value = y0
  .Cells(32, 1).Value = "aWi_P ="
  .Cells(32, 3).Value = aWi0
  .Cells(32, 5).Value = "l ="
  .Cells(32, 6).Value = z0
End With
```

```
'Use the approximated analytical method with the exact covariance matrix
'Getting sensitivity Matrix at the MAP
'Calling sub iterate to use Newton method to get g(m) at MAP

  With ThisWorkbook.Worksheets("check")
    .Cells(1, 1).Value = "gm(j)"
    .Cells(1, 2).Value = "dfpdp"
  End With

  Call iterate1(j, aGmax, aJmax, aWimax, aGp(), aWp(), days(), az(), Bgi, Temp, d1)

  With ThisWorkbook.Worksheets("Check")
   For j = 1 To nd
   dfpdp1(j) = .Cells(j + 1, 2)
   Next j
  End With

  Call Sort_dfpdp1max(dfpdp1())

  dfpdpmax = dfpdp1(UBound(dfpdp1))

  With ThisWorkbook.Worksheets("check_sensitivity")
    .Cells(1, 1).Value = "Gs1"
    .Cells(1, 2).Value = "Gs2"
    .Cells(1, 3).Value = "Gs3"
  End With

  Call sensitivity(j, gm(), dfpdpmax, aGmax, aJmax, aWimax, Bgi, Temp, aGp(), aWp(), days(),
az(), d1)

'Reading sensitivity

   With ThisWorkbook.Worksheets("Check_sensitivity")
   For j = 1 To nd
     For k = 1 To m
       Gsen(j, k) = .Cells(j + 1, k)
     Next k
   Next j
   End With

   'Form the matrix Cd in array Cd
   For i = 1 To nd
     For j = 1 To nd
       Cd(i, j) = 0#
       Cd(j, i) = 0#
     Next j
     Cd(i, i) = sdd ^ 2
   Next i
```

```
'Form matrix Cd^-1
For i = 1 To nd
  For j = 1 To nd
    invCd(i, j) = Application.Index((Application.MInverse(Cd)), i, j)
  Next j
Next i

 'Form the matrix Cm in array Cm
For i = 1 To m
  For j = 1 To m
    Cm(i, j) = 0#
    Cm(j, i) = 0#
  Next j
    If i = 1 Then
       Cm(i, i) = (sdaG ^ 2)
    ElseIf i = 2 Then
       Cm(i, i) = (sdaJ ^ 2)
    Else
        Cm(i, i) = (sdaWi ^ 2)
    End If
Next i

'Form matrix Cm^-1
For i = 1 To m
  For j = 1 To m
    invCm(i, j) = Application.Index((Application.MInverse(Cm)), i, j)
  Next j
Next i

With ThisWorkbook.Worksheets("check")
  .Cells(1, 6).Value = "Cd"
  .Cells(10, 6).Value = "Cd^-1"
  .Cells(1, 15).Value = "Cm"
  .Cells(10, 15).Value = "Cm^-1"
For i = 1 To nd
  For j = 1 To nd
    .Cells(i + 1, j + 5).Value = Cd(i, j)
    .Cells(i + 10, j + 5).Value = invCd(i, j)
  Next j
Next i
For i = 1 To m
  For j = 1 To m
    .Cells(i + 1, j + 13).Value = Cm(i, j)
    .Cells(i + 10, j + 13).Value = invCm(i, j)
  Next j
Next i
End With
```

```
    'From matrix G^T at the MAP in array GsT
    For i = 1 To m
      For j = 1 To nd
        Gt(i, j) = Gsen(j, i)
      Next j
    Next i

    'Form the matrix (Cd^-1*G) in array CdGs
    For i = 1 To nd
      For j = 1 To m
        CdGs(i, j) = Application.Index((Application.MMult(invCd, Gsen)), i, j)
      Next j
    Next i

    'Form the matrix G^T * CdGs in array GtCdGs
    For i = 1 To m
      For j = 1 To m
        GtCdGs(i, j) = Application.Index((Application.MMult(Gt, CdGs)), i, j)
      Next j
     Next i

      ThisWorkbook.Worksheets("check").Cells(10, 1).Value = "Cmapinv(i, j)"

     'Form the matrix G^T*Cd^-1*G+Cm^-1 in array Cmapinv
     'Write the matrix Cmapinv which is the Hessian
     For i = 1 To m
       For j = 1 To m
         Cmapinv(i, j) = GtCdGs(i, j) + invCm(i, j)
         ThisWorkbook.Worksheets("check").Cells(i + 10, j).Value = Cmapinv(i, j)
       Next j
     Next i

     ThisWorkbook.Worksheets("check").Cells(15, 1).Value = "Cmap(i, j)"

     'Call the sub for matixinversion to get the inverse of the matrix Cmapinv
     'Writing the inverse of the matrix Cmapinv
     For i = 1 To m
       For j = 1 To m
         Cmap(i, j) = Application.Index((Application.MInverse(Cmapinv)), i, j)
          ThisWorkbook.Worksheets("check").Cells(i + 15, j).Value = Cmap(i, j)
       Next j
     Next i

  End Sub
```

```
Sub iterate(i As Integer, k As Integer, l As Integer, j As Integer, aG1 As Double, aJ1 As Double,
aWi1 As Double, aGp() As Double, aWp() As Double, days() As Double, az() As Double, Bgi As
Double, d() As Double, sdd As Double, summ() As Double, Temp As Double, d1 As Double)
  Dim Bg As Double
  Dim fp As Double
  Dim dbg As Double
  Dim g As Double
  Dim gi As Double
  Dim g1() As Double
  Dim dfpdp As Double
  Dim Wei As Double
  Dim paqave() As Double
  Dim paqave1() As Double
  Dim We() As Double
  Dim We1() As Double
  Dim prave As Double
  Dim delt As Double
  Dim dWen As Double
  Dim dWenp As Double

  Dim w As Integer
  Dim counter As Integer

  ReDim We(1 To nd)
  ReDim paqave(1 To nd)

  With ThisWorkbook.Worksheets("Data")
   ct = .Cells(2, 6)
   Bw = .Cells(3, 6)
  End With

  Wei = Weif(ct, d1, aWi1)

For j = 1 To nd
  counter = 0
  g = d1 - 5

    Do While w = 0
     counter = counter + 1
     ReDim Preserve g1(counter)
     ReDim Preserve paqave1(counter)
     ReDim Preserve We1(counter)

     If j = 1 Then
        prave = pravef(d1, g)
        delt = deltf(0#, days(j))

        dWen = dWenf(Wei, d1, d1, prave, aJ1, delt)
```

```
      We1(counter) = dWen
      paqave1(counter) = paqavef(d1, We1(counter), Wei)
      dWenp = -0.5 * ct * (1 - Exp(-(aJ1 * delt / (ct * aWi1)))) * aWi1
    Else
      prave = pravef(gm(j - 1), g)
      delt = deltf(days(j - 1), days(j))

      dWen = dWenf(Wei, paqave(j - 1), d1, prave, aJ1, delt)
      We1(counter) = dWen + We(j - 1)
      paqave1(counter) = paqavef(d1, We1(counter), Wei)
      dWenp = -0.5 * ct * (1 - Exp(-(aJ1 * delt / (ct * aWi1)))) * aWi1
    End If

    Bg = 5.02 * az(j) * (Temp + 460) / g            'rb/mscf
    fp = -aG1 * (Bg - Bgi) + aGp(j) * Bg - We1(counter) + aWp(j) * Bw

    dbg = -5.02 * az(j) * (Temp + 460) / (g ^ 2)
    dfpdp = -aG1 * dbg + aGp(j) * dbg - dWenp + aWp(j)

    gi = fp / dfpdp
    g = g - gi

    g1(counter) = g

    If Abs(gi) < 0.00001 Or counter = 100 Then
       gm(j) = g1(counter - 1)
       We(j) = We1(counter - 1)
       paqave(j) = paqave1(counter - 1)
       Exit Do
    ElseIf g1(counter) <= 0 Or g1(counter) >= d1 Then
      gm(j) = d1
      We(j) = We1(counter)
      paqave(j) = paqave1(counter)
      Exit Do
    End If
  Loop

  sum = 0#

  If gm(j) <= 0# Or gm(j) >= d1 Then
    sum = 0
    sum1 = 0
  End If

  sum = sum + ((((d(j) - gm(j))) ^ 2) * (1 / (sdd ^ 2)))
Next j

  summ(i, k, l) = sum
```

```
  With ThisWorkbook.Worksheets("sheet1")
   .Cells((1 + (l - 1) * 102), 104).Value = "Wi =" & aWi(l)
   .Cells((i + 1 + (l - 1) * 102), 1).Value = aJ(i)
   .Cells((1 + (l - 1) * 102), k + 1).Value = aG(k)
   .Cells((i + 1 + (l - 1) * 102), k + 1).Value = summ(i, k, l)
  End With

End Sub

Sub iterate1(j As Integer, aGmax As Double, aJmax As Double, aWimax As Double, aGp() As
Double, aWp() As Double, days() As Double, az() As Double, Bgi As Double, Temp As Double,
d1 As Double)
 Dim Bg As Double
 Dim fp As Double
 Dim dbg As Double
 Dim g As Double
 Dim gi As Double
 Dim g1() As Double
 Dim dfpdp As Double
 Dim Wei As Double
 Dim paqave() As Double
 Dim paqave1() As Double
 Dim We() As Double
 Dim We1() As Double
 Dim prave As Double
 Dim delt As Double
 Dim dWen As Double
 Dim dWenp As Double

 Dim w As Integer
 Dim counter As Integer

 ReDim We(1 To nd)
 ReDim paqave(1 To nd)

 With ThisWorkbook.Worksheets("Data")
  ct = .Cells(2, 6)
  Bw = .Cells(3, 6)
 End With

 Wei = Weif(ct, d1, aWimax)

For j = 1 To nd
 counter = 0
 g = d1 - 5

  Do While w = 0
```

```
  counter = counter + 1
  ReDim Preserve g1(counter)
  ReDim Preserve paqave1(counter)
  ReDim Preserve We1(counter)

  If j = 1 Then
    prave = pravef(d1, g)
    delt = deltf(0#, days(j))

    dWen = dWenf(Wei, d1, d1, prave, aJmax, delt)
    We1(counter) = dWen
    paqave1(counter) = paqavef(d1, We1(counter), Wei)
    dWenp = -0.5 * ct * (1 - Exp(-(aJ1 * delt / (ct * aWi1)))) * aWi1
  Else
    prave = pravef(gm(j - 1), g)
    delt = deltf(days(j - 1), days(j))

    dWen = dWenf(Wei, paqave(j - 1), d1, prave, aJmax, delt)
    We1(counter) = dWen + We(j - 1)
    paqave1(counter) = paqavef(d1, We1(counter), Wei)
    dWenp = -0.5 * ct * (1 - Exp(-(aJ1 * delt / (ct * aWi1)))) * aWi1
  End If

  Bg = 5.02 * az(j) * (Temp + 460) / g                    'rb/mscf
  fp = -aGmax * (Bg - Bgi) + aGp(j) * Bg - We1(counter) + aWp(j) * Bw

  dbg = -5.02 * az(j) * (Temp + 460) / (g ^ 2)
  dfpdp = -aGmax * dbg + aGp(j) * dbg - dWenp + aWp(j)

  gi = fp / dfpdp
  g = g - gi

  g1(counter) = g


  If Abs(gi) < 0.00001 Or counter = 100 Then
     gm(j) = g1(counter - 1)
     We(j) = We1(counter - 1)
     paqave(j) = paqave1(counter - 1)
     Exit Do
  ElseIf g1(counter) <= 0 Or g1(counter) >= d1 Then
    gm(j) = d1
    We(j) = We1(counter)
    paqave(j) = paqave1(counter)
    Exit Do
  End If
Loop
```

```
  ThisWorkbook.Worksheets("Check").Cells(j + 1, 1).Value = gm(j)
  ThisWorkbook.Worksheets("Check").Cells(j + 1, 2).Value = dfpdp
  Next j

End Sub

'This sub us used to calculate the sensitivity coefficient at each point analytically
Sub sensitivity(j As Integer, gm() As Double, dfpdpmax As Double, aGmax As Double, aJmax As Double, aWimax As Double, Bgi As Double, Temp As Double, aGp() As Double, aWp() As Double, days() As Double, az() As Double, d1 As Double)

 Dim zfact As Double
 Dim Bg As Double
 Dim dfpdG As Double
 Dim dfpdJ As Double
 Dim dfpdWi As Double
 Dim dgdG As Double
 Dim dgdJ As Double
 Dim dgdWi As Double
 Dim ra As Double
 Dim Wi As Double
 Dim Wei As Double
 Dim Jindex As Double
 Dim paqave() As Double
 Dim We() As Double
 Dim prave As Double
 Dim delt As Double
 Dim dWen As Double
 Dim dWendj As Double
 Dim dWendWi As Double

 ReDim We(1 To nd)
 ReDim paqave(1 To nd)

 With ThisWorkbook.Worksheets("Data")
  ct = .Cells(2, 6)
  Bw = .Cells(3, 6)
 End With

 Wei = Weif(ct, d1, aWimax)

 For j = 1 To nd

    If j = 1 Then
      prave = pravef(d1, gm(j))
      delt = deltf(0#, days(j))

      dWen = dWenf(Wei, d1, d1, prave, aJmax, delt)
```

```
        We(j) = dWen
        paqave(j) = paqavef(d1, We(j), Wei)
        dWendj = delt * Exp(-delt * aJmax * d1 / Wei) * (d1 - prave)
        dWendWi = ct * (1 - Exp(-(aJmax * delt) / ct * aWimax)) * (0.5 * (-gm(j) - d1) + d1) + _
        (1 - Exp(-(aJmax * delt) / ct * aWimax)) * 0 / aWimax - (Exp(-(aJmax * delt) / ct * aWimax))
* aJmax * ct * (0.5 * (-gm(j) - d1) + d1) / aWimax
     Else
        prave = pravef(gm(j - 1), gm(j))
        delt = deltf(days(j - 1), days(j))

         dWen = dWenf(Wei, paqave(j - 1), d1, prave, aJmax, delt)
         We(j) = dWen + We(j - 1)
         paqave(j) = paqavef(d1, We(j), Wei)
         dWendj = delt * Exp(-delt * aJmax * d1 / Wei) * (paqave(j - 1) - prave)
         dWendWi = ct * (1 - Exp(-(aJmax * delt) / ct * aWimax)) * (0.5 * (-gm(j) - gm(j - 1)) + d1 *
(1 - (We(j - 1) / (ct * d1 * aWimax)))) + _
         (1 - Exp(-(aJmax * delt) / ct * aWimax)) * We(j - 1) / aWimax - (Exp(-(aJmax * delt) / ct *
aWimax)) * aJmax * ct * (0.5 * (-gm(j) - gm(j - 1)) + _
         d1 * (1 - (We(j - 1) / (ct * d1 * aWimax)))) / aWimax
     End If

     Bg = 5.02 * az(j) * (Temp + 460) / gm(j)      'rb/mscf

     dfpdG = -(Bg - Bgi) + aGp(j) * Bg - We(j) + aWp(j) * Bw
     dfpdJ = -dWendj
     dfpdWi = -dWendWi

    dgdG = (1 / dfpdpmax) * dfpdG
    dgdJ = (1 / dfpdpmax) * dfpdJ
    dgdWi = (1 / dfpdpmax) * dfpdWi

    Gs1 = dgdG
    Gs2 = dgdJ
    Gs3 = dgdWi


 ThisWorkbook.Worksheets("Check_sensitivity").Cells(j + 1, 1).Value = Gs1
 ThisWorkbook.Worksheets("Check_sensitivity").Cells(j + 1, 2).Value = Gs2
 ThisWorkbook.Worksheets("Check_sensitivity").Cells(j + 1, 3).Value = Gs3
 Next j

End Sub


Sub Sort_dfpdp1max(ByRef dfpdp1() As Double)
    Dim Temp As Double
    Dim i As Long
    Dim j As Long
```

```
    Application.StatusBar = "                                        Sorting in progress ....."

    For j = 2 To UBound(dfpdp1)
        Temp = dfpdp1(j)
        For i = j - 1 To 1 Step -1
            If (dfpdp1(i) <= Temp) Then GoTo 10
            dfpdp1(i + 1) = dfpdp1(i)
        Next i
        i = 0
10      dfpdp1(i + 1) = Temp
    Next j

End Sub

Sub Find_max0(aG0 As Double, aJ0 As Double, aWi0 As Double, ppriormax As Double, x0 As Integer, y0 As Integer, z0 As Integer, ByVal n As Integer)
    Dim i As Integer, k As Integer, l As Integer
    Dim max_value As Double, x_value As Double, y_value As Double, z_value As Double
    Dim x1 As Integer, y1 As Integer, z1 As Integer

    max_value = -9999999
    For i = 1 To n
        For k = 1 To n
          For l = 1 To n
           If pprior(i, k, l) > max_value Then
               max_value = Val(pprior(i, k, l))
               x_value = Val(aG(i))
               y_value = Val(aJ(k))
               z_value = Val(aWi(l))
               x1 = Val(i)
               y1 = Val(k)
               z1 = Val(l)
           End If
          Next l
        Next k
    Next i

    ppriormax = max_value
    aG0 = x_value
    aJ0 = y_value
    aWi0 = z_value
    x0 = x1
    y0 = y1
    z0 = z1
End Sub
```

```
Sub Find_max(aG2 As Double, aJ2 As Double, aWi2 As Double, pdatamax As Double, x As
Integer, y As Integer, z As Integer, ByVal n As Integer)
    Dim i As Integer, k As Integer, l As Integer
    Dim max_value As Double, x_value As Double, y_value As Double, z_value As Double
    Dim x1 As Integer, y1 As Integer, z1 As Integer

    max_value = -9999999
    For i = 1 To n
        For k = 1 To n
          For l = 1 To n
           If pdata(i, k, l) > max_value Then
               max_value = Val(pdata(i, k, l))
               x_value = Val(aG(i))
               y_value = Val(aJ(k))
               z_value = Val(aWi(l))
               x1 = Val(i)
               y1 = Val(k)
               z1 = Val(l)
           End If
          Next l
        Next k
    Next i

    pdatamax = max_value
    aG2 = x_value
    aJ2 = y_value
    aWi2 = z_value
    x = x1
    y = y1
    z = z1
End Sub

Sub Find_max1(aG3 As Double, aJ3 As Double, aWi3 As Double, ppostmax As Double, x1 As
Integer, y1 As Integer, z1 As Integer, ByVal n As Integer)
    Dim i As Integer, k As Integer, l As Double
    Dim max_value As Double, x_value As Double, y_value As Double, z_value As Double
    Dim x2 As Integer, y2 As Integer, z2 As Integer

    max_value = -9999999
    For i = 1 To n
        For k = 1 To n
          For l = 1 To n
           If Val(ppost(i, k, l)) > max_value Then
               max_value = Val(ppost(i, k, l))
               x_value = Val(aG(i))
               y_value = Val(aJ(k))
               z_value = Val(aWi(l))
               x2 = Val(i)
```

```
            y2 = Val(k)
            z2 = Val(l)
          End If
        Next l
      Next k
   Next i

   ppostmax = max_value
   aG3 = x_value
   aJ3 = y_value
   aWi3 = z_value
   x1 = x2
   y1 = y2
   z1 = z2
End Sub

Function raf(A As Double, teta As Double) As Double
Pi = 4 * Atn(1)
raf = ((43560 * A / Pi) * (360 / teta)) ^ 0.5
End Function

Function Wif(ra As Double, rr As Double, h As Double, phi As Double, teta As Double) As
Double
Pi = 4 * Atn(1)
Wif = (Pi * (ra ^ 2 - rr ^ 2) * h * phi * (teta / 360)) / 5.615
End Function

Function Weif(ct As Double, PAQ As Double, Wi As Double) As Double
Weif = ct * PAQ * Wi
End Function

'J for radial flow finite aquifer with no flow
Function J1(aWe As Double, teta As Double, miu As Double, ra As Double, rr As Double) As
Double
J1 = (0.00708 * aWe * (teta / 360)) / (miu * ((Log(ra / rr) / Log(2.718282)) - 0.75))
End Function

'J for radial flow finite aquifer with constant pressure
Function J2(k As Double, h As Double, teta As Double, miu As Double, ra As Double, rr As
Double) As Double
J2 = (0.00708 * k * h * (teta / 360)) / (miu * (Log(ra / rr) / Log(2.718282)))
End Function

'J for radial flow infinite aquifer
'Function J3(k As Double, h As Double, teta As Double, miu As Double, t As Double, phi As
Double, ct As Double, rr As Double) As Double
'J3 = (0.00708 * k * h * (teta / 360)) / (miu * (Log(0.0142 * k * t / (phi * miu * ct * rr ^ 2) ^ 0.5) /
Log(2.718282)))
```

```
'End Function

Function paqavef(PAQ As Double, We0 As Double, Wei As Double) As Double
paqavef = PAQ * (1 - (We0 / Wei))
End Function

Function pravef(pr0 As Double, pr As Double) As Double
pravef = (pr0 + pr) / 2
End Function

Function deltf(t0 As Double, T As Double) As Double
deltf = T - t0
End Function

Function dWenf(Wei As Double, paqave As Double, PAQ As Double, prave As Double, j As Double, deltn As Double) As Double
   dWenf = (Wei / PAQ) * (paqave - prave) * (1 - Exp(-(j * PAQ * deltn / Wei)))
End Function
```

VITA

Name : Asti Wulandari Aprilia

Address : Jl. Abuserin II no. 7
Cilandak, Jakarta Selatan, Indonesia 12420

Education : Master of Science, Texas A&M University, Petroleum Engineering
Bachelor of Science, University of Indonesia, Civil Engineering